ON THE MECHANISMS OF NON-CONTACT ACL INJURY DURING A SIMULATED JUMP LANDING: EXPERIMENTAL AND THEORETICAL ANALYSES

by

You Keun Oh

A dissertation submitted in partial fulfillment
of the requirements for the degree of
Doctor of Philosophy
(Mechanical Engineering)
in the University of Michigan
2011

Doctoral Committee:

Research Professor James A. Ashton-Miller, Co-Chair
Professor Edward M. Wojtys, Co-Chair
Professor Noel C. Perkins
Assistant Professor Scott G. McLean

To my parents, wife, and daughters

ACKNOWLEDGMENTS

Since the beginning of this long journey, I have received tremendous support from many individuals. Without their help, all of my achievements would not have been possible.

I would like to thank my mentors for their guidance, support, encouragement, and patience throughout the duration of my graduate studies. Prof. James Ashton-Miller has helped me create fresh ideas whenever my research was confronted with a difficult problem. He also taught me the important of capturing the essence of a complicated phenomenon by initially addressing the problem with a simple model. Prof. Edward Wojtys has helped enrich my understating of clinical problems that physicians are facing everyday. I thank both of you for providing me such a great interdisciplinary research environment.

In addition, I would like to thank my dissertation committee members for their valuable feedback. I thank Prof. Scott McLean for providing insightful information for my knee model simulation and Prof. Noel Perkins for his helpful comments and constructive criticism to strengthen the overall dissertation.

I would like to thank Charles Roehm and Dennis Kayer of the Orthopaedic Research Laboratories for their technical assistance in rebuilding the testing apparatus and adding the torsional transformer device. Also, thank you to Prof. Steve Goldstein

who allowed me to use his lab facilities. I would like to thank Dean Muller of the University of Michigan Anatomical Donation Program for the supply of knee specimens.

I would like to thank Jennifer Kreinbrink and David Lipps for their assistance and friendship over the years. Working together with them has been such a joyful experience. Thanks to all my other lab mates in the Biomechanics Research Laboratory for their help and friendship.

I would like to thank my parents, Yongmu Oh and Soyoung Lee, for their unconditional love and support. They have sacrificed so much for me over the years, and have always treated my education as a top priority. Thank you to my sister and brother-in-law, Yeonjoo Oh and WanJei Cho. Remembering the time we spent together in Chicago and Pittsburgh will always makes me smile. Finally, I would like to give heartfelt thanks to my wife Jeonghwa and daughters, Claire and Grace, for making this long journey with me. You have always been a constant source of energy and happiness for me.

Preface

Chapters 2 through 6 were written as separate manuscripts. For this reason, some repetition of material does occur, particularly in the methods section for each chapter. Chapters 2 and 3 have been submitted for publication. Chapter 5 and Appendix B are being published by the *Journal of Bone & Joint Surgery (American Volume)*.

TABLE OF CONTENTS

LIST OF FIGURES

CHAPTER 2

Figure

CHAPTER 3

Figure

CHAPTER 4

Figure

CHAPTER 5

Figure

CHAPTER 6

Figure

APPENDIX A

Figure

APPENDIX B

Figure

LIST OF TABLES

CHAPTER 2

Table

CHAPTER 3

Table

CHAPTER 4

Table

CHAPTER 5

Table

APPENDIX A

Table

APPENDIX B

Table

LIST OF APPENDICES

APPENDIX

ABSTRACT

ON THE MECHANISMS OF NON-CONTACT ACL INJURY DURING A SIMULATED JUMP LANDING: EXPERIMENTAL AND THEORETICAL ANALYSES

by

You Keun Oh

Co-Chairs: James A. Ashton-Miller and Edward M. Wojtys

Of the 350,000 ACL reconstructions performed annually in the U.S., 70% are due to "non-contact" injuries often due to pivot landing maneuvers. Because an ACL injury predisposes the individual to early onset knee osteoarthritis, mechanistic insights are needed into why these injuries occur so they can be better prevented in the future.

A knowledge gap concerns the relative contributions of dynamic internal tibial torque and valgus moment in causing ACL strain under the large impulsive ground reactions and muscle forces typically experienced *in vivo*. The goal of this dissertation, therefore, was to investigate the effect of impulsive axial tibial torque, with and without frontal plane moment, on ACL strain during a realistic jump landing scenario.

Human cadaveric knees were loaded with realistic muscle forces in a simulated pivot landing test scenario. Impulsive compression, flexion moment, internal or external tibial torque, and ab- or adduction moments were simultaneously applied to the knee while recording the 3-D knee loads, muscle forces, tibiofemoral kinematics, and anteromedial ACL relative strain. In addition, a dynamic 3-D biomechanical model of the knee was developed to further explore ACL injury mechanisms.

The results show that internal tibial torque, rather than a knee abduction moment, causes the largest ACL strains during a jump landing. Furthermore, an internal tibial torque induces a 70% larger ACL strain than a similar magnitude of external tibial torque. The presence of either a knee ab- or adduction moment did not significantly alter these results. An insight provided by the knee model is that when the lateral tibial slope exceeds that of the medial tibial plateau, then an abduction moment augments coupled internal tibial rotation, thereby increasing ACL strain, even without medial knee joint opening. Finally, the model simulation found that a steeper lateral tibial slope compared to a medial tibial slope, a more valgus limb alignment, and a shallower medial tibial concavity all increase the ACL strain during a simulated landing.

CHAPTER 1

INTRODUCTION

1.1 Overview

In United States, nearly 350,000 anterior cruciate ligament (ACL) reconstructions are performed every year.[1] Despite recent advances in operative and non-operative treatment of ACL injuries, compromised knee function can be expected in 50% of those injured with 6 months to 11 years.[2] An ACL rupture, regardless of which treatment is chosen, increases the risk of degenerative arthritis ten-fold compared to an age-matched uninjured population.[3-5] Degenerative arthritis is the leading cause of disability among adults in the United States, with the knee being the most commonly affected joint. Degenerative arthritis in young adults is most commonly a result of a previous injury to the knee.[6] Eighty percent of patients who sustain an ACL tear will have a concomitant impaction injury to the articular cartilage (i.e., bone bruise), and greater than 50% will have meniscal tears.[7-11], rendering them at risk for degenerative disease. Daniel et al.[2] demonstrated that a significant percentage of ACL reconstructions with reasonable joint stability developed degenerative changes within a relatively short time. Consequently, even if ACL reconstructions produce normal kinematics at the knee, the concomitant injuries to the menisci, hyaline cartilage, secondary restraints and the neuromuscular

system are believed to predispose these individuals to early degenerative disease over time.[2,3,12-18] Therefore, the best approach to the problem appears to be prevention and a better understanding of the mechanisms of ACL injury is needed in order to improve risk factor surveillance and injury prevention programs.

Over the past decade many ACL injury prevention programs have focused on reducing valgus loading to the knee during jump landings. This is primarily because the knee often appears to pass through a valgus posture on videotapes of athletes who are landing and/or pivoting as they sustain an ACL injury. *Post-hoc* injury video analysis is valuable because it is usually the only way to obtain information at the time of injurious event. However, it provides limited information on the forces and moments that caused injury[19] due to the absence of force plates to accurately measure ground reaction forces, kinematic markers to measure segmental motions, and measures of knee muscle activity which largely determines the loading on the ACL.[20] In addition, a knee valgus angle can occur from a knee abduction, transverse plane rotation of knee joint, or femoral internal rotation and/or adduction.

More importantly, it still remains unclear that if it were the abduction moment at the knee that typically causes the non-contact ACL injury by inducing a medial joint opening, then concomitant medial collateral ligament (MCL) rupture would be seen with most non-contact ACL tears. However, it is estimated that combined ACL/MCL injuries make up to only less than 30% of all ACL injuries. Although this infrequency may be explained by the fact that the failure loads for MCL are greater than the corresponding values for ACL (i.e., ~2300 N vs. 640~2160 N), the difference in those failure loads seem too close to explain this infrequency of combined ACL/MCL injuries.

MR studies of ACL injured knees have demonstrated a bone bruise in the lateral compartment of the knee in up to 80% of acute ACL tears.[10,21] A lateral bone bruise indicates lateral compartment compression or impact either at the time of ACL injury or shortly after. These bone bruise patterns also suggest that large knee abduction moments may be involved under high compressive joint force during an injurious event. However, the same bone bruise patterns can occur under internal tibial rotation with high compressive joint force. Overall, it still remains unclear which of these is the most common form of loading during ACL injury.

Previous studies, performed quasi-statically *in vivo* and *in vitro,* suggest higher ACL strains occur under an internal tibial torque than under an external tibial torque.[22-24] On the other hand, Olsen et al.[25] analyzed 20 videotaped ACL handball injuries and suggested that two-thirds (12 of 19) of the injuries occurred in external rotation during the plant-and-cut maneuver with the knee near full extension, with the remainder (one-third) being injured in internal rotation. Hence, an investigation of the effect of axial tibial torque and interaction between axial tibial torque and frontal plane moment on ACL strain during a realistic jump landing seems warranted, particularly in the presence of direct measurements of the impulsive tibial compressive force, knee flexion moment, muscle forces, tibiofemoral bone kinematics, and ACL strain.

1.2 Objectives and Experimental and Modeling Approach

The objective of this dissertation is to provide a better understanding of ACL behavior under dynamic impulsive loading of the human knee, particularly in

combination with impulsive axial tibial torque and/or frontal plane moment. We adopted an experimental approach involving an in vitro impact testing apparatus to simulate a realistic jump landing in the presence of muscle forces. We also adopted a 3-D knee model simulation approach to help interpret the experimental results and further understand the loading mechanisms of each loading direction. Simply put, our goal was to identify the direction of compound dynamic loading acting on the knee during a pivot landing that caused the largest increase in ACL strain.

1.3 Significance

The significance of this research is in the area of injury prevention. We will demonstrate, for the first time, which is the worst-case dynamic knee loading as far as ACL strain is concerned during a jump landing. The significance is that if the worst-case dynamic loading can be identified then this has implications for ACL injury prevention because minimizing large magnitude loadings of this type would reduce the risk for injury. If knee morphological factors prove to be important, then again these could be the first factors to use imaging to screen athletes in order to reduce injury risk.

1.4 Organization of Dissertation

The dissertation contains nine chapters. Five chapters represent full-length manuscripts either submitted or prepared for publication. Chapter 5 has already been published in a peer-reviewed journal and Chapters 2 and Chapter 3 have been submitted to peer-reviewed journals.

Chapter 2 investigates the effect of axial tibial torque on anteromedial (AM) ACL relative strain. Chapter 3 experimentally examines the relative contributions of an axial tibial torque and frontal plane moment to the AM-ACL relative strain and then further explores how the axial tibial torque and frontal plane moment interact to affect the AM-ACL strain using a 3-D lower-limb model simulation. Chapter 4 investigates how the morphological change in anatomical factors (i.e., lateral tibial slope, frontal plane alignment, and medial tibial concavity) affect the AM-ACL strain during a simulated jump landing. Chapter 5 examines the effect of ACL transection on axial tibial rotation and anterior tibial translation so as to better understand the role of the ACL in limiting axial tibial rotation during a simulated jump landing. Chapter 6 investigates the effect of trans-knee muscle forces on axial tibial rotation in either the ACL-intact or ACL-deficient knee in a quasi-static manner. Chapter 7 contains a general discussion of Chapters 2 - 6 and discusses the strengths and weakness of the overall approach. Finally, Chapter 8 summarizes the conclusions for this research. Appendix A reports the effect of simultaneous hip and knee flexion on hamstring muscle length. Finally, in a secondary analysis, Appendix B reports the correlation between tibiofemoral acceleration and ACL relative strain.

1.5 References

1. Allografts in Sports Medicine: What Do We Know, Need to Know, and Need to Do? Round table discussion: American Orthopaedic Society for Sports Medicine; February 13, 2006; Park City, UT.

2. Daniel DM, Stone ML, Dobson BE, Fithian DC, Rossman DJ, Kaufman KR. Fate of the ACL-injured patient: A prospective outcome study. *Am J Sports Med 1994;*22:632-644.

3. Gillquist J, Messner K. Anterior cruciate ligament reconstruction and the long-term incidence of gonarthrosis. Sports Med 1999;27:143-156.

4. Myklebust G, Holm I, Maehlum S, Engebretsen L, Bahr R. Clinical, functional, and radiologic outcome in team handball players 6 to 11 years after anterior cruciate ligament injury. *Am J Sports Med 2003;*31:981-989.

5. Lohmander, LS, Englund PM, Dahl LL, Roos EM. The long-term consequence of anterior cruciate ligament and meniscus injuries - Osteoarthritis. Am J Sports Med. 2007;35:1756-1769.

6. Roos H, Adalberth T, Dahlberg L, Lohmander LS. Osteoarthritis of the knee after injury to the anterior cruciate ligament or meniscus: The influence of time and age. *Osteoarthritis Cartilage* 1995;3:261-267.

7. Binfield PM, Maffulli N, King JB. Patterns of meniscal tears associated with anterior cruciate ligament lesions in athletes. *Injury 1993;*24:557-561.

8. Caborn DN, Johnson BM. The natural history of the anterior cruciate ligament-deficient knee: A review. *Clin Sports Med 1993;*12:625-636.

9. Fehnel DJ, Johnson R. Anterior cruciate injuries in the skeletally immature athlete: A review of treatment outcomes. *Sports Med 2000;*29: 51-63.

10. Spindler KP, Schils JP, Bergfeld JA, et al. Prospective study of osseous, articular, and meniscal lesions in recent anterior cruciate ligament tears by magnetic resonance imaging and arthroscopy. *Am J Sports Med 1993;*21:551-557.

11. Vellet AD, Marks PH, Fowler PJ, Munro TG. Occult posttraumatic osteochondral lesions of the knee: prevalence, classification, and short-term sequelae evaluated with MR imaging. *Radiology 1991;*178:271-276.

12. Ahmad CS, Cohen ZA, Levine WN, Ateshian GA, Mow VC. Biomechanical and topographic considerations for autologous osteochondral grafting in the knee: *Am J Sports Med* 2001;29:201-206.

13. Ageberg E. Consequences of a ligament injury on neuromuscular function and relevance to rehabilitation – using the anterior cruciate ligament–injured knee as model: *J Electromyography Kinesiol* 2002;12:205-212.

14. Bahr R, Krosshaug T. Understanding injury mechaisms: A key component of preventing injuries in sport. *Brit J Sports Med* 2005;39:324-329.

15. Cameron M, Buchgraber A, Passler H, et al. The natural history of the anterior cruciate ligament-deficient knee: Changes in synovial fluid cytokine and keratan sulfate concentrations. *Am J Sports Med 1997;*25: 751-754.

16. Dye SF, Wojtys EM, Fu FH, Fithian DC, Gillquist I. Factors contributing to function of the knee joint after injury or reconstruction of the anterior cruciate ligament. *Instructional Course Lectures* 48:185-198, 1999.

17. Pinczewski LA, Deehan DJ, Salman LJ, Russell VJ, Clingeleffer A. A five-year comparison of patellar tendon versus four-strand hamstring tendon autograft for arthroscopic reconstruction of the anterior cruciate ligament. *Am J Sports Med 2002;*30:523-536.

18. Roos H. Joint Injury causes knee osteoarthritis in young adults. *Curr Opinion Rheumatol* 2005;17:195-200.

19. Koga H, Nakamae A, Shima Y, Iwasa J, Myklebust G, et al. Mechanisms for noncontact anterior cruciate ligament injuries: Knee joint kinematics in 10 injury situations from female team handball and basketball. *Am J Sports Med.* 2010;38:2218-2225.

20. Pflum MA, Shelburne KB, Torry MR, Decker MJ, Pandy MG. Model prediction of anterior cruciate ligament force during drop landings. *Med Sci Sports Exerc.* 2004;36:1949-1958.

21. Speer KP, Warren RF, Wickiewicz TL, Horowitz L, Henderson L. Observations on the injury mechanism of anterior cruciate ligament tears in skiers. *Am J Sports Med* 1995;23:77-81.

22. Arms SW, Pope MH, Johnson RJ, Fischer RA, Arvidsson I, Eriksson E. The biomechanics of anterior cruciate ligament rehabilitation and reconstruction. Am J Sports Med 1984;12(1):8-18.

23. Fleming BC, Renstrom PA, Beynnon BD, et al. The effect of weightbearing and external loading on anterior cruciate ligament strain. J Biomech 2001;34(2):163-170.

24. Markolf KL, O'Neill G, Jackson SR, McAllister DR. Effects of applied quadriceps and hamstrings muscle loads on forces in the anterior and posterior cruciate ligaments. Am J Sports Med 2004;32(5):1144-1149.

25. Olsen OE, Myklebust G, Engebretsen L, Bahr R. Injury mechanisms for anterior cruciate ligament injuries in team handball a systematic video analysis. Am J Sports Med 2004;32(4):1002-1012.

CHAPTER 2

EFFECT OF AXIAL TIBIAL TORQUE DIRECTION ON ACL RELATIVE STRAIN AND STRAIN RATE IN AN IN VITRO SIMULATED PIVOT LANDING

2.1 Abstract

Anterior cruciate ligament (ACL) injuries most frequently occur under the large loads associated with a unipedal jump landing involving a cutting or pivoting maneuver. We tested the hypotheses that internal tibial torque would increase the anteromedial (AM) bundle ACL relative strain and strain rate more than would the corresponding external tibial torque under the large impulsive loads associated with such landing maneuvers.

Twelve cadaveric female adult knees [mean (SD) age: 65.0 (10.5) years] were tested. Pretensioned quadriceps, hamstring and gastrocnemius muscle-tendon unit forces maintained an initial knee flexion angle of 15º. A compound impulsive test load (compression, flexion moment and internal or external tibial torque) was applied to the distal tibia while recording the 3-D knee loads and tibofemoral kinematics. AM-ACL relative strain was measured using a 3mm DVRT. In this repeated measures experiment, the Wilcoxon Signed-Rank test was used to test the null hypotheses with $p<0.05$ considered significant.

The mean (± SD) peak AM-ACL relative strains were 5.4±3.7 % and 3.1±2.8 % under internal and external tibial torque, respectively. The corresponding mean (± SD) peak AM-ACL strain rates reached 254.4±160.1 %/sec and 179.4±109.9 %/sec, respectively. The hypotheses were supported in that the normalized mean peak AM-ACL relative strain and strain rate were 70% and 42% greater under internal than external tibial torque, respectively ($p=0.023$, $p=0.041$).

We conclude that internal tibial axial torque is a potent stressor of the ACL because it induces a considerably (70%) larger peak strain in the AM-ACL than does a corresponding external tibial torque.

2.2 Introduction

An estimated 350,000 anterior cruciate ligament (ACL) injuries occur annually in the United States, 70 % of which are termed "non-contact".[1,2] Regardless of the treatment, an ACL rupture increases the risk of developing degenerative arthritis in that knee ten-fold compared to an age-matched uninjured population.[3-5] Non-contact ACL injuries frequently occur while landing unipedally from a jump or during a plant-and-cut or pivot maneuver.[6] A current knowledge gap concerns the unknown interaction between lower extremity configuration, external loading direction, and muscle recruitment patterns in causing an ACL rupture. Insights could lead to improved prevention programs.

Previous studies, performed quasi-statically *in vivo* and *in vitro,* suggest higher ACL strains occur under an internally-directed tibial torque than under an externally-directed tibial torque.[7-9] It is known that an internal tibial rotation increases a coupled

anterior tibial translation, thereby increasing ACL strain.[10] *Post hoc* video analyses suggested that ACL injury can occur under a forceful knee valgus loading and internal or external tibial rotation at or near a fully extended knee.[11-12] But the relative contribution of transverse plane tibial rotation to ACL injury remains unclear.[15] Despite some controversy[13-15] (see Discussion), ACL injury prevention programs have focused over the last decade on reducing valgus loading on the knee during jump landings.[16-19] This may be because an apparent valgus knee posture is often observed on injury video tapes of athletes who sustained an ACL injury. However, while *post hoc* injury video analyses can provide valuable information on the timing of gross body and limb postures and movements, they cannot provide the detailed kinematics of the tibia and femur, the direction of the net external load from the ground reaction force and/or moment that act(s) on the tibia, or the concomitant knee muscle forces acting on the knee to cause the ACL injury. Krosshaug et al. showed that the accuracy of a simple visual inspection of injury video is poor[20] and the injury video analysis can be improved by using their model-based image-matching techniques[21]. However, they also commented that their method predicted less accurate axial rotation of the thigh and shank compared to hip and knee flexion and abduction angles.[21] Hence, an investigation of the effect of axial tibial torque on ACL strain and strain rate during a realistic pivot landing seems warranted, particularly in the presence of direct measurements of the impulsive tibial compressive force, knee flexion moment, muscle forces and tibiofemoral joint kinematics.

The goal of the present study, therefore, was to investigate the effects of both internal and external tibial torque on AM-ACL relative strain and strain rate under large compound impulsive loads applied to an instrumented cadaveric knee. The first primary

hypothesis we tested was that peak AM-ACL relative strain should be larger under large internal than external tibial torque during a simulated pivot landing. We also tested the corresponding hypothesis involving strain rate instead of strain. This is because the viscoelastic nature of the ACL causes its resistance to stretch to depend on the strain rate[22], yet we are not aware of any data on the magnitude of the ACL strain rate during a pivot landing.

2.3 Methods

Specimen Procurement and Knee Testing Apparatus

Since a full description of the methods has been published elsewhere[23], only the most pertinent information will be given in what follows. Twelve fresh cadaveric limbs [mean (SD) age: 65.0 (10.5) years; eight female donors] were obtained from the University of Michigan Anatomical Donation Program. Prior to the procurement, assessment of any indication of surgery and severe deformities was performed. In order to standardize specimen length, the lower extremities were cut ~8 in (~20 cm) proximal and distal to the knee joint line. The specimens were then dissected with the ligamentous knee structures and the tendons of the quadriceps, medial and lateral hamstring, and medial and lateral gastrocnemius muscles left intact. The dissected specimens were kept frozen at –20°C until they were needed and were thawed at room temperature for at least twelve hours before testing commenced. During the testing, isotonic saline solution was regularly sprayed on the soft tissues to prevent drying.

Each knee specimen was mounted in a testing apparatus to simulate the position of a single extremity as it strikes the ground while landing onto one leg during a plant-

and-cut or pivot maneuver.[23-25] The quadriceps and medial and lateral gastrocnemius muscles were represented by elastic muscle-equivalent structures (~2 mm diameter woven nylon cord, tensile stiffness ~2 kN/cm) pre-tensioned to 180 N and 70 N each, respectively. Two custom-made constant force springs (pre-tensioned to 70 N each) were used to represent the medial and lateral hamstring muscle forces. In each case the muscle tendon was gripped by a cryoclamp to attach it to the muscle-equivalent along the anatomic line of action, thereby representing its *in vivo* dynamic resistance to sudden stretch. In all trials, an initial knee flexion angle of 15 degrees was maintained by the pretension in the muscle-equivalents. An impulsive jump landing ground reaction force was simulated by releasing a drop weight onto a custom instrumented fixture holding the distal tibia of the inverted knee so as to generate a 2*BW impulsive force peaking in ~50 msec, where BW denotes each donor's postmortem body-weight. In a new departure from the original Withrow et al. apparatus, a specially-designed adjustable torsional transformer device (Figure 2.1) was mounted in series with the distal tibial fixture so that the linear momentum of the drop-weight at impact was transformed into the combination of an axial compressive force and an impulsive axial torque component applied to the tibia. The torsional transformer device consists of two circular plates between which three palls are mounted equidistantly from one another and tangentially to an imaginary cylinder lying orthogonal to and within the two plates. The top circular plate can only translate vertically while the bottom plate can both translate vertically and rotate axially. The direction of the torque could be preselected by setting the inclination of each pall relative to the bottom plate.

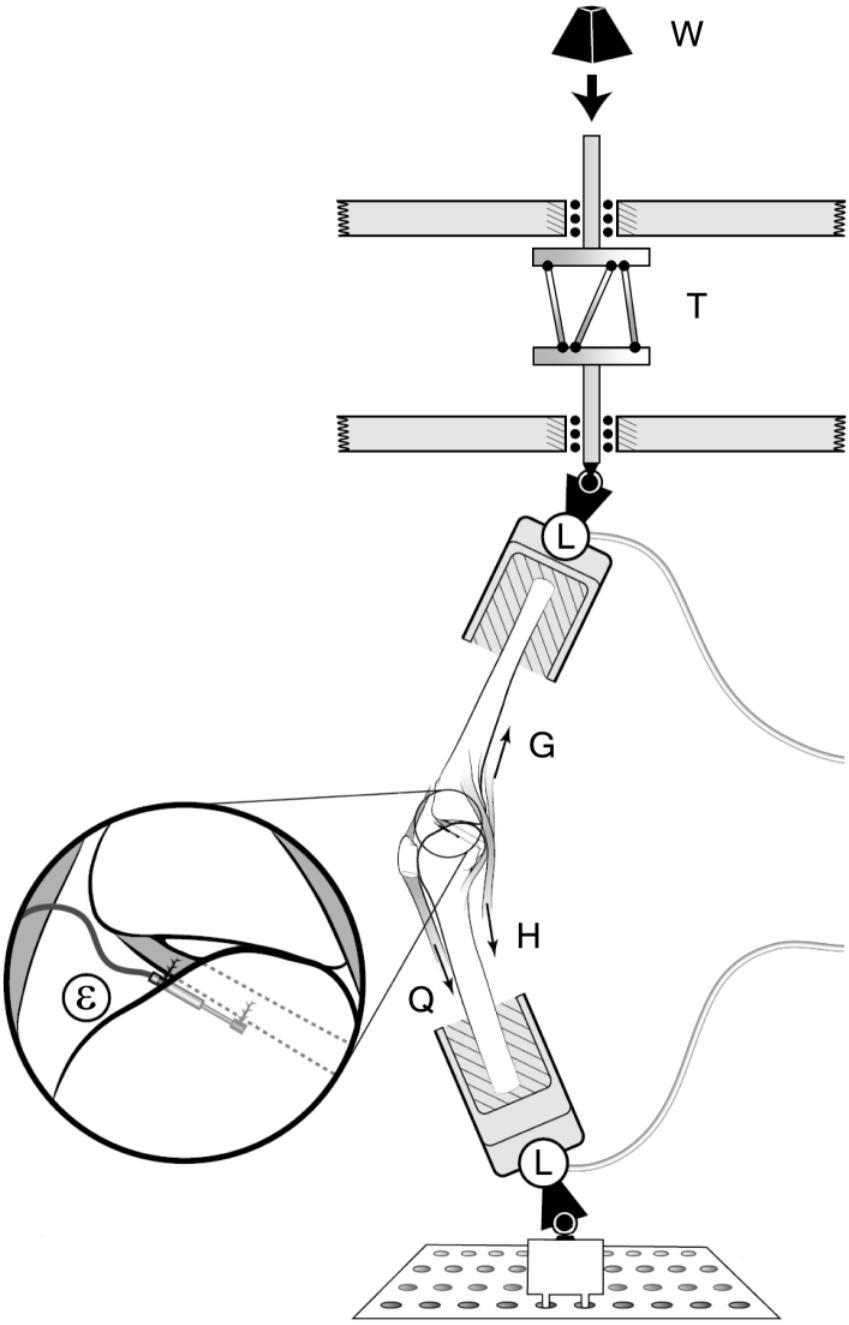

Figure 2.1 Schematic of testing apparatus. A weight (W) is dropped through a standard height onto an impact rod in series with a torsional device (T). Six--axis load cells (L) are located on distal tibia and proximal femur to measure knee input and output loads. Quadriceps (Q), hamstrings (H) and gastrocnemius (G) muscle forces are simulated. Inset shows the DVRT attached to the AM-ACL.

Two 6 degree-of-freedom load cells (MC3A-1000, AMTI, Watertown, MA) measured the 3-D tibial forces and moments delivered to the construct, as well as the 3-D femoral reaction forces and moments. A 3-mm DVRT (Microstrain, Burlington, VT) was mounted on the anteromedial (AM) bundle of the ACL to record relative strain. The anterior knee joint capsule was opened so as to identify the AM bundle and its fiber direction. The transducer was placed under direct vision parallel to the fiber direction at the first quartile of the AM-ACL length measured from the tibial insertion. The knee joint capsule was then closed prior to the testing. Five single degree-of-freedom load cells (TLL-1K, Transducer Techniques, Temecula, CA) measured simulated muscle tensions. Impulsive forces, the five muscle forces and ACL strain data were recorded at 2 kHz, while tibiofemoral kinematic data, defined in accordance with Grood and Suntay[26], were recorded at 400 Hz to the nearest degree and mm using bone screws, infrared diodes and an Optotrak Certus system (Northern Digital, Inc., Waterloo, Canada).

Testing Protocol (Table 2.1)

During the first five pre-conditioning trials, the height of the weight drop was varied to find the drop height that best simulated a two times body-weight (BW) impulsive ground reaction force for the baseline loading condition. That drop height was then maintained throughout all trials to apply the same kinetic energy to the knee specimens. After the five pre-baseline trials ('BASE1'), three blocks of six trials were run on each ACL-Intact specimen in a 'BASE1– B – C – BASE2' repeated measures design, where the blocks 'B' and 'C' were randomized to be either an internally-directed ('INT') or externally-directed ('EXT') tibial torque superposed on the standard baseline

compression force and flexion moment, followed by the post-baseline trial block ('BASE2').

The baseline loading conditions, 'BASE1' and 'BASE2', were designed to simulate a drop landing where the impulsive ground reaction force provides the compressive force on the knee joint and induces the knee flexion, thereby causing sudden stretch of the quadriceps muscle-tendon unit. This stretch of the quadriceps muscle-tendon unit resulted in anterior tibial displacement, thereby increasing the ACL strain via the patellofemoral mechanism.

Table 2.1 Repeated measures experiment protocol proceeded from trial block in top row to bottom row. Two blocks of experimental trials were interposed between the two baseline trial blocks.

Protocol	Loading direction
BASE1	Compression + Flexion moment
INT†	Compression + Flexion moment + Internal tibial torque
EXT†	Compression + Flexion moment + External tibial torque
BASE2	Compression + Flexion moment

† *The order of the experimental blocks was randomized (see text for detail).*

Statistical Analysis

The primary outcomes were AM-ACL relative strain and strain rate in the simulated pivot landing scenario. The peak AM-ACL relative strain for each loading trial was normalized by dividing by the mean peak AM-ACL relative strain obtained during the baseline loading conditions (i.e., 'BASE1' and 'BASE2'). This was done for the last five trials of each loading condition. Then, the five normalized peak AM-ACL relative

strain values were averaged to find a representative strain value for each loading condition. In this repeated measures experiment, a non-parametric Wilcoxon Signed-Rank test was used to test the two hypotheses. An alpha level of 0.05 was considered significant.

2.4 Results

Ten of the twelve knee specimens exhibited significantly greater peak AM-ACL relative strain under the impulsive internal tibial torque than under a similar magnitude of external tibial torque. No differences were found between two baseline loading conditions ('BASE1' and 'BASE2'), thereby confirming the knee specimens were not damaged during the testing. The increases in the AM-ACL relative strain and strain rate under the internal tibial torque were significantly different from the baseline (i.e., $p=0.005$ and $p=0.021$, respectively), while the corresponding values under the external tibial torque were not significantly different. The impulsive compressive force, input moments, and primary and secondary outcome measurements for each loading condition are summarized in Table 2.2. Sample temporal behavior from a single representative specimen and trials are shown in Figure 2.2.

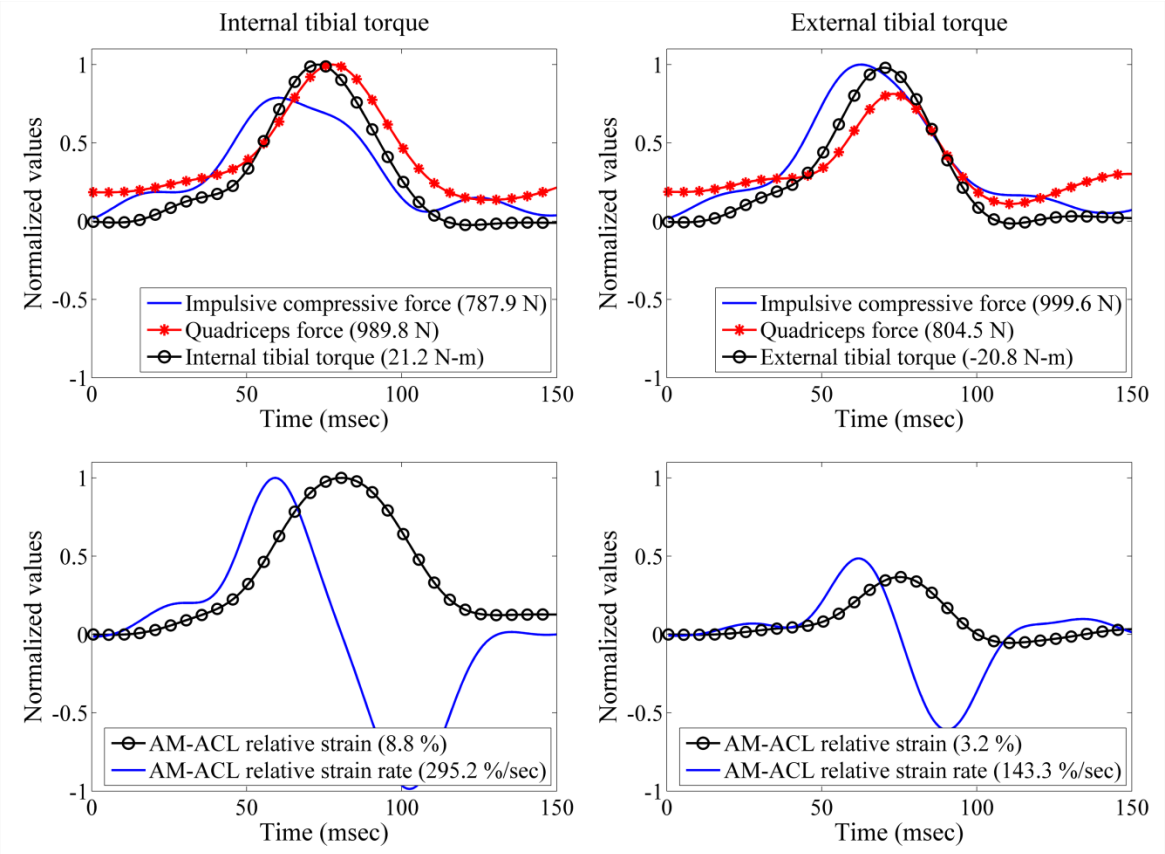

Figure 2.2 Sample temporal behaviors of the impulsive compressive force, quadriceps force, axial tibial torque, and AM-ACL relative strain and strain rate (Specimen ID: F32933R). Measurements are normalized to their maximum values to ease comparison and the pertinent peak values are shown in the legend.

Table 2.2 Mean (± SD) value for the input force and moment, as well as the primary and secondary outcome measurements by testing block (N=12 specimens)

		BASE1	Internal Tibial Torque	External Tibial Torque	BASE2
Input Force	Impulsive Compressive Force (N)	1,286.9 ± 203.4	852.4 ± 98.5	991.9 ± 123.0	1,256.5 ± 193.3
Input Moment	Axial Tibial Torque (N-m)[a]	-	17.3 ± 3.7	-18.0 ± 2.1	-
Primary Outcomes	AM-ACL Relative Strain (%)	3.0 ± 2.0	5.4 ± 3.7	3.1 ± 2.8	2.9 ± 1.7
	AM-ACL Strain Rate (%/sec)	184.2 ± 112.0	252.4 ± 160.1	179.4 ± 109.9	196.1 ±101.3
Secondary Outcomes	Quadriceps Force (N)	1,091.4 ± 305.5	1,093.5 ± 253.7	1,089.2 ± 349.8	1,181.3 ± 344.8
	Knee Flexion Angle (deg)	4.6 ± 1.4	4.8 ± 1.3	2.8 ± 1.3	4.5 ± 1.2
	Anterior Tibial Translation (mm)	1.3 ± 1.0	3.6 ± 2.6	0.8 ± 0.6	1.3 ± 1.0
	Axial Tibial Rotation (deg)[a]	1.8 ± 1.5	12.2 ± 3.1	-11.8 ± 3.7	1.7 ± 1.2

[a] Positive value represents internal tibial torque or rotation.

Effect of axial tibial torque direction on the peak AM-ACL relative strain

In testing the first primary hypothesis, across all 12 specimens, the normalized mean peak AM-ACL relative strain was significantly greater (70 % increase, p=0.023; Figure 2.3) under internal than external tibial torque. The internally-directed loading condition ('INT') caused the normalized mean peak AM-ACL relative strain to be 117 % greater than the baseline loading condition ('BASE1'), whereas the corresponding increase for the externally-directed loading condition ('EXT') was 30 % (Figure 2.3).

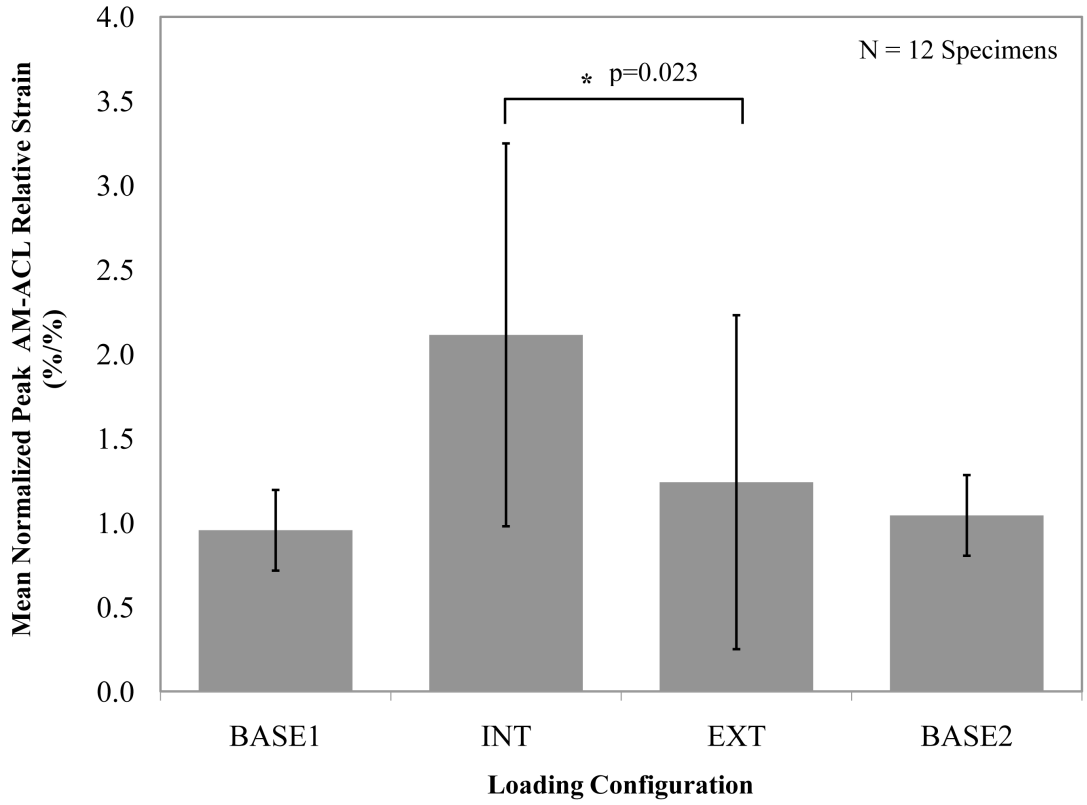

Figure 2.3 Mean (SD, represented by error bars) normalized peak AM-ACL relative *strain* values under each loading condition. In this and the following figure, the asterisk indicates a significant difference.

Effect of axial tibial torque direction on the peak AM-ACL relative strain rate

In testing the secondary hypothesis, the normalized mean peak AM-ACL relative strain rate was significantly greater (42 % increase, p=0.041; Figure 2.4) under internal than external tibial torque. The internally-directed loading condition ('INT') caused the normalized mean peak AM-ACL relative strain rate to increase 51 % when compared to the baseline loading condition ('BASE1'), whereas the corresponding increase for the externally-directed loading condition ('EXT') was 16 % (Figure 2.4).

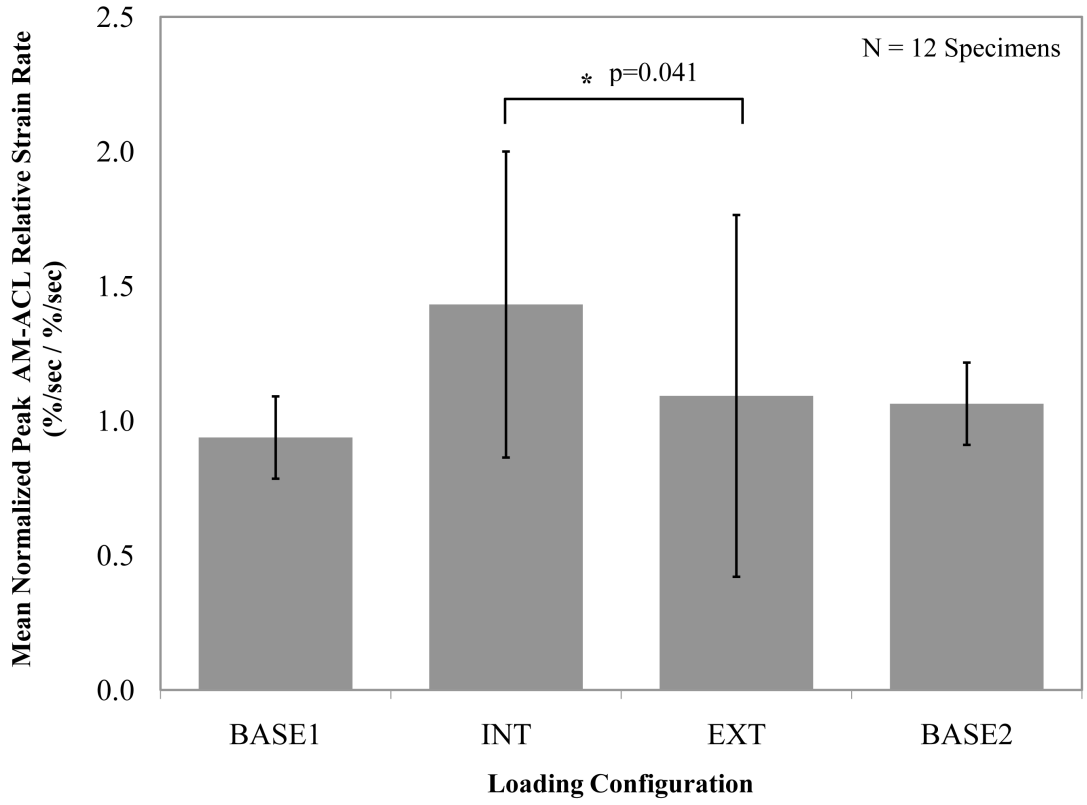

Figure 2.4 Effect of tibial torque direction on mean (SD, represented by error bars) normalized peak AM-ACL relative *strain rate* values across all specimens.

2.5 Discussion

The results demonstrate that the AM-ACL relative strain and strain rate increased significantly more under the internal than external tibial torque in the presence of the realistic impulsive compressive force, flexion moment and muscle forces.[27] Considering the fact that daily mobility task and sports maneuvers induce large dynamic loads on the knee[28], the present study provides useful insights into how the ACL is loaded when such loads include large axial tibial torques.

Our results corroborate and extend the earlier studies, which employed loads that were much less than one body-weight in magnitude and quasi-static in nature.[7-9] For example, Arms et al. found that a quasi-static 13.6 N-m internal tibial torque combined with a simulated quadriceps contraction (~400 N) caused higher ACL strain than a corresponding external tibial torque.[7] Similarly an *in vivo* study performed by Fleming et al. found that the ACL strain was higher when the knee was placed under a 10 N-m internal tibial torque than under a 10 N-m external tibial torque.[8] Furthermore, Markolf et al. measured the ACL tension under a constant 5 N-m of internal or external tibial torque with and without a constant 100 N quadriceps force.[9] They found that the ACL forces were significantly higher under the internal tibial torque than the external tibial torque near full extension. Recently, Meyer et al. showed that the ACL failure occured at about 58 degrees of internal tibial rotation under an average of 33 N-m internal tibial torque.[29] They obtained quite large internal tibial rotations, which might not be observed in actual isolated ACL injury incidents. The large internal tibial rotation likely occurred because they did not incorporate the muscle forces. The qualitative findings, however, are consistent with our findings. Under more physiological loading conditions, the present results unequivocally demonstrate that the ACL relative strain is significantly larger

under simulated landing conditions involving an internal tibial torque than an external tibial torque.

It is interesting that *post hoc* injury video analyses have suggested that the ACL injury can occur under both internal and external tibial rotation, often combined with knee valgus loading. For example, Olsen et al. analyzed 20 videotaped ACL handball injuries and found that two-thirds (12 of 19) of the injuries occurred in apparent external tibial rotation during a plant-and-cut, one-leg landing, and/or deceleration maneuver with the knee near full extension; the remainder were injured in a movement that appeared to generate a torque producing internal tibial rotation.[11] On the other hand, Meyer et al. showed that the external tibial rotation occurred after the ACL failure was caused by the internal tibial torque, thereby suggesting that the observed external tibial rotation in *post hoc* injury video analyses might occur after the ACL was torn.[29] Our results showed that ten of twelve knee specimens exhibited significantly greater ACL relative strain under the internal tibial torque than the similar magnitude of the external tibial torque. One of the remaining two knee specimens in which the peak ACL relative strains were larger under the external tibial torque than the internal tibial torque exhibited the smallest notch height of any knee on frontal plane x-ray images. Thus it is possible that the notch interfered with the DVRT causing an artifact. It is known that ACL impingement can occur under external tibial rotation and knee abduction[30] and a narrow femoral notch width is one risk factor for non-contact ACL injury[31]. In the case of the other knee, there was no obvious morphological difference from the other knees on radiographs or by visual inspection, so we are at a loss to explain why its ACL strain was greater under the external tibial torque. We can speculate that it might have been caused by a lateral movement of the patella,

causing it to apply a greater posteriorly-directed force to the lateral condyle than the medial condyle.

A valgus posture has previously been identified as a primary ACL injury mechanism.[17] Thus, many ACL injury prevention programs have focused on minimizing valgus loading to the knee during jump landings.[16-19] However, the valgus loading mechanism remains controversial because the concomitant medial collateral ligament (MCL) injury, which would be seen with most non-contact ACL ruptures, occurs infrequently.[13] In the review paper by Quatman et al., the authors explain the relative lack of concomitant MCL injuries (i.e., only 4-27% of all ACL injuries) as being due to the failure load of MCL being greater than the corresponding value of ACL (i.e., 2,300 N vs. 640-2,100 N).[13] However, it appears that the difference is not really large enough to explain the relative lack of MCL injuries. Additionally, the lateral compartment bone bruise patterns suggest that either a knee abduction or anterolateral tibial subluxation resulting from internal tibial rotation may be involved under large axial compressive joint loading.[33-35] Unfortunately, it remains unclear which of these is the most crucial loading pattern during ACL injury. Previously, Withrow et al. investigated the effect of valgus loading on the peak AM-ACL relative strain: the normalized peak AM-ACL relative strain was 30% larger in the dynamic valgus loading (i.e., 132.5 ± 29.0 N-m) compared to the sagittally-symmetric baseline loading condition where an impulsive compressive force exceeding two body-weights (~1,500 N) and flexion moment were applied.[26] Using a similar, but improved, testing apparatus to that used by Withrow et al.[26], the present study found that the peak AM-ACL relative strain was 117% greater under the internal tibial torque (i.e., 17.3 ± 3.7 N-m) than the baseline loading condition. This indirect

comparison implies that the internal tibial rotation plays a more important role in increasing the ACL strain than knee valgus loading. This would seem to be a role that cannot be assessed by injury videotape analyses.

As discussed in our recent article[24], our *in vitro* methods include several limitations. The first limitation is that only one initial knee flexion angle (15º) was tested. However, the knee flexion angle at injury is estimated to be 16º in injury video analysis and Li et al. reported the ACL strain to be highest with the knee in 15º of flexion.[11,36] Thus, the initial 15º knee flexion angle used in this study seems reasonable. Second, the ACL strain was measured only in anteromedial (AM) region. The AM-ACL strain may not reflect the strain within the posterolateral (PL) region of the ACL. However, according to the results reported by Gabriel et al., the in situ force in the AM bundle was greater than the corresponding value in the PL bundle in response to a rotatory load (i.e., 10 N-m valgus and 5 N-m internal tibial torque) at 15º of knee flexion angle.[37] Moreover, at 30º of knee flexion angle, the *in situ* force in the AM bundle increased in response to the same rotatory load, while the in situ force in the PL bundle decreased. A similar load sharing pattern was observed in response to a 134 N anterior tibial force for both the knee flexion angles. Thus, measuring the AM-ACL strain under axial tibial torque seems reasonable. The third limitation is that we tested knee specimens from older donors, so our results cannot necessarily be generalized to younger populations. Strocchi et al. reported that in adults and elderly subjects, the maximum diameter of the ACL collagen fibril is significantly decreased compared to younger (<20 years) subjects.[38] The decreased diameter may or may not reduce elastic ACL stiffness. However, this does not necessarily mean that the ACL strain characteristics would be qualitatively different.

Although knee specimens from young donors might show smaller ACL strain values for each loading condition, we expect that the general trend of the normalized AM-ACL strain and strain rate should be maintained.

This study clearly suggests that pivot landing or plant-and-cut maneuvers that apply large impulsive internal tibial torques to the knee are risky from the point-of view of causing excessive AM-ACL strain. It has been shown that a higher coefficient of friction between the shoe-ground interfaces is associated with a greater axial tibial torque transmitted to the knee joint, thereby leading a greater risk of ACL injury.[39] Taken together with existing literature, the present study suggests the necessity for limiting the maximum axial torque that can be applied to a tibia perhaps by changing regulations to limit the maximum frictional torque that can be developed between a shoe sole and a playing surface.

2.6 Conclusions

We conclude that internal tibial axial torque is a potent stressor of the ACL because it induces a considerably (70%) larger peak strain in the AM-ACL than does a corresponding external tibial torque.

2.7 References

1. Allografts in Sports Medicine: What Do We Know, Need to Know, and Need to Do? Round table discussion: *American Orthopaedic Society for Sports Medicine*; February 13, 2006; Park City, UT.

2. McNair PJ, Marshall RN, Matheson JA. Important features associated with acute anterior cruciate ligament injury. *N Z Med J* 1990;103:537-539.

3. Gillquist J, Messner K. Anterior cruciate ligament reconstruction and the long-term incidence of gonarthrosis. *Sports Med*. 1999;27:143-156.

4. Myklebust G, Holm I, Maehlum S, Engebretsen L, Bahr R. Clinical, functional, and radiologic outcome in team handball players 6 to 11 years after anterior cruciate ligament injury. *Am J Sports Med*. 2003;31:981-989.

5. Lohmander, LS, Englund PM, Dahl LL, Roos EM. The long-term consequence of anterior cruciate ligament and meniscus injuries - Osteoarthritis. *Am J Sports Med.* 2007;35:1756-1769.

6. Kirkendall DT, Garrett WE. The anterior cruciate enigma: Injury mechanisms and prevention. *Clin Orthop Rel Res*. 2000;372:64-68.

7. Arms SW, Pope MH, Johnson RJ, Fischer RA, Arvidsson I, Eriksson E. The biomechanics of anterior cruciate ligament rehabilitation and reconstruction. *Am J Sports Med*. 1984;12(1):8-18.

8. Fleming BC, Renstrom PA, Beynnon BD, et al. The effect of weightbearing and external loading on anterior cruciate ligament strain. *J Biomech*. 2001;34(2):163-170.

9. Markolf KL, O'Neill G, Jackson SR, McAllister DR. Effects of applied quadriceps and hamstrings muscle loads on forces in the anterior and posterior cruciate ligaments. *Am J Sports Med*. 2004;32(5):1144-1149.

10. Kanamori A, Woo SL, Ma CB, Zeminski J, Rudy TW, Li G, Livesay GA. The forces in the anterior cruciate ligament and knee kinematics during a simulated pivot shift test: a human cadaveric study using robotic technology. *Arthroscopy*. 2000;16:633-9

11. Olsen OE, Myklebust G, Engebretsen L, Bahr R. Injury mechanisms for anterior cruciate ligament injuries in team handball a systematic video analysis. *Am J Sports Med.* 2004;32(4):1002-1012.

12. Teitz CC. Video analysis of ACL injuries. In: Griffin LY, ed. Prevention of noncontact ACL injuries. Rosemont, IL: American Association of Orthopaedic Surgeons, 2001: 87–92.

13. Quatman CE, Quatman-Yates CC, Hewett TE. A 'plane' explanation of anterior cruciate ligament injury mechanisms - A systematic review. *Sports Medicine*. 2010:40(9);729-746.

14. Markolf KL, Burchfield DM, Shapiro MM, Shepard MF, Finerman GA, Slauterbeck JL. Combined knee loading states that generate high anterior cruciate ligament forces. *J Orthop Res*. 1995;13:930-935.

15. Boden BP, Torg JS, Knowles SB, Hewett TE. Video analysis of anterior cruciate ligament injury: abnormalities in hip and ankle kinematics. *Am J Sports Med*. 2009;37:252-259.

16. Hewett TE, Lindenfeld TN, Riccobene JV, Noyes FR. The effect of neuromuscular training on the incidence of knee injury in female athletes - A prospective study. *Am J Sports Med*. 1999;27:699-706.

17. Hewett TE, Myer GD, Ford KR, et al. Biomechanical measures of neuromuscular control and valgus loading of the knee predict ACL injury risk in female athletes: A prospective study. *Am J Sports Med*. 2005;33:492-501.

18. Lloyd DG. Rationale for training programs to reduce anterior cruciate ligament injuries in Australian football. *J Orthop Sports Phys Ther*. 2001;31:645-654.

19. Myer GD, Ford KR, Hewett TE. Rationale and clinical techniques for anterior cruciate ligament injury prevention among female athletes. *J Athl Training*. 2004;39:352-364.

20. Krosshaug T, Nakamae A, Boden B, Engebretsen L, et al. Estimating 3D joint kinematics from video sequences of running and cutting maneuvers--assessing the accuracy of simple visual inspection. *Gait Posture*. 2007;26(3):378-85.

21. Krosshaug T, Slauterbeck JR, Engebretsen L, Bahr R. Biomechanical analysis of anterior cruciate ligament injury mechanisms: three-dimensional motion reconstruction from video sequences. *Scand J Med Sci Sports*. 2007;17(5):508-19.

22. Grood ES, Noyes FR. Cruciate ligament prosthesis – strength, creep, and fatigue properties. *J Bone Joint Surg AM*. 1976;58(8):1083-1088.

23. Oh YK, Kreinbrink JL, Ashton-Miller JA, Wojtys EM. Effect of ACL transaction on internal tibial rotation in an in vitro simulated pivot landing. *J Bone Joint Surg AM.* 2011;93(4):372-80.

24. Withrow TJ, Huston LJ, Wojtys EM, Ashton-Miller JA. The relationship between quadriceps muscle force, knee flexion, and anterior cruciate ligament strain in an in vitro simulated jump landing. *Am J Sports Med*. 2006;34(2):269-74.

25. Withrow TJ, Huston LJ, Wojtys EM, Ashton-Miller JA. The effect of an impulsive knee valgus moment on in vitro relative ACL strain during a simulated jump landing. *Clin Biomech*. 2006;21(9):977-83.

26. Grood ES, Suntay WJ. A joint coordinate system for the clinical description of three-dimensional motions: application to the knee. *J Biomech Eng*. 1983;105:136-44.

27. Pflum MA, Shelburne KB, Torry MR, Decker MJ, Pandy MG. Model prediction of anterior cruciate ligament force during drop-landings. *Med Sci Sports Exerc*. 2004;36:1949-58.

28. Besier TF, Lloyd DG, Ackland TR, Cochrane JL. Anticipatory effects on knee joint loading during running and cutting maneuvers. *Med Sci Sports Exerc*. 2001;33:1176-81.

29. Meyer EG, Haut RC. Anterior cruciate ligament injury induced by internal tibial torsion or tibiofemoral compression. *J Biomech*. 2008;41(16):3377-83.

30. Fung DT, Zhang LQ. Modeling of ACL impingement against the intercondylar notch. *Clin Biomech*. 2003;18(10):933-941.

31. Uhorchak JM, Scoville CR, Williams GN, Arciero RA, St Pierre P, Taylor DC. Risk factors associated with noncontact injury of the anterior cruciate ligament: A prospective four-year evaluation of 859 west point cadets. *Am J Sports Med*. 2003;31(6):831-842.

32. Graf BK, Cook DA, Desmet AA, et al. Bone bruises on magnetic-resonance-imaging evaluation of anterior cruciate ligament injuries. *Am J Sports Med*. 1993;21(2):220-223.

33. Johnson DL, Urban WP, Caborn DNM, Vanarthos WJ, Carlson CS. Articular cartilage changes seen with magnetic resonance imaging-detected bone bruises associated with acute anterior cruciate ligament rupture. *Am J Sports Med*. 1998;26:409-414.

34. Spindler KP, Schils JP, Bergfeld JA, et al. Prospective study of osseous, articular, and meniscal lesions in recent anterior cruciate ligament tears by magnetic resonance imaging and arthroscopy. *Am J Sports Med*. 1993;21:551-557.

35. Li G, Rudy TW, Sakane M, Kanamori A, et al. The importance of quadriceps and hamstring muscle loading on knee kinematics and in-situ forces in the ACL. *J Biomech.* 1999;32:395-400.

36. Gabriel MT, Wong EK, Woo SLY, et al. Distribution of in situ forces in the anterior cruciate ligament in response to rotatory loads. *J Orthop Res*. 2004;22(1):85-89.

37. Strocchi R, De Pasquale V, Facchini A, et al. Age-related changes in human anterior cruciate ligament (ACL) collagen fibrils. *Ital J Anat Embryol*. 1996;101(4):213-20.

38. Drakos MC, Hillstrom H, et al. The Effect of the Shoe-Surface Interface in the Development of Anterior Cruciate Ligament Strain. *J Biomech Eng-T Asme*. 2010;132(1): 011003.

CHAPTER 3

THE EFFECT OF AXIAL TIBIAL ROTATION AND VARUS OR VALGUS LOADING ON ACL STRAIN DURING A SIMULATED JUMP LANDING

3.1 Abstract

The relative contributions of an axial tibial torque and frontal plane moment to ACL strain during jump landings are unknown. We tested the hypothesis that the peak normalized relative strain in the anteromedial bundle (AM) of the ACL is affected by the direction of the axial tibial torque, but not by the direction of the frontal plane moment applied concurrently during a simulated jump landing.

Fifteen adult male knees with pretensioned knee muscle-tendon unit forces were loaded under a simulated pivot landing test. Compression, a flexion moment, internal or external tibial torque, and knee ab- or adduction moment were simultaneously applied to the distal tibia while recording the 3-D knee loads and tibiofemoral kinematics. AM-ACL relative strain was measured using a 3 mm DVRT. These results were compared to corresponding sagittal loading tests involving compression and flexion moment. The results were analyzed using non-parametric Wilcoxon Signed-Rank tests. A dynamic biomechanical knee model was used to interpret the results.

The mean [SD] peak AM-ACL relative strain was 192% greater ($p<0.001$) under the internal tibial torque combined with a knee ab- or adduction moment (7.0 [4.1]% and 7.0 [3.9]%, respectively), than under external tibial torque and the same moments (2.4 [3.2]% and 2.4 [2.5]%, respectively). A pure abduction moment increased AM-ACL strain via coupled internal tibial rotation.

The worst-case dynamic knee loading as far as ACL strain is concerned is internal tibial torque combined with a knee abduction moment. However, it is an internal tibial torque, rather than a knee abduction moment, that primarily causes large ACL strains during a jump landing. In addition, when the lateral tibial slope exceeds that of the medial tibial plateau, then an abduction moment causes coupled internal tibial rotation, and vice versa. Due to this coupling phenomenon, a knee abduction moment can increase ACL strain, even without medial knee joint opening.

3.2 Introduction

Over 350,000 anterior cruciate ligament (ACL) injuries occur each year in the United States.[14] Eighty percent of patients who sustain an ACL tear exhibit a concomitant impaction injury to the articular cartilage and greater than 50 % will have meniscal tears.[2,4,9,46,48] ACL ruptures increase the risk for developing degenerative joint disease over time.[25] Clearly, better insights into ACL injury mechanisms might improve current ACL injury prevention programs.

Over the past decade many ACL injury prevention programs have focused on reducing valgus loading to the knee during jump landings.[17,18,24,34] This is primarily

because the knee often appears to pass through a valgus posture on video tapes of athletes who are landing and/or pivoting as they sustain an ACL injury (for example, Figure 1.D in Olsen et al. 2004).[36] A valgus posture can result from knee abduction with or without femoral internal rotation and/or adduction. While injury videotapes are valuable, they provide limited information on the forces and moments that caused injury[19] due to the absence of force plates to accurately measure ground reaction forces, kinematic markers to measure segmental motions, and measures of knee muscle activity which largely determines the loading on the ACL[39]. In fact, we do not yet know which combination of 3-D knee forces and moments load the ACL most heavily during a jump landing.

If it were the abduction moment at the knee that typically causes the non-contact ACL injury, then concomitant medial collateral ligament (MCL) injury would be seen with most non-contact ACL tears. However, this occurs infrequently. Additionally, ACL injury usually involves lateral compartment bone bruises[13,46,21] suggesting large knee abduction moments, anterior tibial subluxation or internal tibial torque may be involved under high compressive joint force loading. Unfortunately, it is not known which of these is the most common form of loading during ACL injury. Internal tibial torque and anterior tibial translation are known to cause increases in ACL force during *in vitro* tests involving modest loads of a 100 N of anterior tibial force combined with a 10 N-m of internal tibial torque.[28] Internal torque was found to increase ACL tension more than external tibial torque.[1,11,29,35] Furthermore, when internal axial tibial torque was combined with a knee abduction moment a larger ACL tension was observed than when external tibial torque was combined with a knee abduction moment.[22,28] A limitation of these studies was that no trans-knee muscle forces were used in these quasi-static tests.

The effect of combining varus loading with internal or external tibial torque on ACL tension is not yet known. Fleming et al. applied ±15 N-m knee ab- and adduction moments in weight bearing and non-weight bearing conditions and found no effect on the strain of the anteromedial bundle in the ACL (AM-ACL).[11] On the other hand, Withrow et al. found a 30% increase in AM-ACL strain under a knee abduction moment during a simulated jump landing that applied joint compression and flexion in the presence of muscle forces.[51] Similarly, Shin et al. found a 40% increase in ACL strain using a validated computer simulation.[43] So, these studies suggest that internal tibial torques increase ACL strain more than external tibial torque or abduction moments.

We tested the primary hypothesis that the normalized peak AM-ACL relative strain would be affected by the direction of the axial tibial torque, but not by the direction of the frontal plane moment when applied concurrently. Insights could guide future interventions aimed at reducing the risk for ACL injury in both children and adults. In this paper we shall develop, validate, and then use a simple biomechanical model of the knee to make predictions of the factors causing ACL strain and use it to help interpret our experimental results.

3.3 Methods

Specimen Procurement and Preparation

Fifteen unembalmed cadaveric limbs [mean (SD) age: 70.4 (2.9) years; mean (SD) body-weight: 839.4 (113.0) Newtons; 9 males] were acquired from the University of Michigan Anatomical Donations Program. All lower extremities were visually checked for scars, indication of surgery, malalignments or deformities. Following the

methods of Withrow et al.[50-51] lower extremities were cut 8 inches proximal and distal to the knee joint in order to standardize specimen length. Specimens were then dissected, leaving the ligamentous knee structures and the tendons of quadriceps, medial hamstrings, lateral hamstring and medial and lateral gastrocnemius muscles intact. Each end of the specimen was potted using polymethylmethacrylate.

Knee Testing Apparatus

The Withrow et al.[50-51] testing apparatus was used to simulate the position of a single extremity as it strikes the ground while landing on one leg during a jump or pivot maneuver. The simulated quadriceps muscle was represented by elastic structures pre-tensioned to 180 N. The same elastic structures were used to represent the medial and lateral hamstring and gastrocnemius muscles, initially pretensioned to 70 N each. Each simulated muscle-tendon unit was connected from the femur or tibia to the relevant tendons via cryo-clamps through the anatomical lines-of-action, thereby representing it's *in vivo* dynamic resistance to sudden stretch. In all trials, the initial knee flexion angle was 15 degrees. A jump landing ground reaction force was simulated by dropping a weight onto the distal tibia of an inverted knee generating a 2*BW (BW is each donor's postmortem body-weight) impulsive force. The weight drop was initiated in a standardized manner via a quick-release mechanism mimicking impulsive ground reaction forces typically seen in a jump landing.[5,31,33,47] The linear momentum of the weight at impact was transformed into the combination of an axial compressive force and an impulsive axial torque component (peaking at 70 ms) by a specially-designed torsional

transformer device mounted in series with the distal tibia (Figure 3.1. 'T'). The device consisted of two circular plates between three inclined palls. The angle of the palls to the vertical was adjustable and preset to give the desired gain between the applied compressive force and the rotational torque delivered to the specimen. The peak axial torque was adjusted to reach a nominal value between 20 and 30 N-m. For the "baseline" loading condition, the specimen was oriented such that the impulsive compressive force initially acted 3 cm posterior to the knee in the sagittal plane. For "varus" or "valgus" loading the knee was initially adducted or abducted with the impulsive compressive force inclined at 7 degrees medial or lateral to the sagittal plane, respectively.

Two 6 degree-of-freedom load cells (AMTI, Watertown, MA) measured the 3-D tibial forces and moments delivered to the knee construct, as well as the 3-D femoral reaction forces and moments. A 3-mm differential variable reluctance transducer (DVRT, Microstrain, Burlington, VT) was mounted on the anteromedial (AM) bundle of the ACL to record ACL relative strain. The DVRT was placed on the AM-ACL at a first quartile of the ACL length measured from the tibial attachment site.

Five single degree-of-freedom load cells (Transducer Techniques, Temecula, CA) measured simulated muscle tensions. The impulsive forces and moments, five simulated muscle-tendon unit forces and AM-ACL relative strain data were recorded at 2 kHz using a 16-bit analog-to-digital converter board. Tibiofemoral kinematics[15] were recorded at 400 Hz using an Optotrak Certus system (Northern Digital, Inc., Waterloo, Canada).

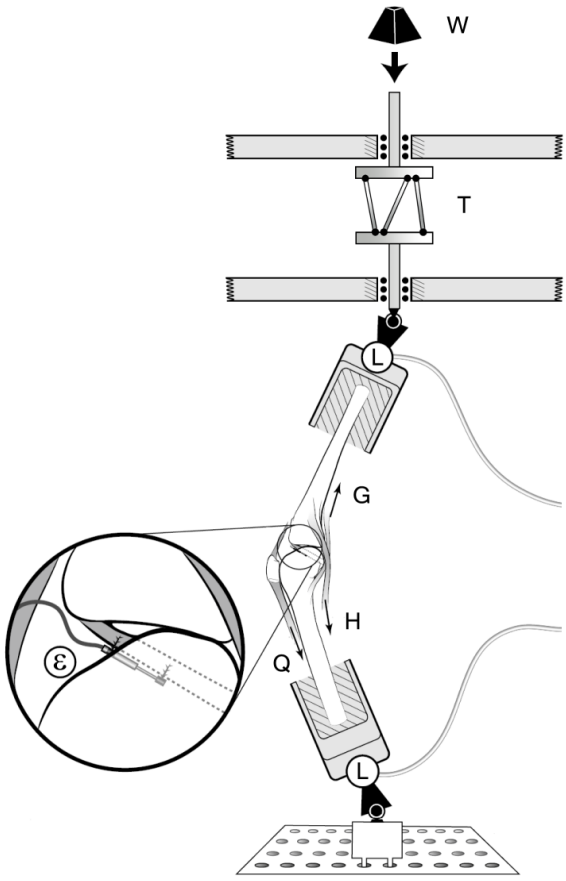

Figure 3.1 Schematic diagram of the test apparatus showing how a weight ('W') dropped from a fixed height onto the torsional transformer device ('T') applies impulsive compression and axial torque to the distal tibia of an inverted knee specimen. The frontal plane moment was applied by initially abducting or adducting the knee specimen. The two load-cells ('L') measure the three components of force and moment applied to the knee specimen in the presence of quadriceps ('Q'), hamstrings ('H') and 'gastrocnemius ('G') forces, while a miniature displacement transducer ('ε') implanted on the surface of the anteromedial bundle of the ACL measures relative strain.

Testing Protocol

Forty trials were completed for each specimen (Table 3.1). During the first five preconditioning trials, the height of the weight drop was varied to find the drop height such that best simulated a 2*BW impulsive ground reaction force for the baseline loading condition ('BASE1', 'BASE2'). That drop height was then maintained throughout all

trials to apply the same kinetic energy to the knee specimens. After the preconditioning trials, six blocks were run on each specimen in a 'BASE1 – A – B – C – D – BASE2' repeated measures design. The first experimental block ('A') was randomized to be either knee abduction or adduction moment combined with either internal or external tibial torque. Then the direction of the frontal plane moment was reversed for the blocks 'B' and 'D', while the direction of the axial tibial torque was reversed for the blocks 'C' and 'D'.

AM-ACL Relative Strain

The initial length of the DVRT was defined as the length of the DVRT in the initial 15º pre-impact static posture under the simulated muscle forces (since it is problematic to find the unloaded zero strain state[10]). The change in DVRT length from this initial length, divided by the initial length, was used to calculate the "relative" strain in the anteromedial (AM) region of the ACL under the impulsive loading.

Statistical Analysis

The peak AM-ACL relative strain for each loading trial was normalized by dividing by the mean peak AM-ACL relative strain in the baseline loading conditions (i.e., 'BASE1' and 'BASE2'). This was done for the last five trials of each testing block. Then, the five normalized peak AM-ACL relative strain values were averaged to find a representative strain value for each loading condition. A non-parametric Wilcoxon Signed-Rank test was used to test the hypothesis. An alpha level of 0.05 was chose for the level of significance.

Table 3.1 Repeated measures experiment protocol proceeded from trial block in top row to bottom row. Four blocks of experimental trials were interposed between the two baseline trial blocks. The order of presentation of the experimental blocks (marked by an asterisk) was randomized (see text for detail).

Protocol	Loading direction	Trials
BASE1	Compression + Flexion moment	5
Internal Tibial Torque + Knee Adduction Moment*	Compression + Flexion moment + Internal tibial torque + Adduction moment	6
Internal Tibial Torque + Knee Abduction Moment*	Compression + Flexion moment + Internal tibial torque + Abduction moment	6
External Tibial Torque + Knee Abduction Moment*	Compression + Flexion moment + External tibial torque + Abduction	6
External Tibial Torque + Knee Adduction Moment*	Compression + Flexion moment + External tibial torque + Adduction	6
BASE2	Compression + Flexion moment	6

3D Dynamic Knee Model

A three-dimensional lower-limb model was constructed to replicate the experimental set-up and to further investigate how the frontal plane moments and axial tibial torques interact to affect the ACL strain under a simulated landing. The segmented femur, tibia, fibula, and patella were obtained from the Visible Human male data set[49] and imported into dynamic simulation software (MD Adams R3, MSC.Software, Inc., Santa Ana, CA). In order to investigate how the medial and lateral posterior tibial slopes affected the interaction between the axial tibial torque and frontal plane moment, the medial and lateral tibial plateaus were modeled with the posterior slope being 5.5 degrees and 8.5 degrees,[30] respectively. The contact forces between the femur and medial and lateral tibial plateau were monitored to detect the medial or lateral joint space opening.

Visco-elastic behavior of the 10 ligaments, 4 anterior and 4 posterior knee joint capsule structures were modeled using Kelvin-Voigt elements consisting of a bi-linear elastic spring[42,43] and a viscous damper in parallel (See Figure 3.2). As described in Shin et al.'s work [42], the force for each ligament or capsular fiber was defined as follows:

$$F(\varepsilon) = \begin{cases} 0 & , \quad \varepsilon < 0 \\ \frac{k}{2}\varepsilon L_O & , \quad 0 \leq \varepsilon < 2\varepsilon_1 \\ k(\varepsilon - \varepsilon_1)L_O, & \quad \varepsilon \geq 2\varepsilon_1 \end{cases}$$

, where L_O is the predefined slack length of each ligament or fiber; ε is the ligament strain defined as $\varepsilon = (L - L_O)/L_O$; the toe region for each ligament or fiber is specified until the strain value reaches $\varepsilon_1 = 0.03$; and k is the stiffness coefficient for each ligament or fiber obtained from previous studies (Table 3.2).

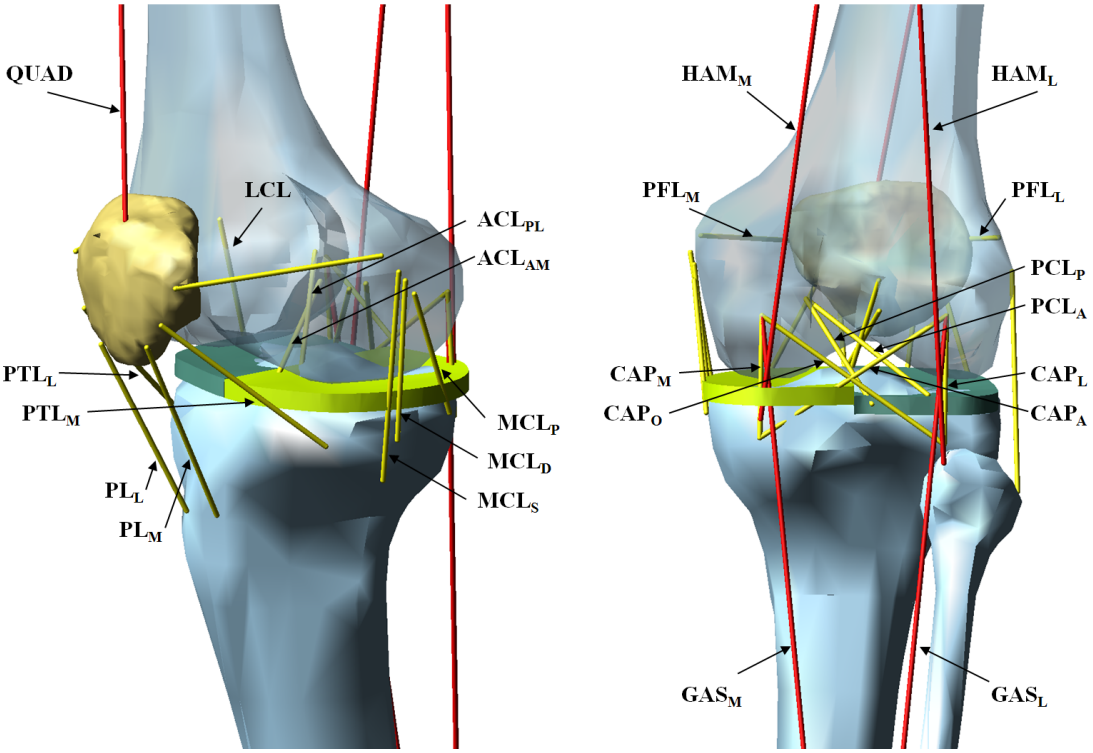

Figure 3.2 Schematic of the knee model showing muscles and ligaments: quadriceps, medial and lateral hamstrings, and medial and lateral gastrocnemius muscles (QUAD, HAM_M, HAM_L, GAS_M, and GAS_L); the anteromedial and posterolateral bundle of ACL (ACL_{AM} and ACL_{PL}); the anterior and posterior bundle of PCL (PCL_A and PCL_P); the lateral collateral ligament and the superficial, deep, and posterior medial collateral ligament (LCL, MCL_S, MCL_D, and MCL_P); the medial and lateral patellofemoral ligament and the medial and lateral patellotibial ligament for the anterior knee capsule (PFL_M, PFL_L, PTL_M, and PTL_L); the medial, lateral, oblique popliteal, and arcuate popliteal fiber for the posterior knee capsule (CAP_M, CAP_L, CAP_O, and CAP_A); and the medial and lateral patellar ligament (PL_M and PL_L).

In order to replicate the initial condition, the quadriceps, medial and lateral hamstrings and gastrocnemius muscles in the simulation model were modeled and pretensioned to the corresponding values, respectively. Then, the 2*BW impulsive compressive force measured from the experiment was imported as the input to drive the knee model with the knee flexion angle being the same as in the experimental set-up. To

validate the model, the quadriceps muscle forces, knee flexion angle, and AM-ACL relative strain values obtained from the simulation model were quantitatively compared to the corresponding values from the experiment by evaluating Pearson correlation coefficients from the time when the impact was initiated and 80 msec. After the validation test, parametric studies were performed to investigate how the axial tibial torques and frontal plane moments would interact to affect the AM-ACL, medial and lateral collateral ligament (i.e., MCL and LCL) strain, and internal-external tibial rotation and knee abduction-adduction angle, thereby identifying the most detrimental loading scenario (Table 3.3).

Table 3.2 Material properties of ligaments.[32,40,42]

Ligament/Fiber	Stiffness (N/mm)	Slack length (mm)
ACL_{AM}	108.0	34.4
ACL_{PL}	108.0	31.7
PCL_{A}	125.0	45.3
PCL_{P}	60.0	35.7
LCL	91.3	56.0
PFL_{M}	48.5	42.0
PFL_{L}	48.5	53.0
PTL_{M}	77.5	50.0
PTL_{L}	77.5	44.5
PL_{M}	300.0	52.5
PL_{L}	300.0	48.7
MCL_{S}	80.0	57.5
MCL_{D}	42.0	41.0
MCL_{P}	56.0	34.0
CAP_{M}	52.6	34.3
CAP_{L}	54.6	38.2
CAP_{O}	21.4	56.0
CAP_{A}	20.8	62.5

Table 3.3 Loading condition for parametric studies

	Loading condition
1	Compression + Flexion moment + Axial tibial torques (-50 N-m ~ 50 N-m) [a]
2	Compression + Flexion moment + Frontal plane moments (-150 N-m ~ 150 N-m) [b]
3	Compression + Flexion moment + Internal tibial torque (20 N-m) + Frontal plane moments (-150 N-m ~ 150 N-m) [b]
4	Compression + Flexion moment + External tibial torque (-20 N-m) + Frontal plane moments (-150 N-m ~ 150 N-m) [b]

[a] Positive value represents internal tibial torque.

[b] Positive value represents knee abduction moment.

3.4 Results

The Interaction between the Frontal Plane Moments and Axial Tibial Torques on ACL Relative Strain

The experimental results support the primary hypothesis: the normalized peak AM-ACL relative strain under the internal tibial torque was significantly greater than the corresponding values under the external tibial torque regardless of the direction of the frontal plane moment (Figure 3.3). The mean peak AM-ACL relative strain under the internal tibial torque combined with the knee ab- or adduction moment (7.0 ± 4.1% and 7.0 ± 3.9%, respectively) was significantly greater 192% than the corresponding values under external tibial torque combined with the knee ab- or adduction moment (2.4 ± 3.2% and 2.4 ± 2.5%, respectively). There was no difference between the two baseline loading conditions, thereby confirming the knee specimens were not damaged during the testing ($p=0.460$). The input force, input moments, and primary and secondary outcome measurements for each loading condition are summarized in Table 3.4. Sample time course data from a single representative specimen and trials are shown in Figure 3.4.

Model Validation

The 3D dynamic knee model was validated by comparing the quadriceps muscle force, knee flexion angle, and AM-ACL relative strain predicted by the simulation with the corresponding values measured from a knee specimen under the baseline loading condition (Figure 3.5). The quadriceps muscle force, knee flexion angles, and AM-ACL relative strain in the experiment and simulation for the first 80 msec were all highly correlated with the Pearson correlation coefficients $r = 0.959$, 0.972, and 0.991.

Table 3.4 Mean (± SD) value for the input force and moments, as well as the primary and secondary outcome measurements by testing block (N=15 specimens)

		BASE1	Internal Tibial Torque + Adduction Moment	Internal Tibial Torque + Abduction M.	External Tibial Torque + Adduction Moment	External Tibial Torque + Abduction Moment	BASE2
Input Force	Impulsive Compressive Force (N)	1,457 ± 131	871 ± 89	844 ± 88	1,113 ± 114	1,121 ± 121	1,429 ± 136
Input Moments	Axial Tibial Torque (N-m)[a]	-	27.0 ± 4.5	26.0 ± 3.4	-25.5 ± 6.0	-24.5 ± 6.3	-
	Frontal Plane Moment (N-m)[b]	-	-44.2 ± 4.5	42.8 ± 4.5	-56.5 ± 5.8	60.0 ± 6.2	-
Primary Outcome	AM-ACL Relative Strain (%)	3.8 ± 2.8	7.0 ± 3.9	7.0 ± 4.1	2.4 ± 2.5	2.4 ± 3.2	3.4 ± 2.7
Secondary Outcomes	Quadriceps Force (N)	772 ± 133	806 ± 135	918 ± 159	835 ± 190	726 ± 150	753 ± 133
	Knee Flexion Angle (deg)	4.4 ± 1.1	5.2 ± 1.0	6.1 ± 1.0	2.6 ± 1.1	1.9 ± 1.0	4.1 ± 1.0
	Anterior Tibial Translation (mm)	1.6 ± 0.7	4.4 ± 1.6	4.5 ± 1.7	1.0 ± 0.9	1.0 ± 0.9	1.6 ± 0.6
	Axial Tibial Rotation (deg)[a]	2.7 ± 1.1	13.5 ± 2.6	13.3 ± 2.2	-15.3 ± 3.6	-15.0 ± 4.2	2.4 ± 0.8
	Frontal Plane Angle (deg)[b]	0.9 ± 0.5	2.2 ± 1.3	2.6 ± 1.5	-3.1 ± 1.6	-3.0 ± 1.5	0.8 ± 0.5

[a] Positive value represents internal tibial torque or rotation.
[b] Positive value represents knee abduction moment or angle.

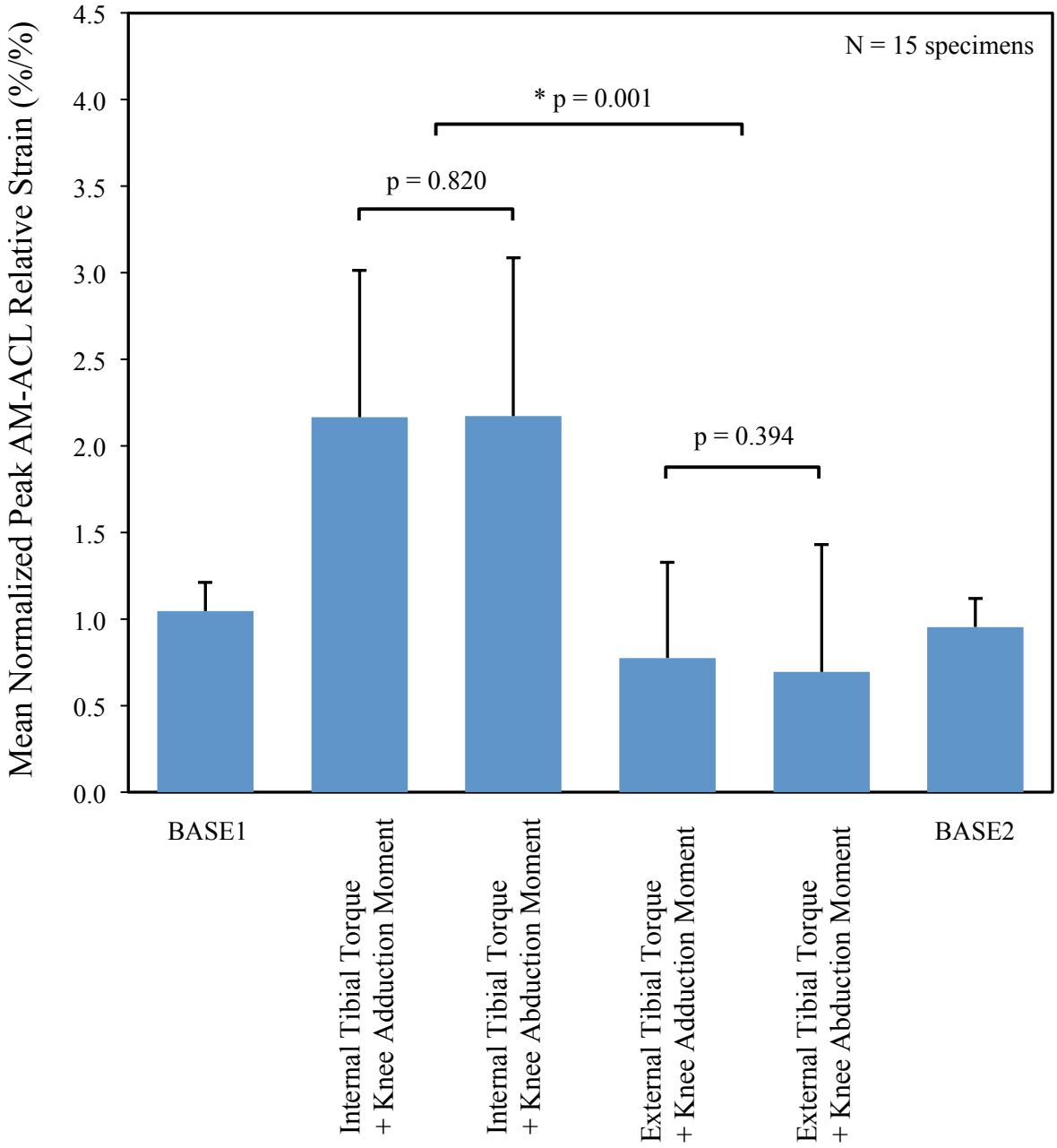

Figure 3.3 Mean (SD, represented by error bars) normalized peak AM-ACL relative strain values under each loading condition. The asterisk indicates a significant difference. Regardless of the direction of the frontal plane moment, the mean normalized peak AM-ACL relative strain was greater under the internal tibial torque than the external tibial torque.

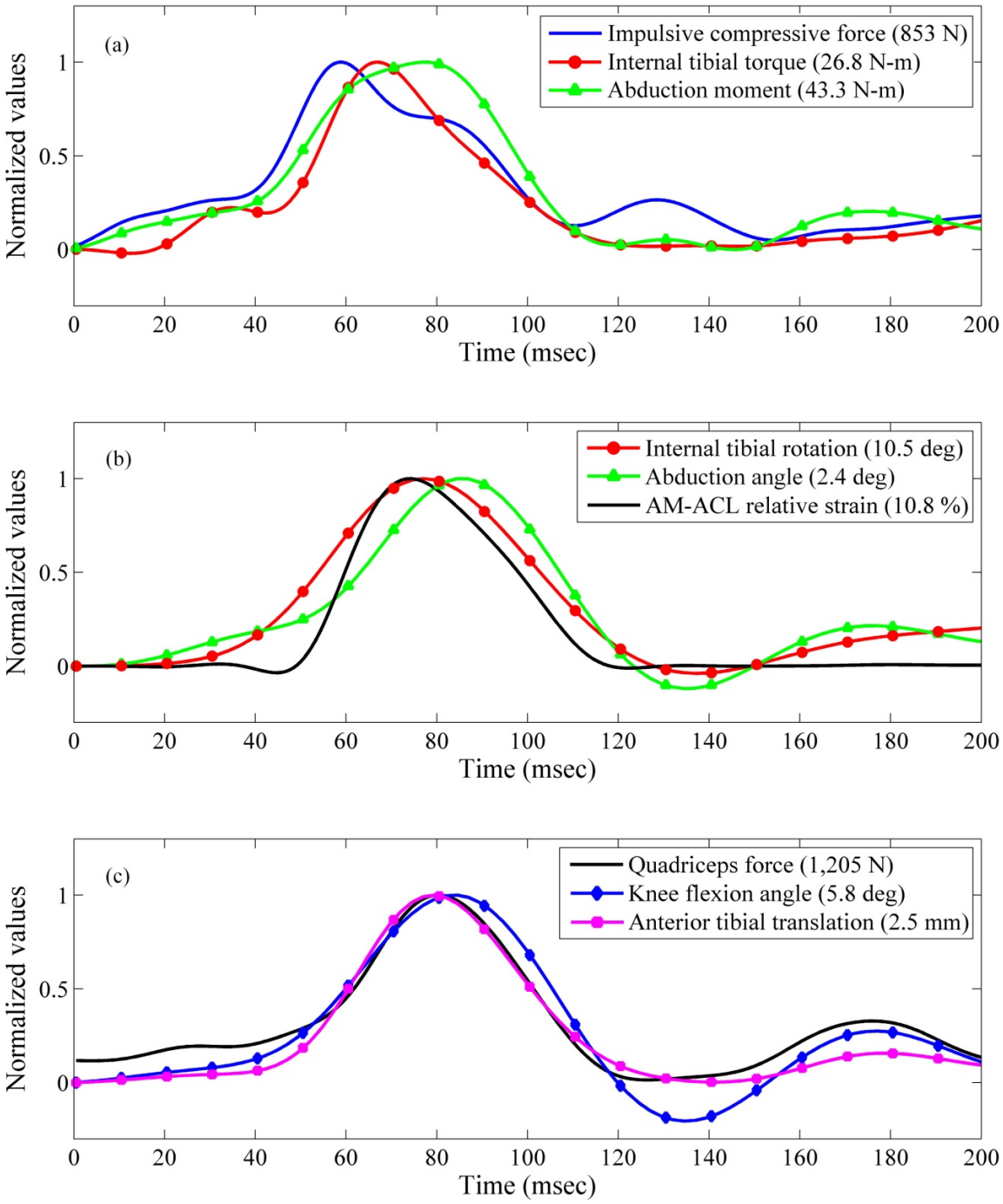

Figure 3.4 Sample temporal behavior: a) the applied impulsive compressive force, internal tibial torque, and knee abduction moment; b) the resultant internal tibial rotation, knee abduction angle and AM-ACL relative strain; c) the resultant quadriceps muscle force, knee flexion angle, and anterior tibial translation. For ease of comparison, measurements are normalized to their peak values in the trial and the pertinent peak values are shown in the legend.

Model-Predicted Effect of Axial Tibial Torque on the AM-ACL Relative Strain

The AM-ACL relative strain increased with internal tibial torque up to 50 N-m; however, the AM-ACL strain decreased as the external tibial torque was increased (Figure 3.6). Interestingly, the axial tibial torque resulted in coupled frontal plane motion due to the effect of the lateral or medial posterior tibial slope. When the lateral tibial slope exceeds that of the medial tibial slope, then an internal tibial torque caused coupled knee abduction, and vice versa (Figure 3.6d). Consistent with previous studies, the LCL and MCL relative strains increased as the internal and external tibial torque increased, respectively (Figure 3.6c).

Model-Predicted Effect of Frontal Plane Moment on the AM-ACL Relative Strain

The AM-ACL relative strain increased when the frontal plane moment was combined with a 20 N-m internal tibial torque (Figure 3.7). As the knee abduction moment was increased, the AM-ACL relative strain tended to increase, while the AM-ACL strain decreased as the adduction moment increased. Just as an axial tibial torque caused the coupled frontal plane motion (see above paragraph), the inverse was true: an abduction and adduction moment resulted in coupled internal and external tibial rotations, respectively. Interestingly, medial or lateral knee joint opening only occurred when the pure abduction or adduction moment exceeded 90 N-m or -110 N-m, respectively. The LCL or MCL relative strain drastically increased when the frontal plane moment exceeded approximately ± 100 N-m, thereby demonstrating the joint opening phenomenon.

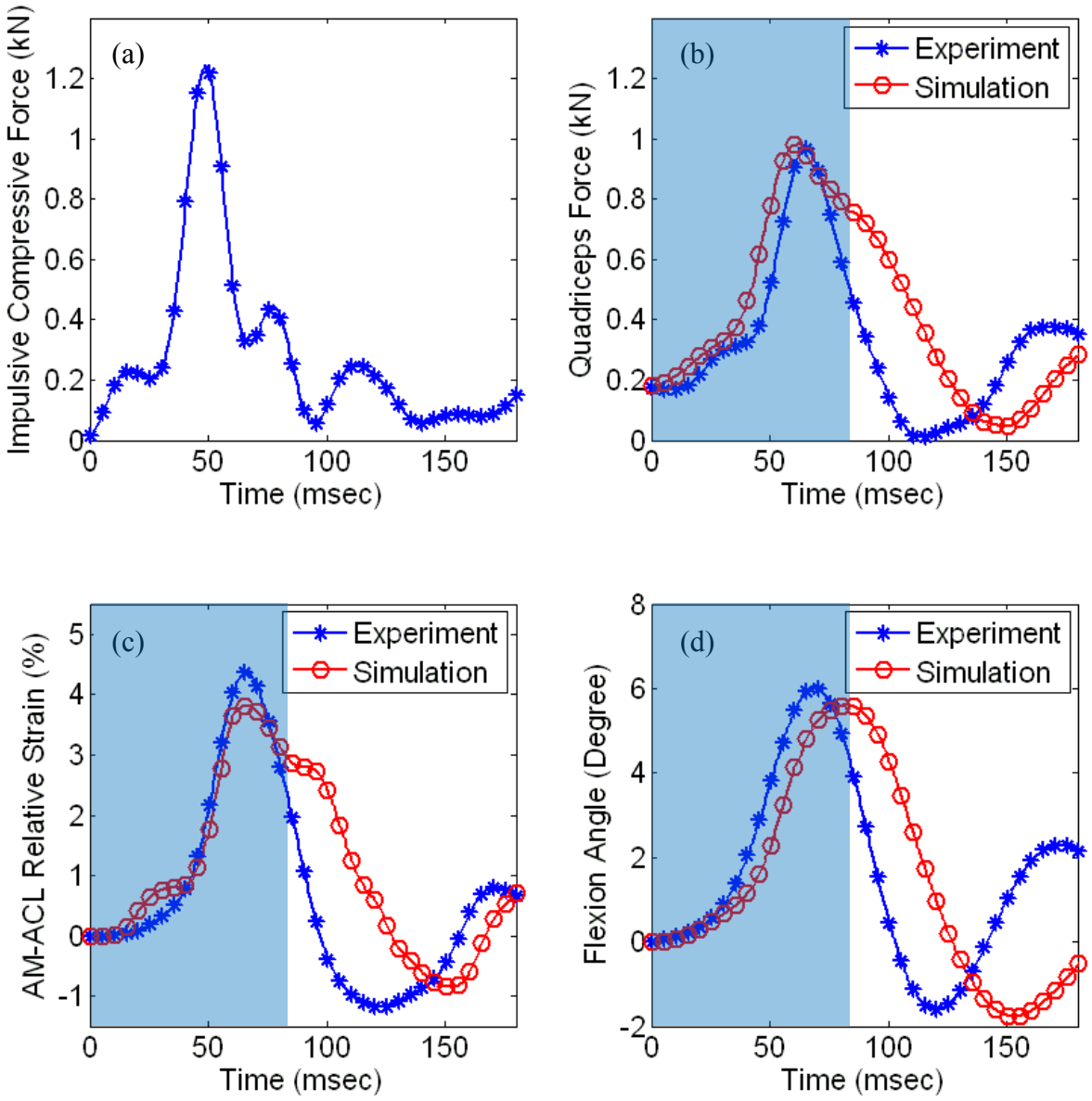

Figure 3.5 Model validation test: a) the impulsive compressive force measured from the experiment was applied as the model input to drive the simulation; b) the quadriceps muscle force, c) AM-ACL relative strain and d) knee flexion angle calculated from the simulation were compared to the corresponding values measured from a single specimen and trial under the baseline loading condition. The shaded area represents the data range used for the validation test. The Pearson correlation coefficients were 0.959, 0.972, and 0.991 for the quadriceps muscle force, knee flexion angle, and AM-ACL relative strain, respectively.

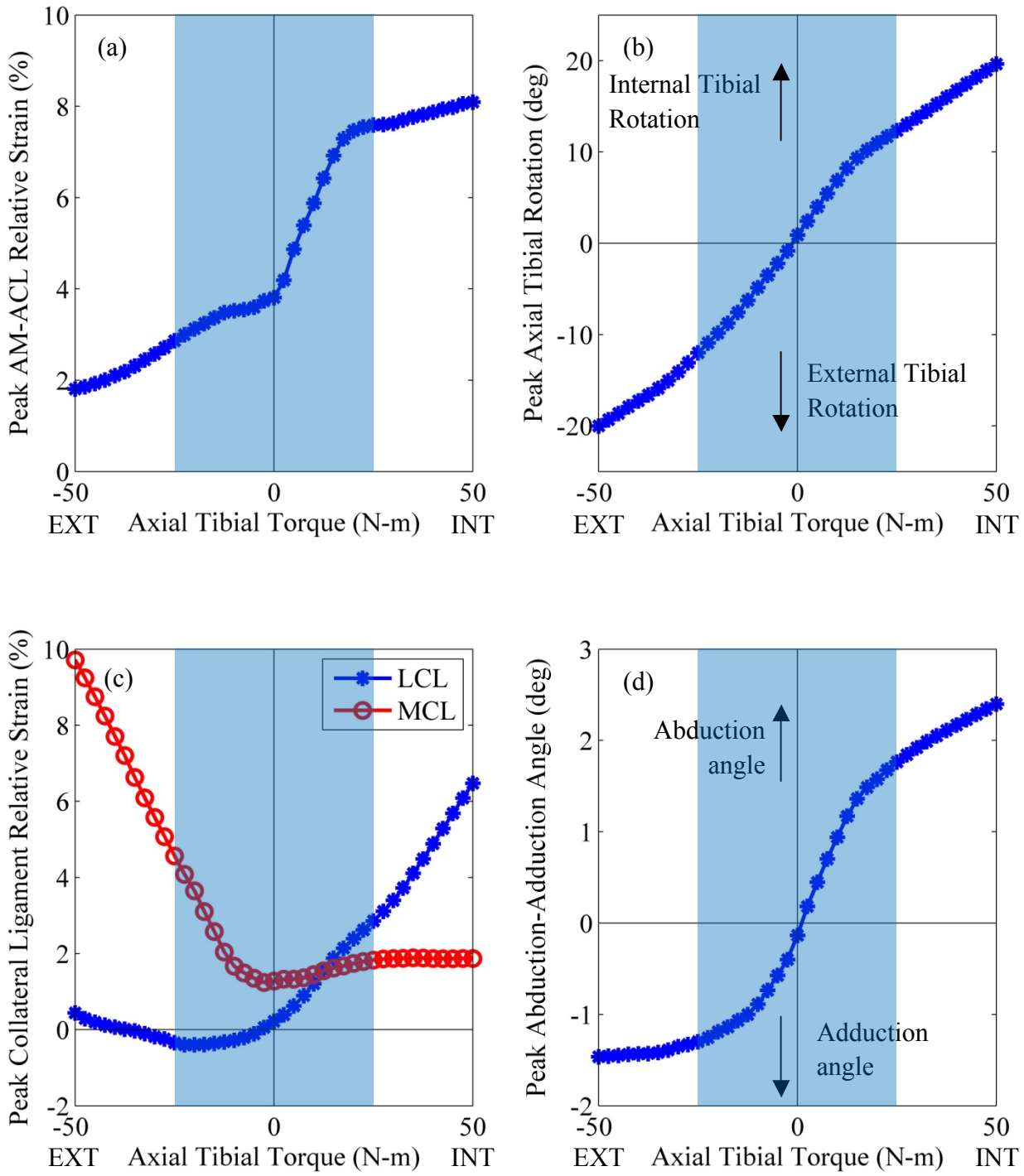

Figure 3.6 Model-predicted effect of the axial tibial torque on the peak AM-ACL relative strain, peak LCL and MCL relative strain, peak axial tibial rotation and peak coupled knee abduction-adduction angle. The positive axial tibial torque values represent the internal tibial torque (INT), while the negative axial tibial torque values represent the external tibial torque (EXT). The shaded area indicates the range of the axial tibial torque applied in the experiment.

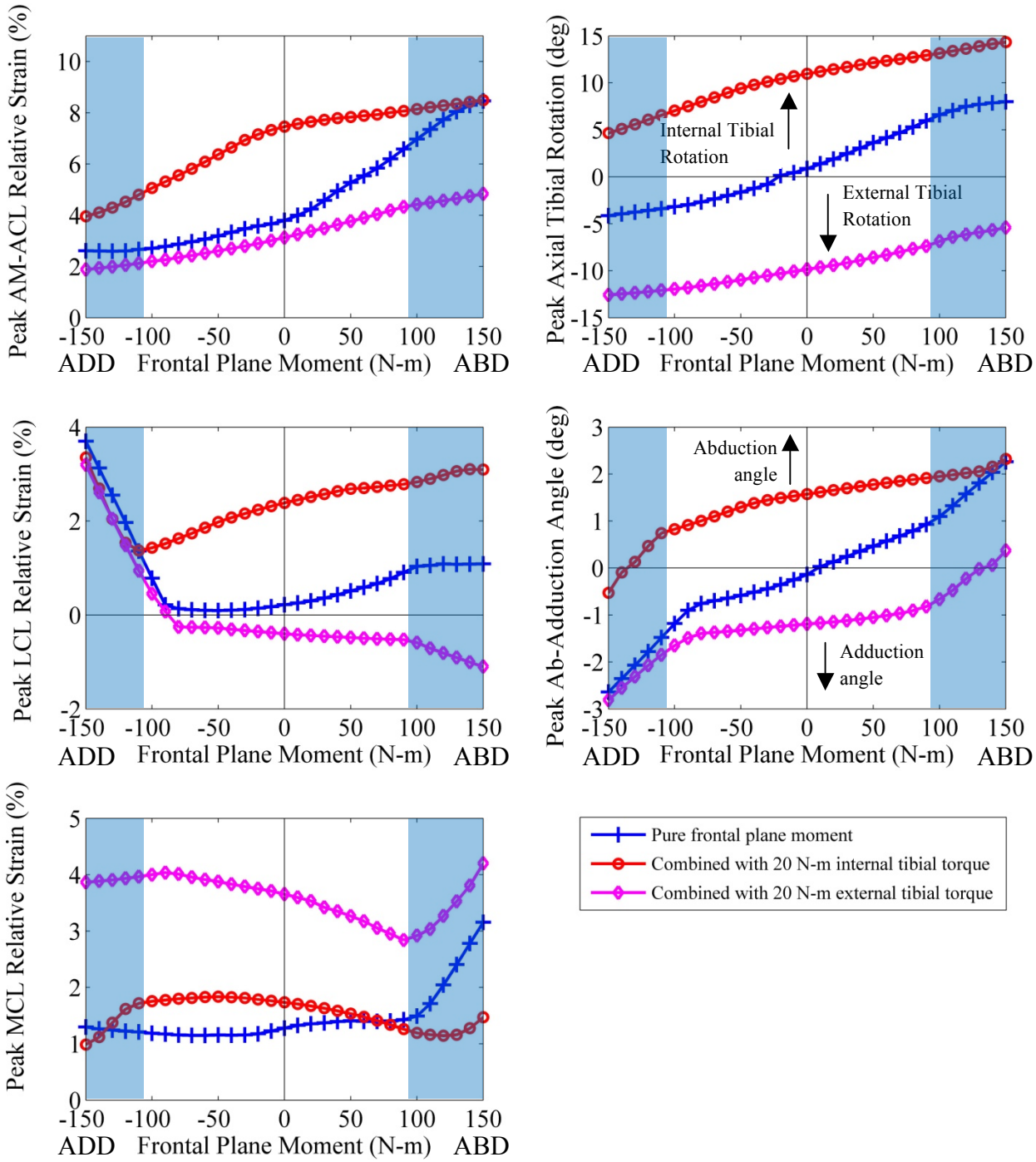

Figure 3.7 Model-predicted effect of the frontal plane moment on the peak AM-ACL relative strain, peak LCL and MCL relative strain, peak axial tibial rotation, and peak knee abduction-adduction angle. The positive frontal plane moment values represent the knee abduction moment (ABD), while the negative frontal plane moment values represent the knee adduction moment (ADD). The shaded area indicates the range of the frontal plane moment where the medial or lateral joint opening occurred.

3.5 Discussion

A new finding is that peak AM-ACL strain was found to be most sensitive to internal axial tibial torque, but not sensitive to the direction of the frontal plane moment. This is consistent with a series of experimental and clinical observations which have employed static or quasi-static loading conditions under much lower test force levels with and without muscle forces.[11,12,22,28] Sports maneuvers, of course, are known to place large dynamic loads on the knee joint.[3,39]

Why did the direction of the frontal plane moments not significantly affect peak AM-ACL strain in our experimental results? This may seem surprising given the current emphasis on minimizing valgus loading in the ACL prevention literature.[17,18,24,34] Part of the explanation can be found in the fact that between -50 N-m (i.e., Adduction) and +50 N-m (i.e., Abduction) frontal plane moments, our knee model predicted the change in ACL strain to be less than 1.5 %, or less than the standard deviation of the experimentally measured strain (c.f., Table 3.4 vs. Figure 3.7). The model simulation backs our experimental findings that ACL strain is relatively insensitive to changes in knee ab- and adduction moment when loaded under large compression forces combined with the axial tibial torque associated with a pivot landing. On the other hand, the model shows that in the absence of an axial tibial torque, an abduction moment also induces ACL strain. These seemingly contradictory results are consistent with previous studies.[43,51] For example, Withrow et al.[51] tested cadaveric human knees under a 2*BW impulsive compressive force, flexion moment, and knee abduction moment reaching 100 N-m during a simulated drop landing. The knee abduction moment caused a 30 % increase in the AM-ACL relative strain compared to when a knee abduction moment was not

applied. Worth noting is that although both internal tibial torque and knee abduction moment independently contribute to an increase ACL strain, in order to achieve the same increase in AM-ACL strain, our model findings suggest that the knee abduction moment would have to be three times as large in order to achieve ~8.5 % of AM-ACL relative strain compared to the internal tibial torque (c.f., Figure 3.6a vs. Figure 3.7a).

Our knee model, with medial and lateral tibial slopes of 5.5 degrees and 8.5 degrees[30], respectively, demonstrates coupled internal tibial rotation and knee abduction. Coupled motion between internal tibial rotation and knee abduction has been observed in many previous studies.[20,37,38] Our study corroborates Simon et al.'s work[45] and extends previous findings by showing the association between dynamic knee loads, coupled motions, tibial slopes and peak AM-ACL strain. A similar phenomenon has been observed *in vivo* in the kinematics of the knee during a dynamic single leg land-and-cut task: both the peak knee abduction angle and peak internal tibial rotation were significantly correlated to the ratio between the medial and lateral tibial slope, where the ratio was dominated by the lateral tibial slope.[30] The coupling phenomenon helps one understand 1) why the AM-ACL relative strain we measured experimentally was not different under the knee ab- and adduction moments, and 2) why the AM-ACL relative strain predicted by the model simulation was less sensitive to the knee abduction moment when it was combined with the axial tibial torque. *As long as medial joint space opening does not occur, the knee abduction moment essentially augments internal tibial rotation. The lateral extra-articular structures, which are known to restrain internal tibial rotation[52], would cause an insensitivity of the AM-ACL relative strain to the knee abduction moment by limiting the internal tibial rotation*.

One advantage of the biomechanical model is that it can be used to predict ACL strain under large frontal plane moments exceeding 100 N-m. The contact force between femur and medial and lateral tibial plateau can then be monitored so as to detect knee joint space opening. The model simulation predicts that knee ab- and adduction moments exceeding 100 N-m are needed to cause medial or lateral joint opening under quadriceps muscle forces that reach ~1,000 N in response to over 1*BW impulsive compressive force (please see sudden increase in MCL or LCL strain in Figure 3.7). In most *in vivo* jump landing studies, frontal plane moments rarely exceeded 100 N-m.[18,44] For example, Sigward et al.[44] reported that the peak abduction moment for those who demonstrated excessive knee abduction moment reached ~70 N-m when the peak vertical ground reaction force reached ~2.9*BW during a cutting maneuver. Furthermore and importantly, as the trans-knee muscular activity level increases, the knee joint compressive force increases and, in turn, the threshold frontal plane moment for knee joint opening increases.[26,27] Therefore, a knee abduction moment will increase the ACL strain via the coupling phenomenon, rather than by the medial joint opening that would place the MCL at risk for injury.

This study has several limitations. First, in order to limit the number of test cycles to each specimen, we only tested one initial knee flexion angle (15 degrees). This angle was chosen because Li et al.[23] reported ACL strain to be highest with the knee in 15 degrees of flexion. More recently in maximum jump landings initial mean (± SD) knee flexion angles of 11 (± 3) degrees at toe contact, and 28 (± 7) degrees at heel contact, have been measured.[47] Also, Olsen et al.[36] used injury videotapes to estimate knee flexion angle at injury to be 16 degrees. Therefore, the initial 15 degrees of knee flexion

we used seems reasonable. A second limitation is that the change of knee flexion angle under the impulsive test load was smaller than in some *in-vivo* studies.[39] Our studies showed an average knee flexion angle change of ~5 degrees in the first 70 msec. This is consistent with Russell et al.[41] who reported a change in knee flexion angle during a single-leg drop landing of less than 10 degrees over the initial 70 msec. Hence, our post-impact ('landing') change in knee flexion angle appears reasonable. A third limitation is that the peak impulsive compressive force under the internal tibial torque was slightly higher than one body-weight, whereas the corresponding value for the baseline loading conditions was about 2 times body-weight. This decrease in the peak impulsive compressive force resulted from the custom torsional transformer device ('T' in Figure 3.1) changing the impedance of the specimen for those tests. We reiterate that the test weight was dropped through the same drop height for every trial and test condition, so the same kinetic energy was applied to the knee specimen for each trial and test conditions. This mirrors landing from the same jump height each time. Withrow et al.[50] showed that the ACL relative strain was highly correlated with the quadriceps force, not the impulsive compressive force. Dikeman et al.[7] and DeMorat et al.[6] also found that an increase in quadriceps force increased ACL strain, and all three experimental models can cause ACL ruptures. These results suggest that the increase in quadriceps force dominates the increase in ACL strain more than does the increase in impulsive compressive force. In our case, for all loading conditions, the quadriceps forces was maintained at the similar value, thereby providing a good opportunity to investigate the effect of the different loading directions and ACL status on the knee joint kinematics. A fourth limitation was that we tested male knee specimens, so our results cannot be generalized to females,

although we do not expect the qualitative results would change. Other limitations include the fact that we could not measure absolute strain in the ACL, but instead relied upon relative strain.[50-51] Finally, a number of standard assumptions and simplifications had to be made in order to develop the model. These include assuming bilinear viscoelastic soft tissue behaviors for ligament and muscle-tendon units, and setting the MCL, LCL and joint capsule slack lengths close to zero when the knee joint is loaded at 15 degrees prior to impact.

Basic biomechanical principles inform us that the maximum internal tibial torque that can be applied to the knee is limited by the torsional coefficient of friction between the shoe and playing surface. If this coefficient of friction is reduced, then the peak internal tibial torque that can be applied to the knee will be reduced, thereby reducing the risk for ACL injury. Clearly, the number of ACL injuries would suggest that the present values of torsional friction are excessive.[8] More reasonable values for this torsional coefficient of friction might be specified by regulatory bodies such as the NFL, NCAA, and state High School Athletic Associations, just as downhill ski bindings can be set to a breakaway torque in order to limit the maximum torque that can be applied to the lower extremity.

3.6 Conclusions

We conclude that the worst-case dynamic knee loading as far as ACL strain is concerned is internal tibial torque combined with a knee abduction moment. However, it is an internal tibial torque, rather than an abduction moment, that causes the most ACL strain.

3.7 References

1. Arms SW, Pope MH, Johnson RJ, Fischer RA, Arvidsson I, Eriksson E. The biomechanics of anterior cruciate ligament rehabilitation and reconstruction. *Am J Sports Med.* 1984;12(1):8-18.

2. Binfield PM, Maffulli N, King JB. Patterns of meniscal tears associated with anterior cruciate ligament lesions in athletes. *Injury*. 1993;24:557-561.

3. Besier TF, Lloyd DG, Ackland TR, Cochrane JL. Anticipatory effects on knee joint loading during running and cutting maneuvers. *Med Sci Sports Exercise*. 2001;33:1176-1181.

4. Caborn DN, Johnson BM. The natural history of the anterior cruciate ligament-deficient knee: A review. *Clin Sports Med*. 1993;12:625-636.

5. Caulfield B, Garrett M. Changes in ground reaction force during jump landing in subjects with functional instability of the ankle joint. *Clin Biomech*. 2004;19:617-621.

6. DeMorat G, Weinhold P, Blackburn T, Chudik S, Garrett W. Aggressive quadriceps loading can induce noncontact anterior cruciate ligament injury. *Am J Sports Med*. 2004;32(2):477-83.

7. Dikeman JS. Experimental simulation of mechanism of injury for non-contact, isolated anterior cruciate ligament ruptures. *Master's Thesis, North Carolina State University*, 1998.

8. Dowling AV, Corazza S, Chaudhari AMW, et al. Shoe-surface friction influences movement strategies during a sidestep cutting task implications for anterior cruciate ligament injury risk. *Am J Sports Med.* 2010;38(3):478-485.

9. Fehnel DJ, Johnson R. Anterior cruciate injuries in the skeletally immature athlete: A review of treatment outcomes. *Sports Med.* 2000;29:51-63.

10. Fleming BC, Beynnon BD, Tohyama H, Johnson RJ, Nichols CE, Renström PA, Pope MH. Determination of a zero strain reference for the anteromedial band of the anterior cruciate ligament. *J Orthop Res*. 1994;12:789-795.

11. Fleming BC, Renstrom PA, Beynnon BD, et al. The effect of weightbearing and external loading on anterior cruciate ligament strain. *J Biomech*. 2001;34(2):163-170.

12. Fukuda Y, Woo SLY, Loh JC, Tsuda E, Tang P, McMahon PJ, Debski RE. A quantitative analysis of valgus torque on the ACL: a human cadaveric study. *J Orthop Res*. 2003; 21:1107-1112.

13. Graf BK, Cook DA, Desmet AA, et al. Bone bruises on magnetic-resonance-imaging evaluation of anterior cruciate ligament injuries. *Am J Sports Med*. 1993;21(2):220-223.

14. Allografts in Sports Medicine: What Do We Know, Need to Know, and Need to Do? Round table discussion: *American Orthopaedic Society for Sports Medicine*; February 13, 2006; Park City, UT.

15. Grood ES, Suntay WJ. A joint coordinate system for the clinical description of three-dimensional motions: application to the knee. *J Biomech Eng*. 1983;105(2):136-44.

16. Hashemi J, Chandrashekar N, Mansouri H, Gill B, Slauterbeck JR, Schutt RC, Dabezies E, Beynnon BD. Shallow medial tibial plateau and steep medial and lateral tibial slopes new risk factors for anterior cruciate ligament injuries. *Am J Sports Med.* 2010;38(1):54-62.

17. Hewett TE, Lindenfeld TN, Riccobene JV, Noyes FR. The effect of neuromuscular training on the incidence of knee injury in female athletes - A prospective study. *Am J Sports Med*. 1999;27:699-706.

18. Hewett TE, Myer GD, Ford KR, et al. Biomechanical measures of neuromuscular control and valgus loading of the knee predict ACL injury risk in female athletes: A prospective study. *Am J Sports Med*. 2005;33:492-501.

19. Koga H, Nakamae A, Shima Y, Iwasa J, Myklebust G, et al. Mechanisms for noncontact anterior cruciate ligament injuries: Knee joint kinematics in 10 injury situations from female team handball and basketball. *Am J Sports Med*. 2010;38:2218-2225.

20. Inoue M, McGurkburleson E, Hollis JM, Woo SLY. Treatment of the medial collateral ligament injury .1. the importance of anterior cruciate ligament on the varus-valgus knee laxity. *Am J Sports Med*. 1987;15:15-21.

21. Johnson DL, Urban WP, Caborn DNM, Vanarthos WJ, Carlson CS. Articular cartilage changes seen with magnetic resonance imaging-detected bone bruises associated with acute anterior cruciate ligament rupture. *Am J Sports Med*. 1998;26:409-414.

22. Kanamori A, Zeminski J, Rudy TW, Li G, Fu FH, Woo SLY. The effect of axial tibial torque on the function of the anterior cruciate ligament: A biomechanical study of a simulated pivot shift test. *Arthroscopy*. 2002;18(4):394-398

23. Li G, Rudy TW, Sakane M, Kanamori A, Ma CB, Woo SLY. The importance of quadriceps and hamstring muscle loading on knee kinematics land in-situ forces in the ACL. *J Biomech*. 1999;32(4):395-400.

24. Lloyd DG. Rationale for training programs to reduce anterior cruciate ligament injuries in Australian football. *J Orthop Sports Phys Ther*. 2001;31:645-654.

25. Lohmander, LS, Englund PM, Dahl LL, Roos EM. The long-term consequence of anterior cruciate ligament and meniscus injuries - Osteoarthritis. *Am J Sports Med.* 2007;35:1756-1769.

26. Markolf KL, Mensch JS, Amstutz CH. Stiffness and laxity of the knee—the contribution of the supporting structures. A quantitative in vitro study. *J Bone Joint Surg Am.* 1978;58:583-593.

27. Markolf KL, Bargar WL, Shoemaker SC, Amstutz HC. The role of joint load in knee stability. *J Bone Joint Surg Am*. 1981;63:570-585.

28. Markolf KL, Burchfield DI, Shapiro MM, Shepard ME, Finerman GAM, Slauterbeck JL. Combined knee loading states that generate high anterior cruciate ligament forces. *J Orthop Res*. 1995;13(6):930-935.

29. Markolf KL, O'Neill G, Jackson SR, McAllister DR. Effects of applied quadriceps and hamstrings muscle loads on forces in the anterior and posterior cruciate ligaments. *Am J Sports Med*. 2004;32(5):1144-1149.

30. McLean SG, Lucey SM, Rohrer S, et al. Knee joint anatomy predicts high-risk in vivo dynamic landing knee biomechanics. *Clin Biomech*. 2010;25(8):781-788.

31. McNitt-Gray JL, Hester DM, Mathiyakom W, Munkasy BA. Mechanical demand and multi-joint control during landing depends on orientation of the body segments relative to the reaction force. *J Biomech*. 2001;34:1471-1482.

32. Merican AM, Sanghavi S, Iranpour F, Amis AA. The structural properties of the lateral retinaculum and capsular complex of the knee. *J Biomech*. 2009;42:2323-2329.

33. Mizhari J, Susak K. Analysis of affecting force attenuation during landing in human vertical free fall. *Eng. Med*. 1982;11:141-147.

34. Myer GD, Ford KR, Hewett TE. Rationale and clinical techniques for anterior cruciate ligament injury prevention among female athletes. *J Athl Training*. 2004;39:352-364.

35. Oh YK, Kreinbrink JL, Ashton-Miller JA, Wojtys EM. Effect of ACL transaction on internal tibial rotation in an in vitro simulated pivot landing. *J Bone Joint Surg AM.* 2011;93(4):372-80.

36. Olsen OE, Myklebust G, Engebretsen L, Bahr R. Injury mechanisms for anterior cruciate ligament injuries in team handball a systematic video analysis. *Am J Sports Med.* 2004;32(4):1002-1012.

37. Oster, DM, Grood ES, Feder SM, Butler DL, Levy MS. Primary and coupled motions in the intact and the ACL-deficient knee - An in vitro study in the goat model. *J Orthop Res*. 1992;10:476-484.

38. Ostgaard SE, Helmig P, Nielsen S, Hvid I. Anterolateral instability in the anterior cruciate ligament deficient knee - A cadaver study. *Acta Orthop Scand*. 1991;62:4-8.

39. Pflum MA, Shelburne KB, Torry MR, Decker MJ, Pandy MG. Model prediction of anterior cruciate ligament force during drop landings. *Med Sci Sports Exerc*. 2004;36:1949-1958.

40. Robinson, JR, Bull AMJ, Amis AA. Structural properties of the medial collateral ligament complex of the human knee. *J Biomech*. 2005;38:1067-1074.

41. Russell KA, Palmieri RM, Zinder SM, Ingersoll CD. Sex differences in valgus knee angle during a single-leg drop jump. *J Athl Training*. 2006;41(2):166-171.

42. Shin CS, Chaudhari AM, Andriacchi TP. The influence of deceleration forces on ACL strain during single-leg landing: A simulation study. *J Biomech*. 2007;40(5):1145-1152.

43. Shin CS, Chaudhari AM, Andriacchi TP. The effect of isolated valgus moments on ACL strain during single-leg landing: A simulation study. *J Biomech*. 2009;42(3):280-285.

44. Sigward, SM, Powers CM. Loading characteristics of females exhibiting excessive valgus moments during cutting. *Clin Biomech*. 2007;22, 827-833.

45. Simon RA, Everhart JS, Nagaraja HN, Chaudhari AM. A case-control study of anterior cruciate ligament volume, tibial plateau slopes and intercondylar notch dimensions in ACL-injured knees. *J Biomech*. 2010;43:1702-1707.

46. Spindler KP, Schils JP, Bergfeld JA, et al. Prospective study of osseous, articular, and meniscal lesions in recent anterior cruciate ligament tears by magnetic resonance imaging and arthroscopy. *Am J Sports Med*. 1993;21:551-557.

47. Urabe Y, Kobayashi R, Sumida S, Tanaka K, Yoshida N, Nishiwaki GA, et al. Electromyographic analysis of the knee during jump landing in male and female athletes. *Knee*. 2005;12(2):129-34.

48. Vellet AD, Marks PH, Fowler PJ, Munro TG. Occult posttraumatic osteochondral lesions of the knee: prevalence, classification, and short-term sequelae evaluated with MR imaging. *Radiology*. 1991;178:271-276.

49. Viceconti M, et al. Visible Human Male – Bone Surface from The BEL Repository, http://www.tecno.ior.it/VRLAB/.

50. Withrow TJ, Huston LJ, Wojtys EM, Ashton-Miller JA. The relationship between quadriceps muscle force, knee flexion, and anterior cruciate ligament strain in an in vitro simulated jump landing. *Am J Sports Med*. 2006;34(2):269-74.

51. Withrow TJ, Huston LJ, Wojtys EM, Ashton-Miller JA. The effect of an impulsive knee valgus moment on in vitro relative ACL strain during a simulated jump landing. *Clin Biomech*. 2006;21(9):977-83.

52. Wroble RR, Grood ES, Cummings JS, Henderson JM, Noyes FR. The role of the lateral extraarticular restraints in the anterior cruciate ligament-deficient knee. *Am J Sports Med*. 1993;21:257-263.

CHAPTER 4

EFFECT OF LATERAL TIBIAL SLOPE, FRONTAL PLANE ANLIGNMENT AND MEDIAL TIBIAL CONCAVITY ON ACL STRAIN DURING A SIMULATED JUMP LANDING

4.1 Abstract

The incidence of anterior cruciate ligament (ACL) injury still remains high. Recently, it has been the focus of investigations to find the explicit link between injurious loading mechanisms and morphological characteristics of knee joint. It remains unclear what variations in the morphological factors influence ACL strain to increase injury risk.

The purpose of this study was to determine how changes in lateral tibial slope, frontal plane alignment, and medial tibial concavity affect ACL strain during a simulated jump landing. A three-dimensional lower-limb model was constructed using sagittal MR scans to replicate the experimental set-up. The simulation model was validated by matching the quadriceps force, ACL strain, knee flexion angle, internal tibial rotation, and knee abduction angle to the corresponding values obtained from our previous experiment. The model simulation was repeated with 1) lateral tibial slope altered in 1-degree increment ranging from 5.5-degrees to 13.5-degrees, 2) frontal plane alignment altered in 1-degree increment ranging from 7.5-degrees of varus to 10.0-degrees of

valgus, 3) medial tibial depth of concavity morphed in 0.5-mm increment ranging from 2-mm to 5-mm.

The model simulation predicted that the ACL strain was most sensitive to the change in the lateral tibial slope (i.e., 1.0 % ACL strain increase per 1.0-degree increase). Every 1.0-degree increase in the frontal plane lower limb alignment resulted in 0.1% ACL strain increase, while every 0.5-mm decrease in the medial tibial depth of concavity resulted in 0.7 % ACL strain decrease. These results corroborate previous studies in that a steeper lateral tibial slope, more valgus limb alignment, and shallower medial tibial depth can be used as risk factors for ACL injury.

4.2 Introduction

The incidence of anterior cruciate ligament (ACL) injury still remains high. In United States, nearly 350,000 ACL reconstructions are performed every year.[1] An ACL injury predisposes an individual to early development of degenerative osteoarthritis.[2] The fundamental basis for knee trauma prevention research is that injuries occur not in random events, but in patterns that reflect underlying risk factors.[3] Thus, it is required to better understand risk factors for ACL injury in order to identify at-risk individuals who are most vulnerable. Recently, it has been the focus of investigations to find the explicit link between injurious loading mechanisms and morphological characteristics of knee joint. It remains unclear what variations in the morphological factors influence ACL strain to increase injury risk.

The association between ACL injury and posteriorly inclined tibial slope has been identified.[4,5] In addtion, Stijak et al.[6] reported that an examined group with a diagnosed ACL lesion has significantly greater tibial slope on the lateral plateau and lower tibial slope on the medial plateau than a control group with a diagnosed patellofemoral pain, suggesting that the tibial slope of the medial and lateral plateau should be compared separately. Similarly, Simon et al.[7] found a significantly steeper lateral tibial slope in an ACL injured group than an uninjured group while the medial tibial slopes between two groups were not significantly different. Then, they explained that these difference between the medial and lateral tibial slope would allow an axial force to cause the lateral side of the femur to slide more posteriorly off of the lateral tibial plateau, using the medial tibial plateau as a pivoting point: in other words, increased internal tibial rotation or anterolateral tibial subluxation. McLean et al.[8] demonstrated a similar phenomenon during in vivo land-and-cut tasks: both the peak knee abduction angle and peak internal tibial rotation were significantly correlated to the ratio between the medial and lateral tibial slope, where the ratio was dominated by the lateral tibial slope. Our previous work demonstrated that when the lateral tibial slope exceeds that of the medial tibial plateau, then an abduction moment causes coupled internal tibial rotation, and vice versa and a knee abduction moment can increase ACL strain even without medial knee joint opening due to this coupling phenomenon. Since this coupled phenomenon resulted from the different medial and lateral slopes is accentuated under large compressive loading, it is warranted to investigate how much the variation in slope difference between medial and lateral tibial plateau will affect to increase ACL strain.

Static frontal plane lower limb alignment has been identified as a risk factor for ACL injury.[9,10] Similarly, it is suggested that a high static Q-angle is related to an increased risk of ACL injury.[11-14] On the other hand, other studies showed that a static measurement of frontal plane limb alignment does not appear to be related to a dynamic frontal plane limb alignment or ACL injury risk during dynamic moment.[15-18] For example, a static valgus knee angle in young athletes with higher Q-angle was not significantly greater compared to those who showed lower Q-angle.[18] Despite the fact that a static frontal-plane lower limb alignment is clinically easy to determine, the evidence to support the relationship between a static frontal plane limb alignment and a potential risk factor for ACL injury remains inconsistent. Thus, it is required to study if a static frontal plane limb alignment can affect to increase ACL strain and if so, how sensitive the effect would be.

Recently, a shallow medial tibial depth of concavity has been identified as a risk factor for ACL injury.[5] Hashemi et al.[5] reported that ACL injured participants had smaller medial tibial depth of concavity along with greater lateral tibial slope compared to ACL uninjured controls in both male and female groups. Similarly, Khan et al.[19] found a significantly steep lateral tibial slope in the injured group for both genders or male only and a significantly shallow medial tibial concavity only in the female injured group. Interestingly, Hashemi et al.[5] estimated that the injury risk would be affected more by the decreased (shallower) medial tibial concavity than by the increased (steeper) lateral tibial slope, while Khan et al.[19] estimated that the lateral tibial slope would contribute to ACL injury more than the medial tibial concavity would do.

Therefore, the purpose of this study was to investigate which morphological factor (i.e., lateral tibial slope, frontal plane limb alignment, and medial tibial concavity) would contribute more to increase ACL strain by developing a 3D lower limb model during a simulated jump-landing scenario.

4.3 Methods

A three-dimensional lower-limb model was constructed to replicate the experimental set-up (Figure 4.1) and to further investigate how the coronal plane alignment, medial tibial concavity, and lateral tibial slope affect the ACL strain under a simulated landing. T2-weighted 3D magnetic resonance imaging (MRI) scans were acquired from a male thawed cadaveric limb (age: 80, weight: 82.5 kg, height: 174.4 cm) prior to impact testing (Philips 3T Scanner, 3D-PD sequence, TR/TE: 1000/35 ms, slice thickness: 0.35 mm, pixel spacing: 0.35 mm x 0.35 mm, field of view: 160mm). For the segmentation, the sagittal plane MRI scans were imported into a 3D Computer-Aided Design Software (SolidWorks 2010, Dassault Systèmes SolidWorks Corp., Concord, MA) and the outer edges of each bone were traced using splines. Then, a set of the splines for each bone was combined to form a smooth surface (Rhinoceros, McNeel North America, Seattle, WA). The segmented distal femur, proximal tibia, proximal fibula, and patella were imported into a dynamic simulation software (MD ADAMS R3, MSC.Software, Inc., Santa Ana, CA).

As described in our earlier work,[20] eighteen visco-elastic elements consisting of a bi-linear elastic spring and a viscous damper in parallel (See Figure 4.2) were used to

describe the mechanical behavior of the knee joint ligament and capsular structure. The attachment sites and slack lengths of the ligament were based on the MR scans and were adjusted to match the simulation results with the experiment. As described in Shin et al.'s work[21], the force for each ligament or capsular fiber was defined as follows:

$$F(\varepsilon) = \begin{cases} 0 & , \quad \varepsilon < 0 \\ \frac{k}{2}\varepsilon L_O & , \quad 0 \leq \varepsilon < 2\varepsilon_1 \\ k(\varepsilon - \varepsilon_1)L_O, & \quad \varepsilon \geq 2\varepsilon_1 \end{cases}$$

, where L_O is the predefined slack length of each ligament or fiber; ε is the ligament strain defined as $\varepsilon = (L - L_O)/L_O$; the toe region for each ligament or fiber is specified until the strain value reaches $\varepsilon_1 = 0.03$; and k is the stiffness coefficient for each ligament or fiber obtained from previous studies (Table 4.1).

In order to replicate the experimental set-up,[20,24] the quadriceps, medial and lateral hamstrings and gastrocnemius muscles in the simulation model were modeled and pretensioned to a 180 N for quadriceps and 70 N for each flexor muscle, respectively, with the knee initially in 15 degrees of flexion. Then, the impulsive compressive force, internal tibial torque, and knee abduction moment measured from the experiment were applied as the input to drive the knee model. In the *in vitro* experiment (Figure 4.1), the impulsive compressive force, flexion moment, internal tibial torque, and knee abduction moment were simultaneously applied while recording the 3-D knee loads at the proximal and distal end of the knee, muscle forces, tibiofemoral kinematics using the Optotrak Certus motion capture system, and AM_ACL relative strain using a 3-mm DVRT (Microstrain, Burlington, VT). To validate the model, the quadriceps muscle forces, AM-ACL strain, knee flexion angle, internal tibial rotation and knee abduction angle obtained

from the simulation model were quantitatively compared to the corresponding values from the experiment by evaluating Pearson correlation coefficients from the time when the impact was initiated and 100 msec (Figure 4.2).

Table 4.1 Material properties of ligaments.[21-23]

Ligament/Fiber	Stiffness (N/mm)	Slack length (mm)
ACL_{AM}	108.0	32.9
ACL_{PL}	108.0	28.8
PCL_{A}	125.0	39.4
PCL_{P}	60.0	31.9
LCL	91.3	44.2
PFL_{M}	50.0	56.6
PFL_{L}	50.0	37.3
PTL_{M}	80.0	46.6
PTL_{L}	80.0	39.2
PL_{M}	300.0	55.7
PL_{L}	300.0	54.6
MCL_{S}	80.0	53.4
MCL_{D}	42.0	39.0
MCL_{P}	56.0	27.5
CAP_{M}	52.6	29.9
CAP_{L}	54.6	30.2
CAP_{O}	21.4	52.9
CAP_{A}	20.8	62.4

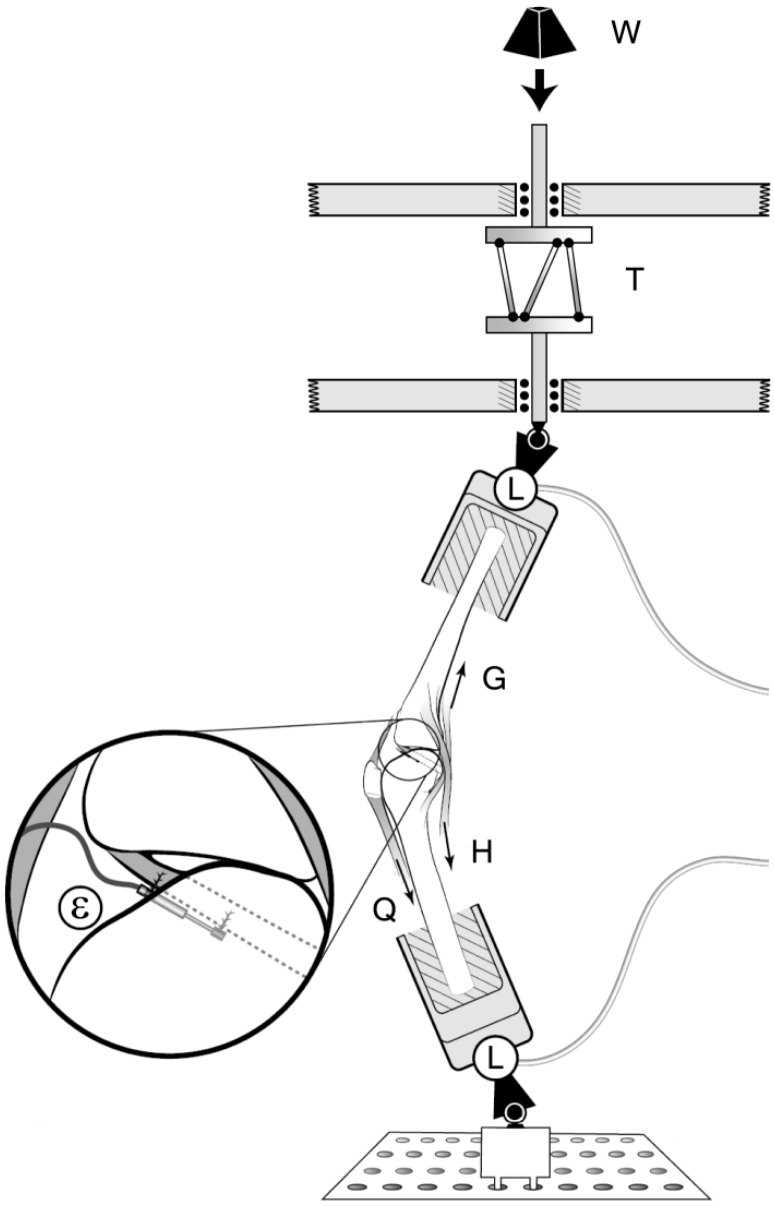

Figure 4.1 Schematic diagram of the test apparatus showing how a weight ('W') dropped from a fixed height onto the torsional transformer device ('T') applies impulsive compression and axial torque to the distal tibia of an inverted knee specimen. The frontal plane moment was applied by initially abducting or adducting the knee specimen. The two load-cells ('L') measure the three components of force and moment applied to the knee specimen in the presence of quadriceps ('Q'), hamstrings ('H') and 'gastrocnemius ('G') forces, while a miniature displacement transducer ('ε') implanted on the surface of the anteromedial bundle of the ACL measures relative strain.

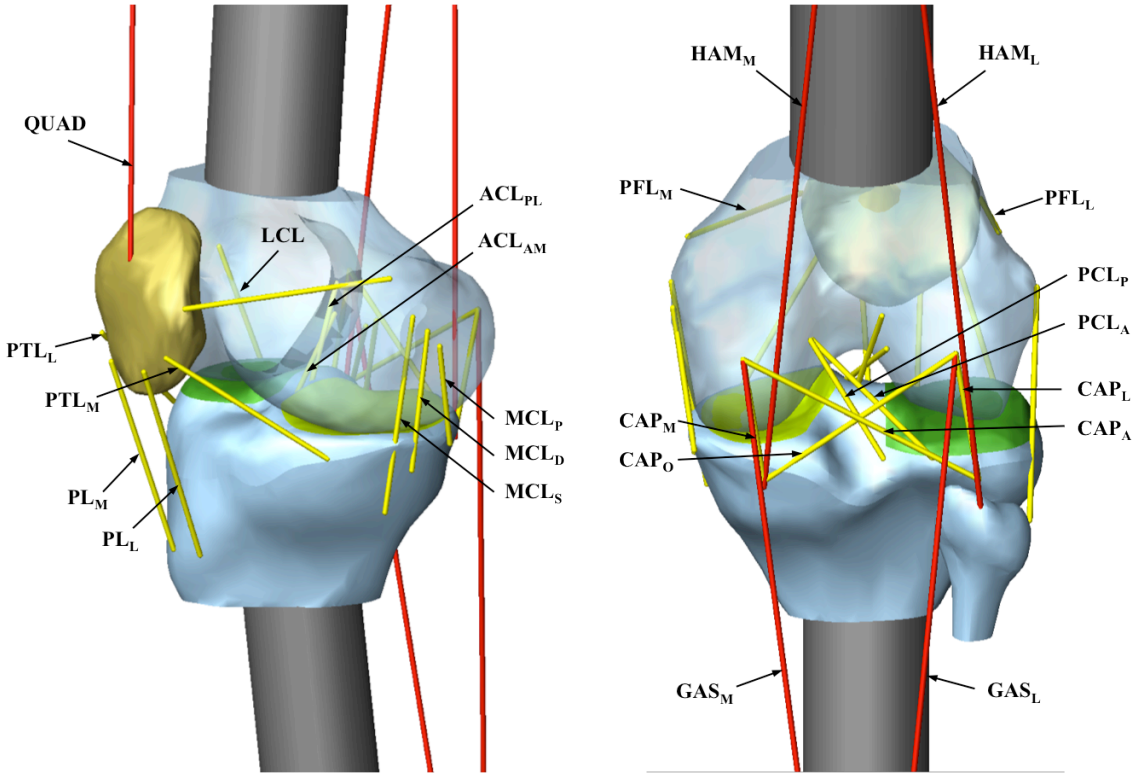

Figure 4.2 Schematic of the knee model showing muscles (red lines) and ligaments (yellow lines): quadriceps, medial and lateral hamstrings, and medial and lateral gastrocnemius muscles (QUAD, HAM_M, HAM_L, GAS_M, and GAS_L); the anteromedial and posterolateral bundle of ACL (ACL_{AM} and ACL_{PL}); the anterior and posterior bundle of PCL (PCL_A and PCL_P); the lateral collateral ligament and the superficial, deep, and posterior medial collateral ligament (LCL, MCL_S, MCL_D, and MCL_P); the medial and lateral patellofemoral ligament and the medial and lateral patellotibial ligament for the anterior knee capsule (PFL_M, PFL_L, PTL_M, and PTL_L); the medial, lateral, oblique popliteal, and arcuate popoliteal fiber for the posterior knee capsule (CAP_M, CAP_L, CAP_O, and CAP_A); and the medial and lateral patellar ligament (PL_M and PL_L).

After the validation test, sensitivity analysis was performed to investigate how the lateral tibial slope, coronal plane alignment, and medial tibial concavity would affect the AM-ACL strain during a simulated jump landing, thereby identifying which morphological factor would be the most detrimental to ACL injury. In addition, the anterior tibial translation, internal tibial rotation, and knee abduction angle were also

calculated to interpret how the morphological change would cause the change in the AM-ACL strain value. In order to investigate the effect of the lateral tibial slope on AM-ACL strain, a segment corresponding to the lateral tibial plateau was separated from the reconstructed proximal tibia (Figure 4.3). The original lateral tibial slope was measured to be 8.5-degrees posteriorly from the sagittal plane MR scans using methods similar to those reported by Stijak et al.[6] and Hashemi et al.[5] Then, the model simulation was repeated for every 1-degree increment in the lateral tibial slope ranging from 5.5-degrees to 13.5-degrees. The lateral tibial slope was changed by rotating the separated lateral tibial plateau about an axis located on the center of mass for the lateral tibial plateau.

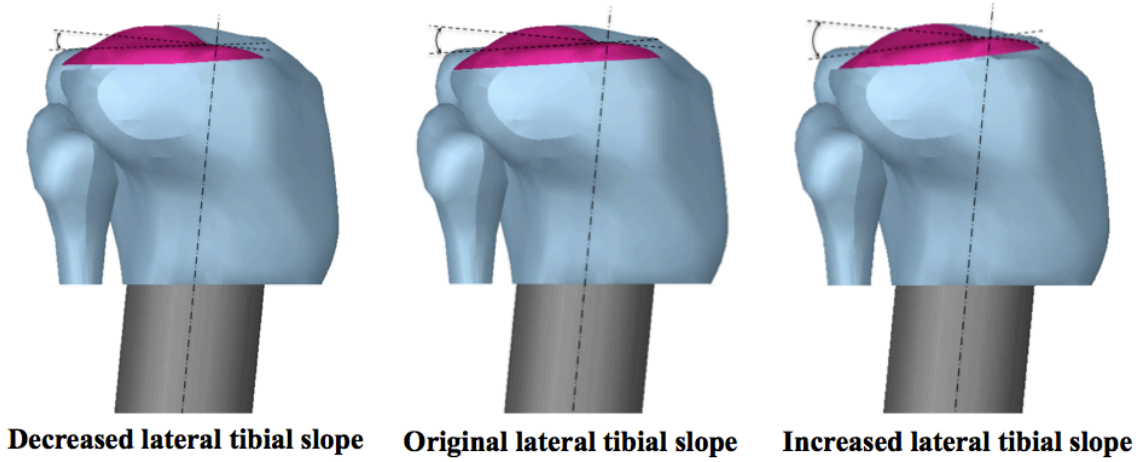

Figure 4.3 Schematic diagram of how the lateral tibial slope was altered. The lateral tibial slope was altered by rotating the separated lateral tibial plateau about an axis located on the center of mass for the lateral tibial plateu and perpendicular to the sagittal plane. The original lateral tibial slope was measured to be 8.5-degrees, then the change was repeated for every 1.0-degree ranging from 5.5-degrees and 13.5-degrees.

Similarly, the effect of the coronal plane alignment on AM-ACL strain was tested. To determine the lower limb coronal alignment, the mechanical axes of the femoral and

tibial shaft were used. The coronal alignment was altered by rotating the femoral shaft about an axis located on the tibial spine and perpendicular to the coronal plane (Figure 4.4). The model simulation was repeated for every 2.5-degrees ranging from 7.5-degree of varus to 10-degrees of valgus. For the neutral alignment (i.e., 180-degrees), the line of action for the quadriceps force (i.e., rectus femoris) was aligned with a Q-angle of 14.0-degrees[25]. As the coronal plane alignment changes, the line-of-action for the quadriceps force was also rotated by the corresponding angle in the same manner.

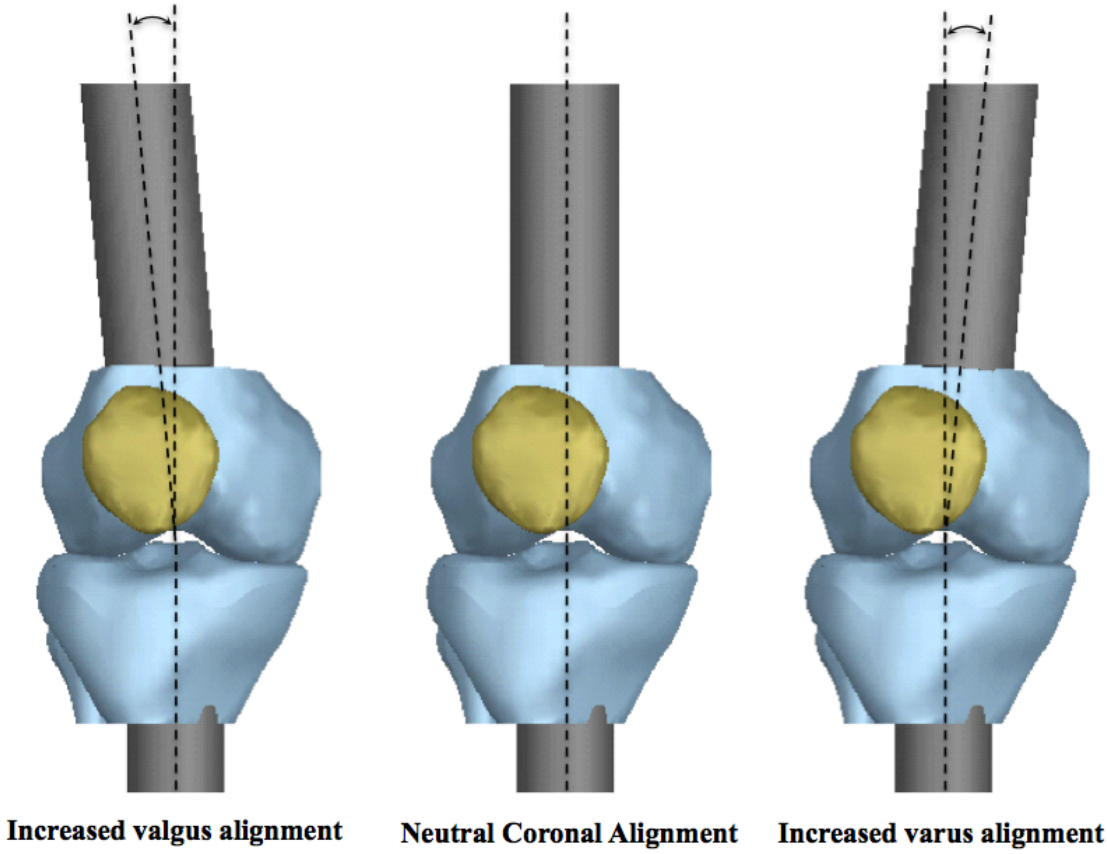

Figure 4.4 Schematic diagram of how the lower extremity coronal alignment was altered. The lower extremity coronal alignment was altered by rotating the femoral shaft, which represents a femoral mechanical axis, about an axis located on the tibial spine and perpendicular to the coronal plane. Starting from the neutral alignment, the change was repeated for every 2.5-degrees ranging from 7.5-degrees of varus and 10.0-degrees of valgus.

In order to investigate the effect of the medial tibial concavity, the depth of the medial concavity was altered by morphing the original geometry. Similar to the method used by Hashemi et al.[5], the medial tibial depth of the original geometry was measured to be 3-mm. To measure the medial tibial depth of the original geometry, the deepest point of the medial tibial plateau was found. A line connecting the anterior and posterior crests of the medial tibial plateau was drawn in the sagittal plane where the deepest point was included. Another line to parallel to this line was drawn to be tangent to the deepest point of the medial tibial plateau. The medial tibial depth was then defined as the distance between two parallel lines. The model simulation was repeated for every 0.5-mm ranging from 2.0-mm to 5.0-mm. (Figure 4.5)

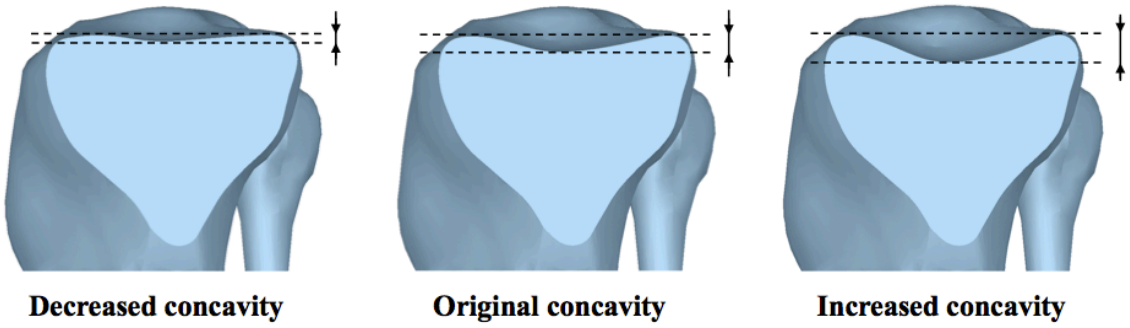

Figure 4.5 Schematic diagram of how the medial tibial concavity was altered. The medial tibial concavity was altered by morphing the concave geometry of the medial tibial plateau. The change was repeated for every 0.5-mm ranging from 2.0-mm to 5.0-mm.

4.4 Results

Model validation (Figure 4.6)

The 3D dynamic knee model was validated by comparing the quadriceps muscle force, AM-ACL strain, knee flexion angle, internal tibial rotation, and knee abduction angle predicted by the simulation with the corresponding values measured from a knee specimen under the baseline loading condition (Figure 4.6). The quadriceps muscle force, AM-ACL strain, knee flexion angle, internal tibial rotation, and knee abduction angle in the experiment and simulation for the first 100 msec were highly correlated with the Pearson correlation coefficients r = 0.988, 0.985, 0.981, 0.976, and 0.817 respectively.

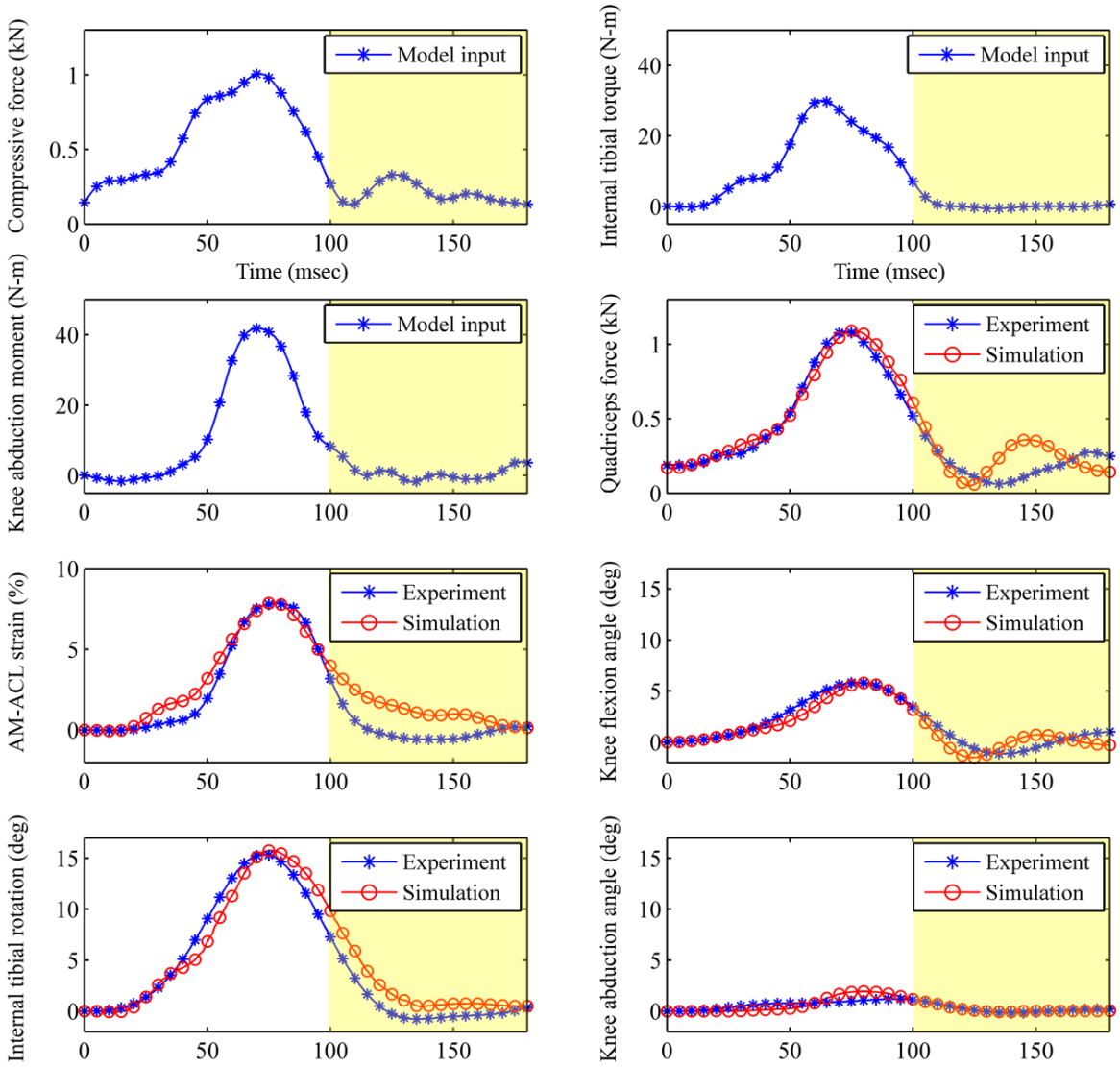

Figure 4.6 Model validation test: a) the impulsive compressive force, b) internal tibial torque, and c) knee abduction moment measured from the experiment were applied as the model input to drive the simulation; c) the quadriceps muscle force, d) AM-ACL strain, e) knee flexion angle, f) internal tibial rotation, and g) knee abduction angle calculated from the simulation were compared to the corresponding values measured from a single specimen and trial under the same input loading condition. The un-shaded area represents the data range used for the validation test.

Model-Predicted Effect of Lateral Tibial Slope on AM-ACL Strain (Figure 4.7)

As the lateral tibial slope increased, the peak AM-ACL strain increased under the identical input loading conditions. Approximately, the model predicted 1.5 % increase in the peak AM-ACL strain for every 1-degreee increase in the lateral tibial slope. In addition, the model simulation demonstrated that the increase in the lateral tibial slope resulted in the increases in the peak anterior tibial translation, peak internal tibial rotation, and peak knee abduction angle.

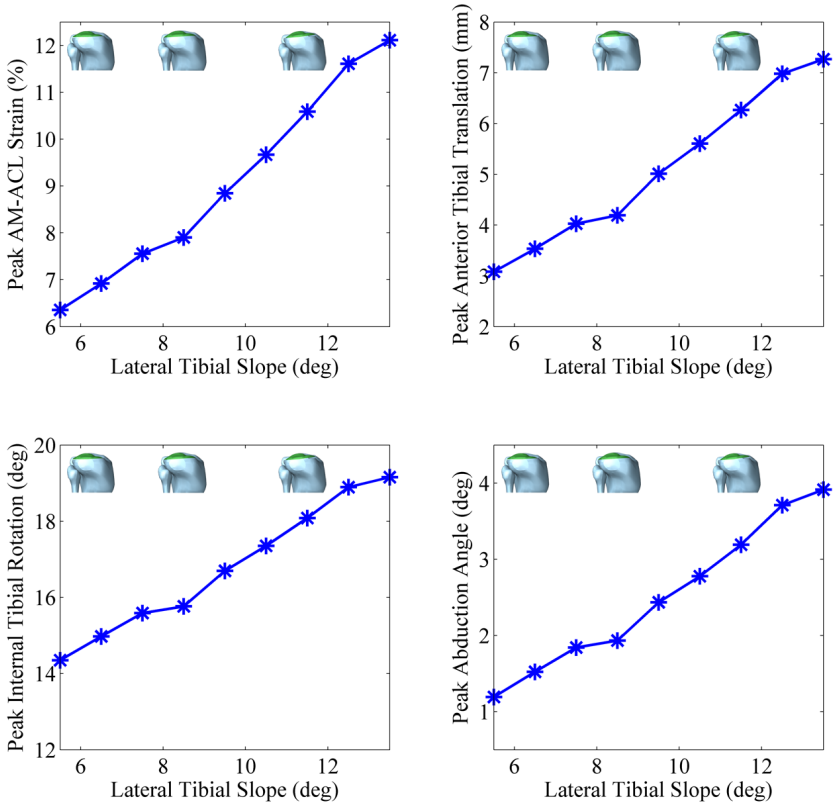

Figure 4.7 Model-predicted effect of the lateral tibial slope on the peak AM-ACL strain. As the lateral tibial slope increases, the difference between the medial and lateral tibial slope becomes greater. Under the impulsive compressive force, this difference in the medial and lateral tibial slope resulted in more pronounced effect of the coupled motion between 1) anterior tibial translation and internal tibial rotation and 2) internal tibial rotation and knee abduction angle.

Model-Predicted Effect of Frontal Plane Alignment on AM-ACL Strain (Figure 4.8)

Similarly, as the coronal plane alignment increased, the peak AM-ACL strain increased under the identical input loading conditions. However, the model predicted that the change of the coronal plane alignment ranging between -7.5-degrees and 10.0-degrees resulted in less than 2 % change in the AM-ACL strain. In addition, the model simulation demonstrated that the increase in the AM-ACL strain was explained by the increases in the peak anterior tibial translation, peak internal tibial rotation, and peak knee abduction angle.

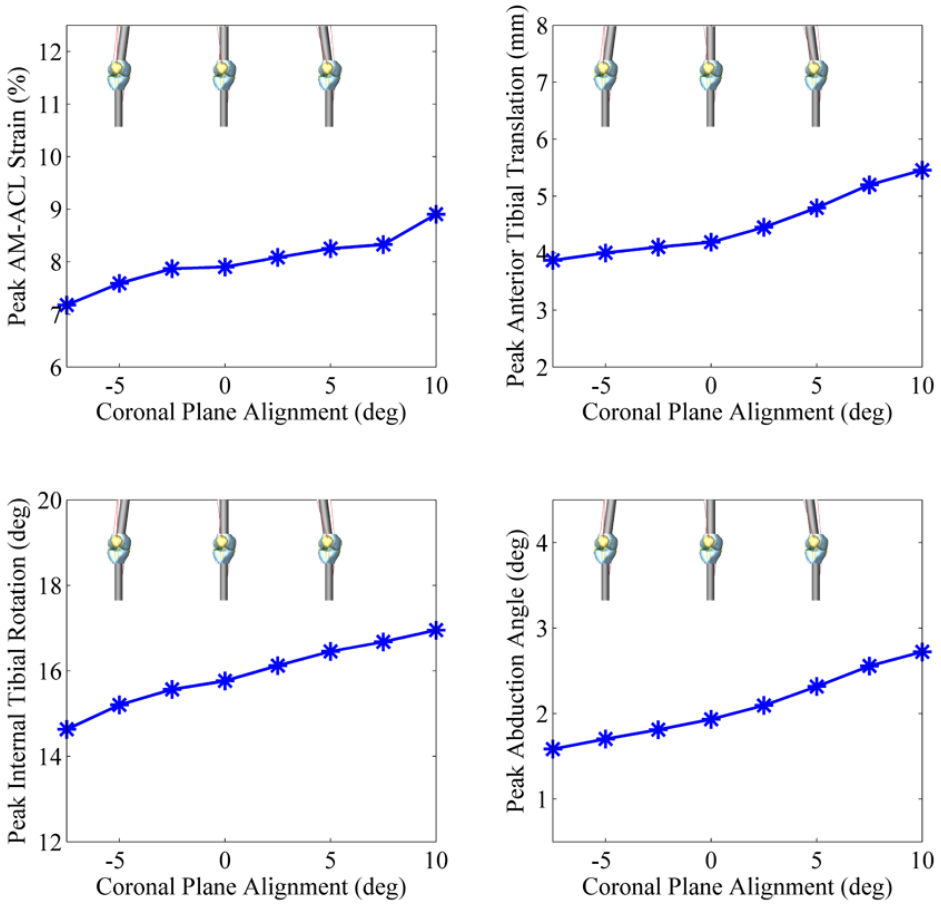

Figure 4.8 Model-predicted effect of the coronal plane alignment on the peak AM-ACL strain, peak anterior tibial translation, peak internal tibial rotation, and peak knee abduction angle.

Model-Predicted Effect of Medial Tibial Concavity on AM-ACL Strain (Figure 4.9)

As the medial tibial depth of concavity increased, the peak AM-ACL strain decreased under the same input loading conditions. Although the change in the AM-ACL strain was less than 2 % over the variation of the medial tibial depth between 2-mm and 5-mm, the model simulation consistently predicted an inverse relationship between the AM-ACL strain and the medial tibial depth of concavity. The decrease in the AM-ACL strain due the the increase in the medial tibial depth can be explained by the decreases in the anterior tibial translation and internal tibial rotation.

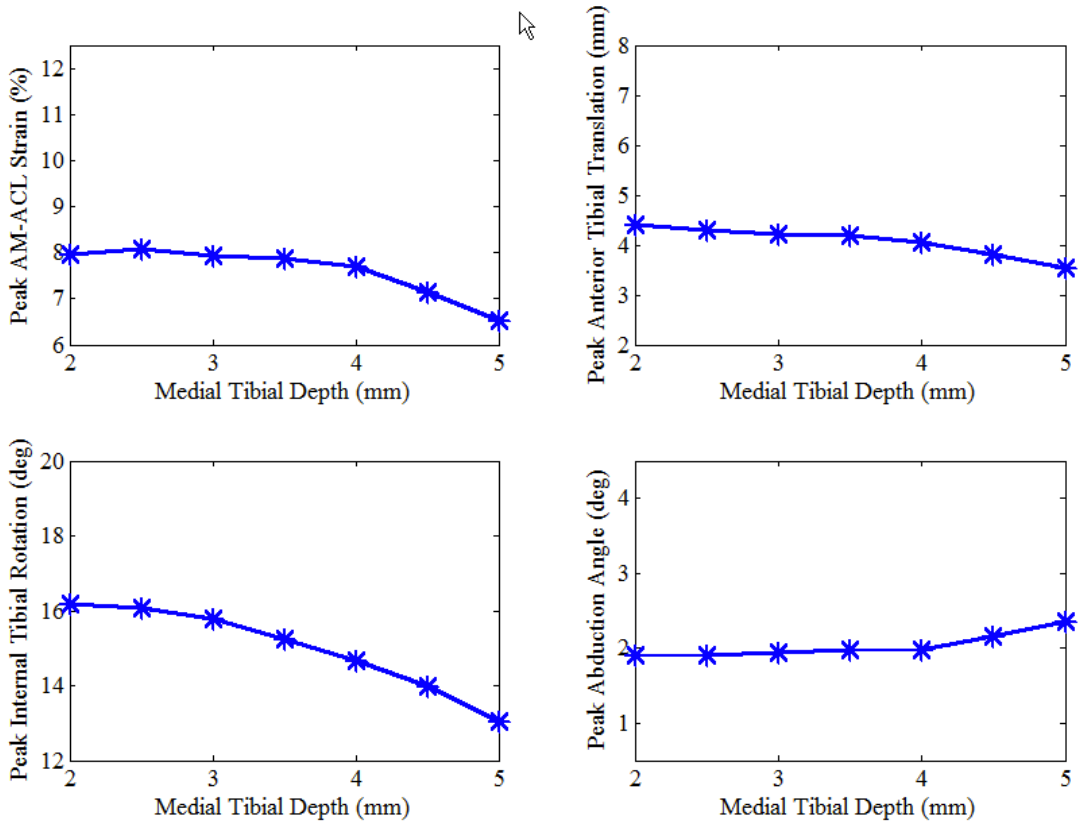

Figure 4.9 Model-predicted effect of the medial tibial concavity on the peak AM-ACL strain, peak anterior tibial translation, peak internal tibial rotation, and peak knee abduction angle.

4.5 Discussion

In our previous study, we performed an experiment of in vitro human cadaveric knees and a dynamic knee model simulation to replicate the experiment. One insight from the experiment was that although the worst-case loading condition as far as ACL strain is concerned is an internal tibial torque combined with a knee abduction moment, it is an internal tibial rotation, rather than a knee abduction moment, that primarily increases ACL strain during a jump landing. Another insight provided by the knee model simulation was that when the lateral tibial slope exceeds that of the medial tibial plateau, then an abduction moment causes a coupled internal tibial rotation along with the increased abduction angle. The model simulation also demonstrated that a knee abduction moment augments internal tibial rotation due to this coupling phenomenon and thus increases ACL strain, even without medial knee joint opening. The current study was designed to investigate the isolated effect of morphological factors on ACL strain under the worst-case loading condition, where an internal tibial torque and knee abduction moment were combined with an impulsive compressive force and knee flexion moment.

The present study demonstrated that the increase in the lateral tibial slope with the medial tibial slope unchanged accentuated the coupling phenomenon between internal tibial rotation and knee abduction angle, thereby increasing ACL strain. The ACL strain was the most sensitive to the increase in the lateral tibial slope, more precisely (i.e., 1.0 % ACL strain increase per 1.0-degree change), the increase in the difference between the medial and lateral tibial slope. This result corroborates McLean et al.'s work in that peak knee abduction angle and peak internal tibial rotation are both significantly correlated with a ratio between medial and lateral tibial slope when the lateral tibial slope is greater

than the medial tibial slope.[8] As Simon et al. conceptually explained, the difference between the medial and lateral tibial plateau with the lateral tibial slope greater causes the lateral side of the femur to slide posteriorly off of the lateral tibial plateau when an axial compressive force is applied.[7] Previous studies report that acute ACL injury is usually associated with the posterior lateral compartment bone bruises suggesting that large knee abduction moment, anterolateral subluxation of the tibia, or internal tibial rotation may cause those bone bruise patterns.[26-29] Collectively, the mechanism causing the posterior lateral tibial bone bruise patterns can be narrowed down to internal tibial rotation since anterolateral subluxation can be another expression of internal tibial rotation and knee abduction moment can result in internal tibial rotation due to the coupling phenomenon. Thus, the lateral tibial slope or the difference in the medial and lateral tibial slope should be considered a risk factor for ACL injury.

This study corroborates previous findings in that a static frontal plane limb alignment can be used as a risk factor for ACL injury. The ACL strain was varied within 2 % when the frontal plane alignment was altered ranging from 7.5-degrees varus alignment to 10.0-degrees valgus alignment. The contribution from the frontal plane alignment to the increase in ACL strain was relatively smaller (i.e., 0.1 % ACL strain increase per 1.0-degree change) compared to the effect of the lateral tibial slope. In current literature, the association between a static measurement of either frontal plane limb alignment or Q-angle and ACL injury risk is not in agreement. This inconsistency in the role of the static frontal plane limb alignment to increase ACL injury risk may be explained by the relatively smaller contribution in our results.

The medial tibial depth of concavity showed a modest effect on ACL strain. When the medial tibial depth was decreased so as to make the medial tibial plateau flatter, the ACL strain slightly increased and appeared to be saturated. However, the increase in medial tibial depth resulted in more pronounced decrease in ACL strain (i.e., 0.7 % ACL strain decrease per 1.0-mm change). Interestingly, the increase curvature of the medial tibial plateau resulted in the decreased internal tibial rotation and anterior tibial translation, thereby reducing the ACL strain. From an engineering perspective, the increased curvature of the medial tibial plateau, particularly the increased slope in the anterior portion of the medial tibial plateau, caused more of the axial compressive force to counteract to the applied internal tibial torque. Overall, our results corroborate the previous works in that a shallow medial tibial concavity could be used as a risk factor for ACL injury.

There are several limitations to this study. First, the knee model is not specimen-specific. Two different knees were used to get MR images for the reconstruction and the experimental data for the model validation, respectively. However, the knee for the experimental data was chosen since the temporal data were a representative sample of all other knees tested in our previous study. In addition, the knee for the MR images showed close measurements in the medial and lateral tibial slope and the medial tibial concavity compared to other studies.[5,8] If we generalize the results in this study to all other knees, although some minor differences could be seen, we do not expect that the qualitative trends of the effect of lateral tibial slope, frontal plane limb alignment, and medial tibial concavity would change. Second, the material properties were adapted from literatures. In addition, the location of the origin and insertion for the ligamentous structures was

adjusted starting from the MR scans in order to match the simulation to the experimental data. Although the errors in the material properties may affect the results in this study, the relative contribution from those three structural factors should be preserved. Third, in this model, the meniscus was not considered. Although the addition of the meniscus may result in the increase of the concavity, the effect is likely to be minor. Finally, when the knee reached an equilibrium state at 15-degrees knee flexion angle prior to impact, the initial strain values for the medial and lateral collateral ligament and posterior joint capsular structures were set close to zero.

4.6 Conclusions

In conclusion, the current study demonstrates that the increased difference in medial and lateral tibial slopes accentuates the coupled motion between internal tibial rotation and knee abduction angle, thereby increasing ACL strain during a simulated jump landing in the presence of muscle forces. Although the effect of changing frontal plane limb alignment was smaller compared to the tibial slope effect, the increased valgus limb alignment resulted in the increased ACL strain. The increased medial tibial depth of concavity also contributed to the decreased ACL strain. Therefore, this study supports that a greater difference in medial and lateral tibial slope, more valgus limb alignment, and shallower medial tibial concavity should be considered risk factors for ACL injury.

4.7 References

1. Allografts in Sports Medicine: What Do We Know, Need to Know, and Need to Do? Round table discussion: American Orthopaedic Society for Sports Medicine; February 13, 2006; Park City, UT.

2. Lohmander, LS, Englund PM, Dahl LL, Roos EM. The long-term consequence of anterior cruciate ligament and meniscus injuries - Osteoarthritis. Am J Sports Med. 2007;35:1756-1769.

3. Renstrom P, Ljungqvist A, Arendt E, Beynnon B, et al. Non-contact ACL injuries in female athletes: an International Olympic Committee current concepts statement. Br J Sports Med. 2008;42(6):394-412.

4. Brandon ML, Haynes PT, Bonamo JR, Flynn MI, Barrett GR, Sherman MF. The association between posterior-inferior tibial slope and anterior cruciate ligament insufficiency. Arthroscopy. 2006;22:894-899.

5. Hashemi J, Chandrashekar N, Mansouri H, et al. Shallow medial tibial plateau and steep medial and lateral tibial slopes new risk factors for anterior cruciate ligament injuries. Am J Sports Med. 2010;38(1):54-62.

6. Stijak L, Herzog RF, Schai P. Is there an influence of the tibial slope of the lateral condyle on the ACL lesion? A case-control study. Knee Surg Sports Traumatol Arthrosc. 2008;16:112–117.

7. Simon RA, Everhart JS, Nagaraja HN, Chaudhari AM. A case-control study of anterior cruciate ligament volume, tibial plateau slopes and intercondylar notch dimensions in ACL-injured knees. J Biomech. 2010;43:1702-1707.

8. McLean SG, Lucey SM, Rohrer S, et al. Knee joint anatomy predicts high-risk in vivo dynamic landing knee biomechanics. Clin Biomech. 2010;25(8):781-788.

9. Huston LJ, Greenfield M. Wojtys EM. Anterior cruciate ligament injuries in the female athlete: potential risk factors, Clinical Orthopaedics and Related Research. 2000;372:50–63.

10. Moul JL. Differences in selected predictors of anterior cruciate ligament tears between male and female NCAA division I collegiate basketball players, Journal of Athletic Training. 1998;33:118–121.

11. Buchanan PA. Developmental perspectives on basketball players' strength, knee position in landing, and ACL injury gender differences. Dissertation, Indiana University, Bloomington, 2003.

12. Heiderscheit BC, Hamill J, Caldwell GE. Influence of Q-angle on lower-extremity running kinematics. J Orthop Sports Phys Ther. 2000;30:271–278

13. Mizuno Y, Kumagai M, Mattessich SM, et al. Q-angle influences tibiofemoral and patellofemoral kinematics. J Orthop Res. 2001;19:834–840

14. Shambaugh JP, Klein A, Herbert JH. Structural measures as predictors of injury in basketball players. Med Sci Sports Exerc. 1991;23:522–527

15. Endsley ML, Ford KR, Myer GD, Slauterbeck JR, Hewett TE. The effects of gender on dynamic knee stability and Q-angle in young athletes. Ohio Physical Therapy Association fall conference. Cleveland State University, Cleveland, 2003

16. Gray J, Taunton JE, McKenzie DC, Clement DB, McConkey JP, Davidson RG. A survey of injuries to the anterior cruciate ligament of the knee in female basketball players. Int J Sports Med 1985;6:314–316

17. Myer GD, Ford KR, Hewett TE. The effects of gender on quadriceps muscle activation strategies during a maneuver that mimics a high ACL injury risk position. J Electromyogr Kinesiol. 2005;15:181–189

18. Pantano KJ, White SC, Gilchrist LA, Leddy J. Differences in peak knee valgus angles between individuals with high and low Q-angles during a single limb squat. Clin Biomech. 2005;20:966–972

19. Khan MS, Seon JK, Song EK. Risk factors for anterior cruciate ligament injury: assessment of tibial plateau anatomic variables on conventional MRI using a new combined method. Int Orthop. 2011. (in press)

20. Oh YK, Lipps DB, Ashton-Miller JA, Wojtys EM. The effect of axial tibial rotation and varus or valgus loading on ACL strain during a simulated jump landing (submitted to AJSM)

21. Shin CS, Chaudhari AM, Andriacchi TP. The influence of deceleration forces on ACL strain during single-leg landing: A simulation study. J Biomech. 2007;40(5):1145-1152.

22. Merican AM, Sanghavi S, Iranpour F, Amis AA. The structural properties of the lateral retinaculum and capsular complex of the knee. J Biomech. 2009;42:2323-2329.

23. Robinson, JR, Bull AMJ, Amis AA. Structural properties of the medial collateral ligament complex of the human knee. J Biomech. 2005;38:1067-1074.

24. Oh YK, Kreinbrink JL, Ashton-Miller JA, Wojtys EM. Effect of ACL transection on internal tibial rotation in an in vitro simulated pivot landing. J Bone Joint Surg Am. 2011 Feb;93(4):372-80.

25. Aglietti P, Insall JN, Cerulli G. Patellar pain and incongruence. I: Measurements of incongruence. Clin Orthop Relat Res. 1983;176:217-24.

26. Graf BK, Cook DA, Desmet AA, et al. Bone bruises on magnetic-resonance-imaging evaluation of anterior cruciate ligament injuries. Am J Sports Med. 1993;21(2):220-223.

27. Johnson DL, Urban WP, Caborn DNM, Vanarthos WJ, Carlson CS. Articular cartilage changes seen with magnetic resonance imaging-detected bone bruises associated with acute anterior cruciate ligament rupture. Am J Sports Med. 1998;26:409-414.

28. Spindler KP, Schils JP, Bergfeld JA, et al. Prospective study of osseous, articular, and meniscal lesions in recent anterior cruciate ligament tears by magnetic resonance imaging and arthroscopy. Am J Sports Med. 1993;21:551-557.

29. Nishimori M, Deie M, Adachi N, Kanaya A, Nakamae A, Motoyama M, Ochi M. Articular cartilage injury of the posterior lateral tibial plateau associated with acute anterior cruciate ligament injury. Knee Surg Sports Traumatol Arthrosc. 2008 Mar;16(3):270-4.

CHAPTER 5

EFFECT OF ACL TRANSECTION ON INTERNAL TIBIAL ROTATION IN AN *IN VITRO* SIMULATED PIVOT LANDING

5.1 Abstract

The amount of resistance provided by the anterior cruciate ligament (ACL) to axial tibial rotation remains controversial. The goal of this study was to test the primary hypotheses that under the large impulsive loads associated with a simulated pivot landing ACL transection would not significantly affect the resulting tibial rotation, but would increase the anterior tibial translation.

Twelve cadaveric knees [mean (SD) age: 65.0 (10.5) years] were mounted in a custom testing apparatus to simulate a single-leg pivot landing. A compound impulsive load was applied to the distal tibia with compression (~800 N), flexion moment (~40 N-m), and axial tibial torque (~17 N-m) in the presence of five trans-knee muscle forces. A DVRT mounted on the anteromedial aspect of the ACL measured relative strain. With the knee initially in 15 degrees flexion, after five combined compression and flexion moment ('baseline') loading trials, six trials were conducted with the addition of either internal or external tibial torque ('internal' or 'external' loading), and then the six 'baseline' trials were repeated. The ACL was then sectioned, six 'baseline' trials were

repeated and then six trials of either 'internal' or 'external' loading condition, whichever initially resulted in the larger relative ACL strain. Tibiofemoral kinematics were measured optoelectronically. The results were analyzed by a non-parametric Wilcoxon Signed-Rank test.

Following ACL transection, the increase in the normalized internal tibial rotation was statistically significant, but small (0.7 ± 0.3 to 0.8 ± 0.3 degrees/N-m, p=0.012), while anterior tibial translation significantly increased (3.8 ± 2.9 to 7.0 ± 2.9 mm, p=0.017).

ACL transection leads to a small increase in internal tibial rotation, equivalent to a 13% decrease in the dynamic rotational resistance, under the large forces associated with a simulated pivot landing, but a significant increase in the anterior tibial translation.

5.2 Introduction

Over 200,000 anterior cruciate ligament (ACL) injuries are reconstructed each year in the United States.1 Despite surgical treatment, the development of post-traumatic degenerative disease has been reported, perhaps due to sub-optimally restored knee joint kinematics. As part of an effort to better restore knee joint kinematics and reduce the risk of degenerative changes of the knee joint, alternative surgical techniques have been introduced including a double-bundle reconstruction and a single-bundle reconstruction with more oblique ACL graft orientation in the sagittal and coronal plane.2 Both techniques attempt to improve knee joint kinematics in axial tibial rotation in addition to anterior tibial translation. While it is well documented that the ACL plays a primary role

in restraining anterior tibial translation, the role of the ACL in limiting axial tibial rotation remains controversial in the literature.3

Previous in vivo and in vitro studies regarding the role of ACL in limiting axial tibial rotation are not in agreement.[4-9] Recently, Markolf et al. reported the largest increase in internal tibial rotation under a 5 N-m internal tibial torque during passive knee extension test, i.e., 7.3 ± 3.4 and 4.0 ± 2.8 degrees at 0 and 30 degrees knee flexion angle, respectively.[4] Similarily, Lipke et al. found that sectioning the ACL caused less than 5 degrees increase in internal tibial rotation with being significant when the cadaveric knee specimens were quasi-statically tested under 10 N-m of axial tibial torques in the presence of the quadriceps muscle force.[5] An *in vivo* study by DeFrate et al. showed that ACL deficiency resulted in a significant increase in both anterior tibial translation (i.e., ~3 mm) and internal tibial rotation (i.e., ~ 2 degrees) at a low knee flexion angle during a quasi-static lunge.[10] On the other hand, Lane et al. performed an *in vitro* study in that a 5 N-m of internal or external tibial torque was quasi-statically applied to the quadriceps-stabilized knee specimens varying the knee flexion angle from 0 to 60 degrees.[6] The increases in the internal tibial rotation were less than 4 degrees with being statistically insignificant for both weight-bearing (89 N) and non-weight-bearing conditions. Similarly, Wroble et al. reported that the 2~3 degrees increase in internal tibial rotation was too small to be clinically important despite the statistical significance[8]. These differing observations on the functional implications of ACL deficiency regarding knee axial rotational resistance have been quantified using quasi-static biomechanical outcome measurements, usually in the absence of muscle forces or under modest test loads. Snyder-Mackler et al. have demonstrated that passive joint laxity is poorly correlated

with the patient's functional or dynamic ability.[11] Given how common large dynamic knee loads are *in vivo*,[12] it would seem worthwhile to investigate how ACL transection affects axial tibial rotation in the presence of muscle forces and under the large dynamic loads associated with a pivot landing involving an internal tibial torque.

The anterior tibial translation that is coupled with tibial rotation has been measured in order to determine the degree of 'rotational resistance' provided by the ACL under axial tibial torques.[13-15] Kanamori et al. observed significant increases in both the internal tibial rotation and the coupled anterior tibial translation in response to either a 10 N-m of internal tibial torque or a combined torque of 10 N-m of internal tibial torque and 10 N-m valgus moment.[13] Although the increased internal tibial rotation was statistically significant, the magnitude of the internal tibial rotation was less than 3 degrees at low flexion angles. Diermann et al. employed a robotic methodology to investigate the effect of ACL deficiency under a combined torque of 10 N-m valgus moment and 4 N-m internal tibial torque.[16] They found similar results: ACL deficiency caused a significant increase in anterior tibial translation, but not in internal tibial rotation. Thus they concluded that the anterior tibial translation should be evaluated rather than internal tibial rotation for objective assessments of the contribution provided by the ACL on resisting a combined rotatory load. Worth noting is that these data appear to be contradictory because the internal tibial rotation can cause ACL strain, but the increase in internal tibial rotation following ACL transection is not as large as might be expected. Hence, it would be worthwhile to investigate how these contradictory observations might be reconciled by comparing the effect of ACL transection on knee behavior under a realistic pivot landing scenario.

The goal of this study, therefore, was to examine the effect of ACL transection on axial tibial rotation and anterior tibial translation in cadaveric knees placed under compound impulsive loading in the presence of simulated muscle forces. The primary hypotheses were that transecting the ACL would not increase tibial axial rotation, but would increase anterior tibial translation.

5.3 Methods

Specimen Procurement and Preparation

Twelve unembalmed cadaveric limbs [mean (SD) age: 65.0 (10.5) years; eight females] were acquired from the University of Michigan Anatomical Donations Program. All lower extremities were visually checked for scars, indication of surgery, severe misalignments or deformities. Prior to specimen procurement, frontal plane digital images of axially compressed and fully extended knees were taken to determine the natural alignment angle. Following the methods of Withrow et al.[17-19] lower extremities were cut ~8 inches proximal and distal to the knee joint in order to standardize specimen length. Specimens were then dissected, leaving the ligamentous knee structures and the tendons of quadriceps, medial hamstrings (sartorius, gracilis, semitendinosus, semimembranosus), lateral hamstring (biceps femoris) and medial and lateral gastrocnemius muscles intact. Each end of the specimen was potted using polymethylmethacrylate. The frontal plane alignment of the knee specimens was reproduced based upon the above frontal plane digital images. The dissected specimens were frozen at -20°C until needed and thawed at room temperature for at least 12 hours before testing commenced.

Knee Testing Apparatus

The Withrow et al.[17-19] testing apparatus was used to simulate the position of a single extremity as it strikes the ground while landing on one leg during a jump or pivot maneuver. The simulated quadriceps and medial and lateral gastrocnemius muscles were represented by elastic structures (~2 mm woven nylon cord, tensile stiffness ~2 kN/cm) pre-tensioned to 180 N and 70 N each, respectively.[17] Two custom-made constant force springs (pre-tensioned to 70 N each) were used to represent the medial and lateral hamstring muscle forces. Each simulated muscle-tendon unit was connected from the femur or tibia to the relevant tendons via cryo-clamps through the anatomical lines-of-action, thereby representing its *in vivo* dynamic resistance to sudden stretch. In all trials, an initial knee flexion angle of 15 degrees was maintained. A jump landing ground reaction force was simulated by dropping a weight onto the distal tibia of an inverted knee so as to generate a 2*BW (where BW is each donor's postmortem body-weight) impulsive force. The weight drop was initiated in a standardized manner via a quick-release mechanism. A customized shock absorber (ACE Controls Inc., Farmington, MI) was attached in series at the distal end of the drop weight so that the ground reaction force peaked at 50 msec. In a new departure from the original Withrow et al. apparatus, the linear momentum of the weight at impact was transformed into the combination of an axial compressive force and an impulsive axial torque component (peaking at 70 ms) by a specially-designed torsional transformer device mounted in series with the distal tibia (Figure 5.1). The device consisted of two circular plates between which three inclined palls are located, the angle of the palls to the vertical being adjustable and preset to give the desired gain between the applied compressive force and the rotational torque

delivered to the specimen. The peak axial torque was adjusted to reach a nominal value between 10 and 25 Nm and recorded.

As in Withrow's et al. apparatus,[17-19] two 6 degree-of-freedom load cells (AMTI, Watertown, MA) measured the 3-D tibial forces and moments delivered to the construct, as well as the 3-D femoral reaction forces and moments. A 3-mm DVRT (Microstrain, Burlington, VT) was mounted on the anteromedial (AM) bundle of the ACL to record ACL relative strain. In order to standardize the location of the DVRT on the AM-ACL, it was placed at a first quartile of the ACL length measured from the tibial attachment site of the ACL.

Five single degree-of-freedom load cells (Transducer Techniques, Temecula, CA) measured simulated muscle tensions. Impulsive forces, the five muscle forces and ACL strain data were recorded at 2 kHz using a 16-bit analog-to-digital converter board, while tibiofemoral kinematics, which was defined in accordance with the work of Grood and Suntay[20], was recorded at 400 Hz using an Optotrak Certus system (Northern Digital, Inc., Waterloo, Canada).

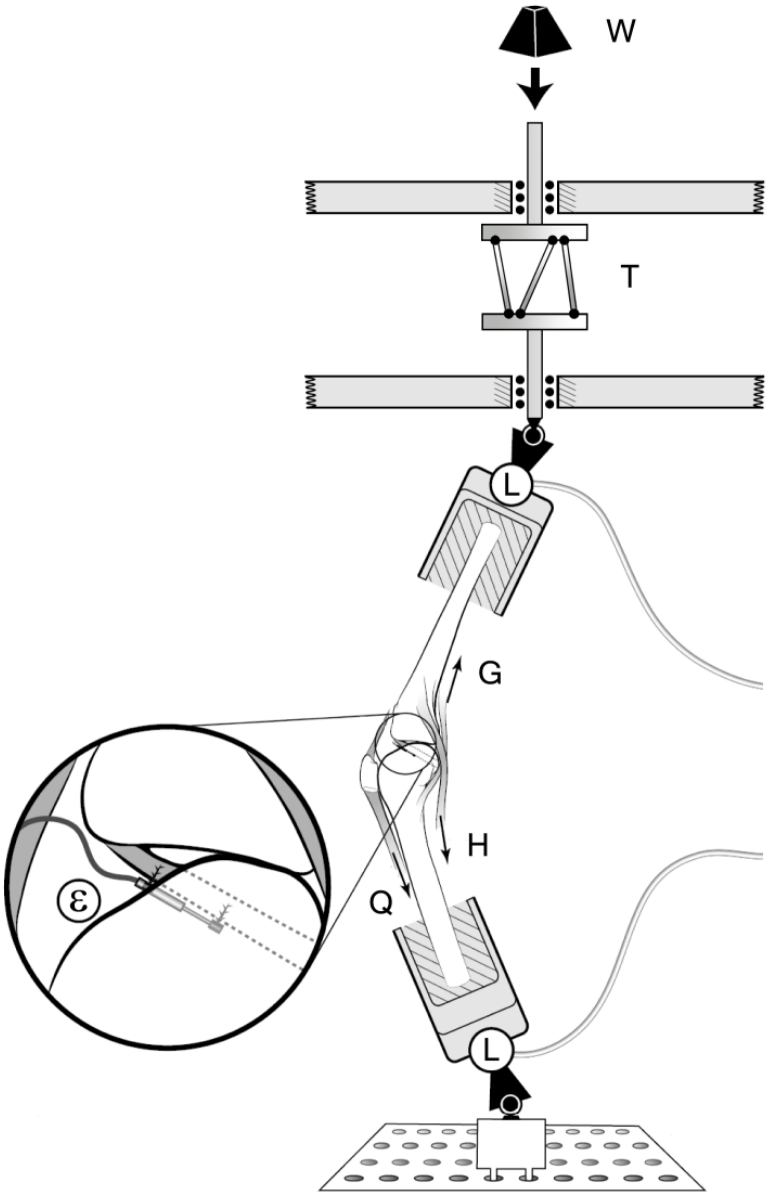

Figure 5.1 Schematic diagram showing how a weight ('W') dropped from a fixed height onto the torsional transformer device ('T') applies impulsive compression and axial torque to the distal tibia of an inverted knee specimen. The two load transducers ('L') measure the three components of force and moment applied to the knee specimen in the presence of quadriceps ('Q'), hamstrings ('H') and 'gastrocnemius ('G') forces, while a miniature displacement transducer ('ε') implanted on the surface of the anteromedial bundle measures strain.

Testing Protocol (Table 5.1)

The baseline loading condition ('Base1', 'Base2', and 'Base3') was designed to simulate a drop landing where the impulsive ground reaction force provides the compressive force on the knee joint and induces the knee flexion, thereby causing sudden stretch of the quadriceps muscle-tendon unit. In addition, the stretch of the quadriceps muscle-tendon unit resulted in the posterior femoral displacement thereby straining the ACL. For the axially-directed loading condition ('Int1', 'Ext1', 'Int2', and 'Ext2'), either internal or external tibial torque was added to the baseline loading condition.

During the first five pre-conditioning trials, the height of the weight drop was varied to find the drop height that best simulated a 2*BW impulsive ground reaction force for the baseline loading condition. That drop height was then maintained throughout all trials to apply the same kinetic energy to the knee specimens. After the five pre-baseline trials ('Base1'), three blocks of six trials were run on each ACL-Intact specimen in a 'Base1 – B – C – Base2' design, where the blocks 'B' and 'C' were randomized to be either an internally-directed ('Int1') or externally-directed ('Ext1') axial tibial torque combined with a standard compression force and a flexion moment, followed by the post-baseline trial block ('Base2'). The ACL was then transected. Two blocks of six trials were then repeated on each ACL-Deficient specimen in an 'Base3 – D' design, where 'Base3' was the baseline trial for ACL-Deficient specimens and 'D' (either 'Int2' or 'Ext2') was applied in the direction of the axial tibial torque trial that resulted in the larger ACL relative strain in the 'B' and 'C' conditions. The first trial for each configuration was considered a pre-conditioning trial and the last five trials were used to calculate the biomechanical variables.

Table 5.1 Testing protocol (see text for abbreviations).

Protocol	Loading type
ACL-Intact Condition	
Base1	Compression + Flexion moment
Int1*	Compression + Flexion moment + Internal tibial torque
Ext1*	Compression + Flexion moment + External tibial torque
Base2	Compression + Flexion moment
ACL-Deficient Condition	
Base3	Compression + Flexion moment
Int2 or Ext2**	Compression + Flexion moment + Internal or External tibial torque

* The sequence of Int1 and Ext1 tests was randomized.
** The direction of the axial tibial torque was chosen based on Int1 and Ext1

Statistical Analysis

The peak internal tibial rotation for each of the 10 specimens that fulfilled the 'Int2' condition during the internally-directed trials was normalized by the peak internal tibial torque. This was done for the last five trials from each loading condition (i.e., 'Int1' and 'Int2') and averaged for each specimen. The primary hypotheses were tested that (a) the normalized peak internal tibial rotation for the ACL-Deficient state would be no different than that for the ACL-Intact state, and (b) the anterior tibial translation would significantly increase following ACL transection. A non-parametric Wilcoxon Signed-Rank test was used to test the hypotheses. An alpha level of 0.05 was chosen for the level of significance.

5.4 Results

Ten of the 12 specimens [mean (SD) age: 65.0 (11.2) years, mean (SD) body-weight: 655.0 (147.2) N, eight females] exhibited larger peak ACL relative strain under the internal tibial axial torque than under the external tibial torque. According to the protocol, these 10 were therefore re-tested after ACL transection under the combination of the standard compression force, flexion moment, and internal tibial torque in the testing condition, 'D', in order to test the primary hypotheses. The remaining two specimens were tested under external tibial torque. Sample temporal behaviors from a single specimen and trial are shown in Figure 5.2.

There were no differences between two baseline loading conditions for the ACL-Intact state (i.e., 'Base1' and 'Base2'), thereby confirming the knee specimens were not damaged during the testing.

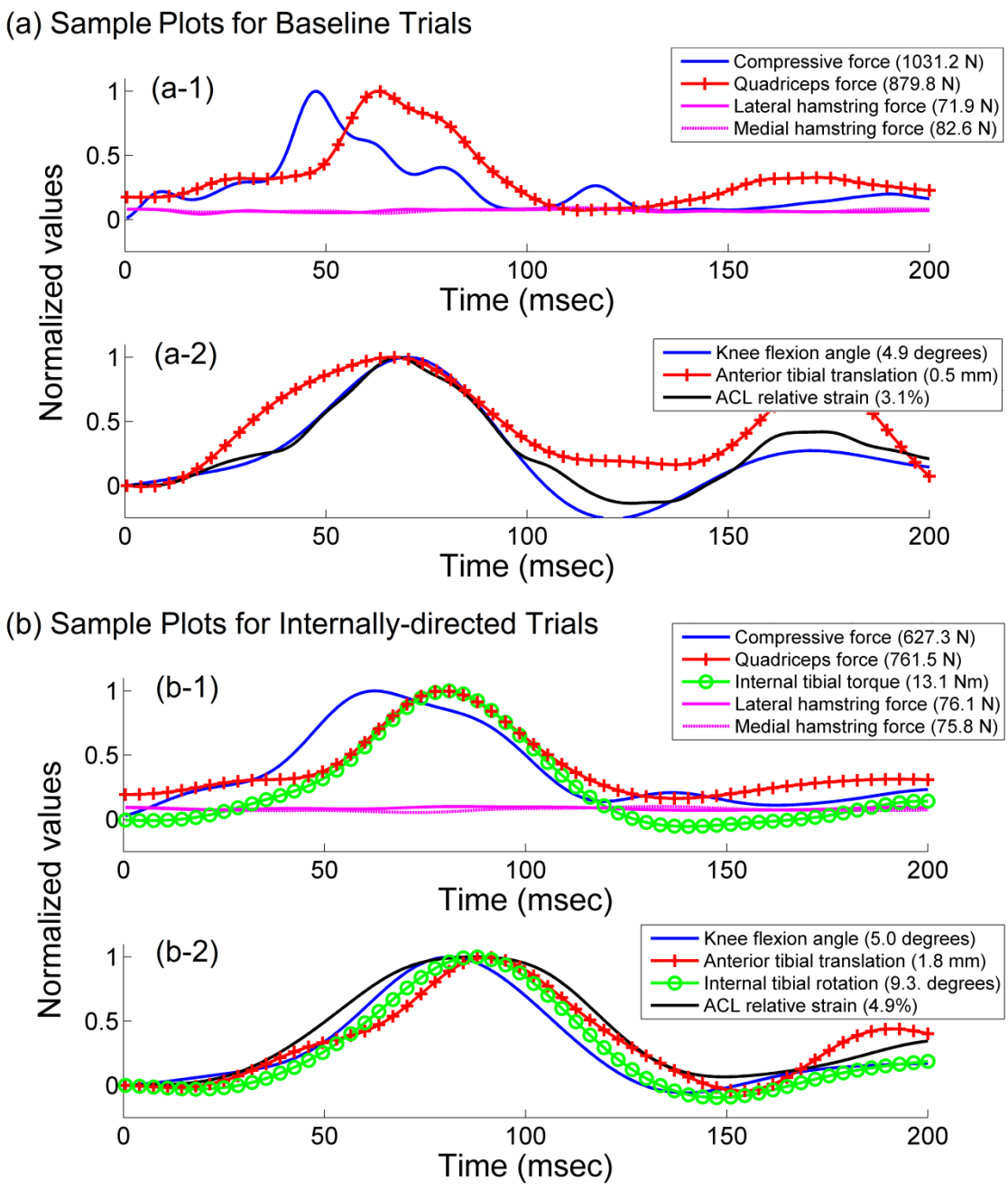

Figure 5.2 Sample temporal behavior of the applied impulsive compressive force, resulting quadriceps force, internal tibial torque, knee flexion angle, anterior tibial translation, internal tibial rotation, and ACL relative strain from a single loading trial under the (a) baseline and (b) internally-directed loading condition for specimen F32797L. Measurements have been normalized to their peak values (see legends).

Effect of ACL Transection on the Internal Tibial Rotation

Under the baseline loading conditions, in the absence of any applied axial tibial torque, the resulting internal tibial rotations were 1.6 ± 1.2 degrees and 2.5 ± 1.5 degrees for the ACL-Intact ('Base1') and ACL-Deficient ('Base3') conditions, respectively (Figure 5.3). The internal tibial torque induced internal tibial rotations of 11.6 ± 2.8 degrees and 12.1 ± 3.0 degrees for the ACL-Intact ('Int1') and ACL-Deficient ('Int2') conditions, respectively (Figure 5.3).

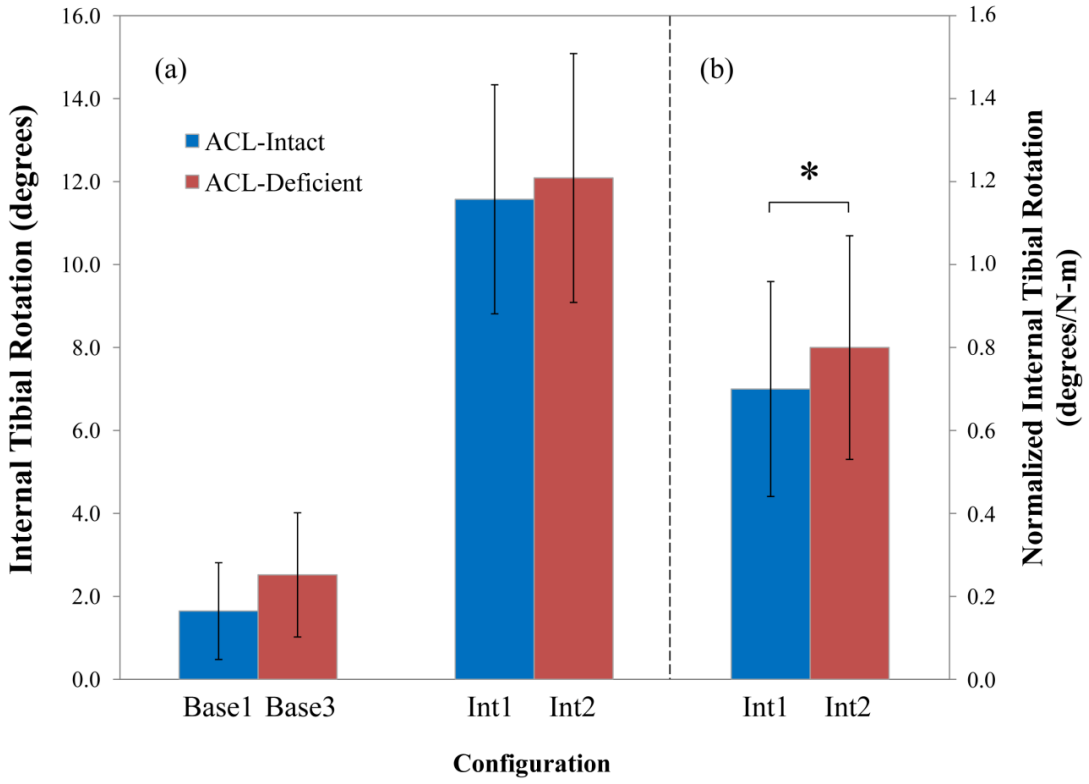

Figure 5.3 (a) Mean (SD, represented by error bars) peak internal tibial rotation under the baseline and internally-directed loading conditions for the ACL-Intact ('Base1' and 'Int1') and ACL-Deficient ('Base3' and 'Int2') state. ACL transection resulted in an increase of 0.9 degrees and 0.5 degrees, respectively, in internal tibial rotation for the baseline and internally-directed loading conditions, respectively. (b) Normalized internal tibial rotation in the presence of the internal tibial torque for the ACL-Intact ('Int1') and ACL-Deficient ('Int2'). In this and the following figure, the asterisks indicate a significant difference (see text).

In a test of the first primary hypothesis, the increase in the normalized internal tibial rotation caused by ACL transection was significant under the compound loading with internal tibial torque: 0.7 ± 0.3 degrees/N-m and 0.8 ± 0.3 degrees/N-m for the ACL-Intact ('Int1') and the ACL-Deficient ('Int2') states, respectively (p=0.012, Figure 5.3). This corresponds to a 13 % decrease in the dynamic rotational resistance compared to the ACL-Intact states.

Effect of ACL Transection on the Anterior Tibial Translation

In the absence of any applied axial tibial torque, the anterior tibial translations of the center of the tibial plateau were 1.2 ± 1.1 mm and 3.9 ± 2.1 mm for the ACL-Intact ('Base1') and ACL-Deficient ('Base3') condition, respectively (Figure 5.4, p=0.009). In the presence of the internal tibial torque, ACL transection caused the anterior tibial translations of the center of the tibial plateau to increase from 3.8 ± 2.9 mm for the ACL-Intact ('Int1') to 7.0 ± 2.9 mm for the ACL-Deficient ('Int2') condition, respectively, supporting the second primary hypothesis (Figure 5.4, p=0.017).

In order to investigate the portion of the anterior tibial translation caused by the internal tibial torque, the increments due to the addition of internal tibial torque to the baseline loading condition were calculated by subtracting the anterior tibial translation for the baselines (e.g., 'Base1' or 'Base3') from the corresponding value for the internally-directed loading conditions (e.g., 'Int1' or 'Int2'). After ACL transection, these increments were 2.6 ± 2.0 mm and 3.0 ± 1.5 mm for the ACL-Intact and ACL-Deficient state, respectively (cf., 'Δ1' vs. 'Δ2', Figure 5.4).

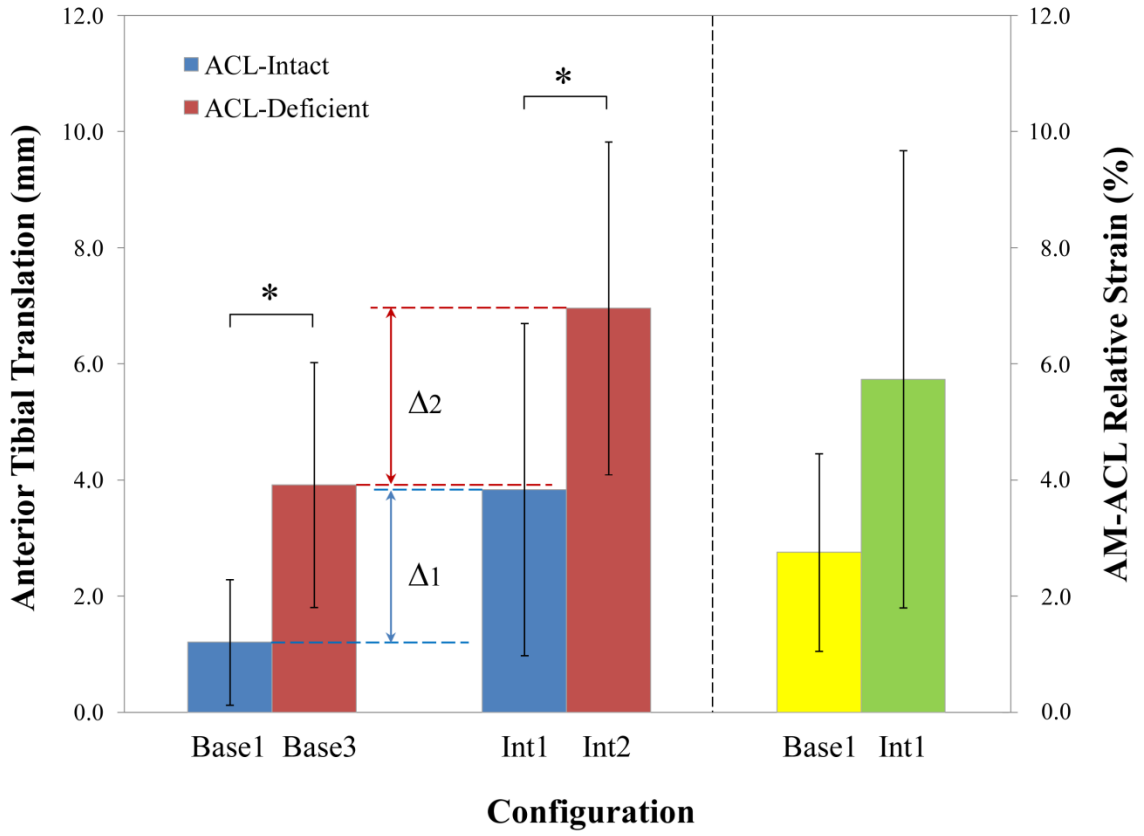

Figure 5.4 Mean (SD) anterior tibial translation (mm, at left) and AM-ACL relative strain (%, at right) across all specimens. The addition of the internal tibial torque to the baseline loading condition increased the AM-ACL relative strain by 108 % (at right). This increase in the AM-ACL relative strain is consistent with the increase in the anterior tibial translation (c.f., 'Base1' vs 'Int1', at left). Following the ACL transection, the anterior tibial translation significantly increased for both baseline and internally-directed loading conditions.

Summary of Flexion Angle, Impulsive Compressive Force, Quadriceps Force, and Internal Tibial Torque

Table 5.2 summarizes the mean (SD) peak values of knee flexion angle, impulsive compressive force, quadriceps force, and internal tibial torque over the test conditions. In the absence of any applied axial tibial torque, the peak knee flexion angles were 5.0 ± 1.3 and 5.3 ± 1.4 for the ACL-Intact ('Base1') and ACL-Deficient ('Base3') condition, respectively. In the presence of the internal tibial torque, the peak knee flexion angles were 5.0 ± 1.3 and 4.9 ± 3.0 for the ACL-Intact ('Int1') and ACL-Deficient ('Int3') condition, respectively. The peak impulsive compressive forces under the internally-directed tibial torque were ~1.3*BW and ~1.2*BW for the ACL-Intact ('Int1') and ACL-Deficient ('Int2'), respectively, whereas the corresponding values in the absence of any applied axial tibial torques were 1,299.3 ± 217.6 N (1.7*BW ~ 2.3*BW) and 1,206.8 ± 126.5 N (1.6*BW ~ 2.0*BW) for the ACL-Intact ('Base1') and ACL-Deficient ('Base3') conditions, respectively. On the other hand, the resulting quadriceps forces were 1,040.9 ± 235.0 N and 1,079.4 ± 182.8 N for the ACL-Intact ('Base1') and ACL-Deficient ('Base3') conditions, respectively; these were similar to the corresponding values under the internally-directed loading conditions (Table 5.2).

Table 5.2 Mean (SD) values of peak impulsive compressive force, internal tibial torque and quadriceps force for all ACL-Intact and ACL-Deficient knees loaded under internal tibial torques

	Impulsive Compressive Force (N)	Internal Tibial Torque (N-m)	Quadriceps Force (N)
ACL-Intact	866.1 (101.0)	17.1 (3.9)	1,055 (226)
ACL-Deficient	777.7 (140.6)	16.6 (4.7)	1,108 (163)

5.5 Discussion

This study was designed to evaluate the contribution of the ACL to restraining axial rotation of the tibia under dynamic loading conditions similar to a pivot landing maneuver involving internal tibial axial rotation. Previous *in vitro* and *in vivo* studies have employed static or quasi-static loading conditions employing low force levels. Those studies are relevant because clinical examinations are often performed quasi-statically to measure the degree of passive knee laxity. However, Snyder-Mackler et al.[11] have demonstrated that passive joint laxity is poorly correlated with the patient's functional or dynamic ability. Because daily mobility tasks and sports maneuvers induce large dynamic loads on the knee[21,22], we investigated here the effect of ACL transection on knee kinematics under combinations of impulsive loading conditions (compressive force, flexion moment, and axial tibial torque) with simulated muscle-tendon unit forces. In our baseline testing, the dynamic loading caused the increase in the knee flexion angle to stretch the quadriceps muscle-tendon unit and increase its force, thereby causing the femur to translate posteriorly relative to the tibia so as to increase ACL strain. Then, internal tibial torque was added to the baseline loading configuration. Overall, the ACL played a secondary role by providing 13% of the total dynamic rotational resistance to the applied internal tibial torque. Although the internal tibial rotation was increased due to the ACL deficiency, it is probably too small to be clinically significant.

The ACL transection resulted in a statistically significant increase in the normalized internal tibial rotation. However, the increase in the internal tibial rotation was small (i.e., 0.5 degrees difference between the ACL-Intact ('Int1') and ACL-Deficient ('Int2') state, Figure 5.3). In previous studies of smaller quasi-static forces in

the absence of muscle forces, or in the presence of low level muscle forces, larger increases in internal tibial rotation following ACL transection have been reported. For example, Markolf et al.[4] reported the largest increase in internal tibial rotation (i.e., 7.3 ± 3.4 and 4.0 ± 2.8 degrees at 0 and 30 degrees knee flexion angle, respectively) under a 5 N-m internal tibial torque during passive knee extension test. Similarly, Lipke et al.[5] and Lane et al.[6] also found 4~5 degrees increase in internal tibial rotation. Other studies observed less than or slightly larger than 3 degrees increase in internal tibial rotation after ACL transection.[7, 8, 13, 16, 23, 24] The most plausible explanation for the larger values of internal tibial rotation in those studies is the absence of either large muscle forces or large compressive force. Previous studies found that axial compressive load induced by either external load or quadriceps muscle contraction reduces the total anterior-posterior translation of the tibia relative to the femur.[25, 26] More directly, Wojtys et al. demonstrated that the internal tibial rotation in the presence of active muscle contractions was smaller compared to the passive muscle state.[27] The large trans-knee external and muscular compressive forces acting in the present study may have resulted in better conformity of the femoral condyle, tibial plateau, and meniscus leading to increased resistance to internal tibial torque. In addition, a large quadriceps force translates the femur posteriorly, thereby tightening the peripheral ligaments to make them more effective in resisting internal tibial torque. Wroble et al. showed that cutting the ACL only produced a small but statistically significant increase in internal tibial rotation, but that subsequent sectioning of the anterolateral structures produced a significant increase in internal tibial rotation.[8] They concluded that the internal tibial rotation is restrained

more by the lateral extra-articular structures than the ACL. So, our results imply that the increase in internal tibial rotation due to ACL insufficiency is typically small. (CME)

The contribution by the ACL to the dynamic rotational resistance was estimated by calculating the difference in the reciprocal of the normalized internal tibial rotation between the ACL-Intact ('Int1') and ACL-Deficient ('Int2') states. In our pivot landing scenario the mean contribution by the ACL corresponds to 13 % of the dynamic rotational resistance for the ACL-Intact knees. This is a modest contribution when compared to Butler et al.'s results that ACL resists 86 % of anterior tibial force.[3] This minor contribution of the ACL to the dynamic rotational resistance can be explained by the functional anatomy, i.e., the attachment site of the ACL on the tibial plateau is near the longitudinal axis of the knee joint,[28, 29] thus the moment arm is too short to be effective in resisting the internal tibial torque.[30]

As shown in Figure 5.4, the addition of the internal tibial torque to the baseline loading condition increased the anterior tibial translation, thereby straining the ACL by a factor of 2. However, despite the resulting stretch on the ACL, which would have contributed to the dynamic rotational resistance, the increase in the internal tibial rotation was small (cf., 'Int1' vs. 'Int2', Figure 5.3.a). Previous quasi-static studies have observed coupled anterior tibial translation under an isolated internal tibial torque, or a combined internal tibial torque and valgus torque.[16, 31] In ACL-Deficient knees compared to the ACL-Intact, Diermann et al.[16] found no significant increase in the internal tibial rotation, but a significant increase in the anterior tibial translation under a combined 10 N-m valgus moment and 4 N-m internal tibial torque after ACL transection. Our results

corroborate their findings that anterior tibial translation was the primary variable altered following ACL transection when the knee was subjected to the combined rotatory load. These findings appear to be contradictory because the internal tibial rotation can cause the coupled anterior tibial translation, thereby straining the ACL, but the contribution of the induced ACL force in limiting internal tibial rotation is minor. However, they can be reconciled considering that the attachment site of the ACL on the tibial plateau is close to the longitudinal axis resulting in the short moment arm. Hence, an internal tibial torque primarily loads the ACL in its role as a primary restraint to anterior tibial translation. Furthermore, these results imply that the decrease in the dynamic rotational resistance due to the ACL insufficiency could be reduced even more if ACL reconstruction were to restore physiological anterior tibial translation.

The strength of this *in vitro* study is that we were able to compare the knee kinematics for the ACL-Intact and ACL-Deficient knee states while simulating a realistic jump landing scenario under highly controlled conditions that would be hard to achieve *in vivo*. Pflum et al. predicted the ACL force during drop landings using their computer model.[22] In their study the drop landing data including kinematics, muscle EMG data, and ground reaction force were collected from a healthy male athlete. As shown Figure 5.2 (a), the ground reaction force and simulated muscle forces for the baseline loading condition in the present study are consistent with their ground reaction force and *in vivo* muscle EMG pattern. A pivot landing scenario was simulated by adding the impulsive axial tibial torque to the baseline loading condition. During an *in vivo* pivot landing, the magnitude and direction of the axial tibial torque applied to the knee joint depends on the

body's axial angular momentum while landing, thereby making this pivot landing scenario realistic.

There are several limitations to this study. First, only one initial knee flexion angle (15 degrees) was tested because Li et al.[32] reported the ACL strain to be highest with the knee in 15 degrees of flexion. More recently, in maximum jump landings, initial mean (± SD) knee flexion angles of 11 (± 3) degrees at toe contact, and 28 (± 7) degrees at heel contact, have been measured.[33] Finally, Olsen et al.[12] used injury videotapes to estimate knee flexion angle at injury to be 16 degrees. Therefore, the initial 15 degrees of knee flexion we used seems reasonable, but other angles could be investigated in the future. A second limitation is that the change of knee flexion angle under the impulsive test load was smaller than in some *in-vivo* studies. For example, Pflum et al.[22] reported that the knee flexion angle change in the first 70 msec was ~35 degrees. Our studies showed an average knee flexion angle change of ~5° in the first 70 msec. This is consistent with Russell et al.[34] who reported a change in knee flexion angle during a single-leg drop landing of less than 10 degrees over the initial 70 msec. Hence, our knee flexion angle change appears reasonable. A third limitation is that the peak impulsive compressive force for the internally-directed trials was slightly higher than 1.2 times body-weight, whereas the corresponding value for the baseline loading conditions was about 2 times body-weight. This decrease in the peak impulsive compressive force resulted from the custom torsional transformer device ('T' in Figure 5.1). However, by maintaining the height of the drop weight at the same level across all trials, the same kinetic energy was applied to the knee specimen under all test conditions. Withrow et

al.[17] showed that the ACL relative strain was highly correlated with the quadriceps force, not the impulsive compressive force. Dikeman et al.[35] and DeMorat et al.[36] also found that an increase in quadriceps force increased ACL strain. These results suggest that the increase in quadriceps force dominates the increase in ACL strain more than does the increase in impulsive compressive force. In our case, for all loading conditions, the quadriceps forces were maintained at the same force level, thereby providing a good opportunity to investigate the effect of the different loading directions and ACL status on the knee joint kinematics. A fourth limitation is that the effect of the iliotibial band was not simulated although it reduces the anterior tibial translation of the lateral tibial plateau, thereby limiting the internal tibial rotation and the coupled anterior tibial translation under a rotatory load. Yamamoto et al. investigated the effect of the iliotibial band force on the coupled anterior tibial translation, internal tibial rotation, and *in situ* ACL force in response to a combined 10 N-m valgus moment and 5 N-m internal tibial torque.[37] They reported that all three measurements were generally decreased as the iliotibial band force increased (i.e., 0 N, 22 N, 44 N, 88 N). However, the effect of the iliotibial band force level on internal tibial rotation was not significant. Additionally, the coupled anterior tibial translation was significantly affected by the iliotibial band force only at high knee flexion (i.e., 45 deg and 60 deg) under their highest iliotibial band force (i.e., 88 N). In our study, the initial knee flexion angle for all trials was maintained at 15 degrees and the knee flexion angle changes were less than 10 degrees. The results from Yamamoto et al. suggest that the iliotibial band force can be ignored for our low initial knee flexion angle and small knee flexion angle change.[37] Finally, we do not have a complete set of knees under the external tibial torque: only two knees were tested under the external tibial

torque following the ACL transection because we were concerned about knee specimen deterioration due to too many trials.

5.6 Conclusions

Our results show that transection of the ACL leads to a small increase in the internal tibial rotation, equivalent to a 13 % decrease in the dynamic rotational resistance, under the large forces associated with a simulated jump landing, but a significant increase in the anterior tibial translation. Therefore, an ACL reconstruction that restores both ligament orientation and stiffness will provide major resistance to anterior tibial translation, but provide minor resistance to axial tibial rotation.

5.7 References

1. Gasser S, Uppal R. Anterior cruciate ligament reconstruction: A new technique for Achilles tendon allograft preparation. *Arthroscopy-the Journal of Arthroscopic and Related Surgery*. 2006;22(12).

2. Noyes FR. The Function of the Human Anterior Cruciate Ligament and Analysis of Single- and Double-Bundle Graft Reconstructions. *Sports Health: A Multidisciplinary Approach.* 2009;1:66-75.

3. Butler DL, Noyes FR, Grood ES. Ligamentous Restraints to Anterior-Posterior Drawer in the Human Knee - Biomechanical Study. *Journal of Bone and Joint Surgery-American Volume*. 1980;62(2):259-70.

4. Markolf KL, Park S, Jackson SR, McAllister DR. Anterior-Posterior and Rotatory Stability of Single and Double-Bundle Anterior Cruciate Ligament Reconstructions. *Journal of Bone and Joint Surgery-American Volume.* 2009;91A(1):107-18.

5. Lipke JM, Janecki CJ, Nelson CL, McLeod P, Thompson C, Thompson J, et al. The Role of Incompetence of the Anterior Cruciate and Lateral Ligaments in Anterolateral and Anteromedial Instability - A Biomechanical Study of Cadaver Knees. *Journal of Bone and Joint Surgery-American Volume*. 1981;63(6):954-60.

6. Lane JG, Irby SE, Kaufman K, Rangger C, Daniel DM. The Anterior Cruciate Ligament in Controlling Axial Rotation - An Evaluation of Its Effect. *American Journal of Sports Medicine.* 1994 Mar-Apr;22(2):289-93.

7. Reuben JD, Rovick JS, Schrager RJ, Walker PS, Boland AL. 3-Dimensional Dynamic Motion Analysis of the Anterior Cruciate Ligament Deficient Knee-Joint. *American Journal of Sports Medicine*. 1989 Jul-Aug;17(4):463-71.

8. Wroble RR, Grood ES, Cummings JS, Henderson JM, Noyes FR. The Role of the Lateral Extraarticular Restraints in the Anterior Cruciate Ligament-Deficient Knee. *American Journal of Sports Medicine*. 1993;21(2):257-63.

9. Andersen HN, Dyhre-Poulsen P. The anterior cruciate ligament does play a role in controlling axial rotation in the knee. *Knee Surg Sports Traumatol Arthrosc*. 1997;5(3):145-9.

10. DeFrate LE, Papannagari R, Gill TJ, Moses JM, Parhare NP, Li G. The 6 Degrees of Freedom Kinematics of the Knee After Anterior Cruciate Ligament Deficiency: An In Vivo Imaging Analysis. *American Journal of Sports Medicine.* 2006;34:1240-1246.

11. Snyder- Mackler L, Fitzgerald GK, Bartolozzi AR, Ciccotti MG. The relationship between passive joint laxity and functional outcome after anterior cruciate ligament injury. *American Journal of Sports Medicine*. 1997;25(2):191-5.

12. Olsen OE, Myklebust G, Engebretsen L, Bahr R. Injury mechanisms for anterior cruciate ligament injuries in team handball a systematic video analysis. *American Journal of Sports Medicine.* 2004;32(4):1002-12.

13. Kanamori A, Woo SLY, Ma CB, Zeminski J, Rudy TW, Li GA, et al. The forces in the anterior cruciate ligament and knee kinematics during a simulated pivot

shift test: A human cadaveric study using robotic technology. *Arthroscopy-the Journal of Arthroscopic and Related Surgery*. 2000;16(6):633-9.

14. Yagi M, Wong EK, Kanamori A, Debski RE, Fu FH, Woo SLY. Biomechanical analysis of an Anatomic anterior cruciate ligament reconstruction. *American Journal of Sports Medicine.* 2002 Sep-Oct;30(5):660-6.

15. Zantop T, Schumacher T, Diermann N, Schanz S, Raschke MJ, Petersen W. Anterolateral rotational knee instability: role of posterolateral structures. *Archives of Orthopaedic and Trauma Surgery*. 2007;127:743-52.

16. Diermann N, Schumacher T, Schanz S, Raschke MJ, Petersen W, Zantop T. Rotational instability of the knee: internal tibial rotation under a simulated pivot shift test. *Archives of Orthopaedic and Trauma Surgery*. 2009;129(3):353-8.

17. Withrow TJ, Huston LJ, Wojtys EM, Ashton-Miller JA. The relationship between quadriceps muscle force, knee flexion, and anterior cruciate ligament strain in an in vitro simulated jump landing. *American Journal of Sports Medicine*. 2006;34(2):269-74.

18. Withrow TJ, Huston LJ, Wojtys EM, Ashton-Miller JA. The effect of an impulsive knee valgus moment on in vitro relative ACL strain during a simulated jump landing. *Clinical Biomechanics*. 2006;21(9):977-83.

19. Withrow TJ, Huston LJ, Wojtys EM, Ashton-Miller JA. Effect of varying hamstring tension on anterior cruciate ligament strain during in vitro impulsive

knee flexion and compression loading. *Journal of Bone and Joint Surgery-American Volume.* 2008;90A(4):815-23.

20. Grood ES, Suntay WJ. A joint coordinate system for the clinical description of three-dimensional motions: application to the knee. *J Biomech Eng*. 1983;105(2):136-44

21. Besier TF, Lloyd DG, Ackland TR, Cochrane JL. Anticipatory effects on knee joint loading during running and cutting maneuvers. *Medicine and Science in Sports and Exercise*. 2001;33(7):1176-81.

22. Pflum MA, Shelburne KB, Torry MR, Decker MJ, Pandy MG. Model prediction of anterior cruciate ligament force during drop-landings. *Medicine and Science in Sports and Exercise*. 2004;36(11):1949-58.

23. Zantop T, Diermann N, Schumacher T, Schanz S, Fu FH, Petersen W. Anatomical and nonanatomical double-bundle anterior cruciate ligament reconstruction - Importance of femoral tunnel location on knee kinematics. *American Journal of Sports Medicine.* 2008;36(4):678-85.

24. Kanamori A, Zeminski J, Rudy TW, Li G, Fu FH, Woo SLY. The effect of axial tibial torque on the function of the anterior cruciate ligament: A biomechanical study of a simulated pivot shift test. *Arthroscopy-the Journal of Arthroscopic and Related Surgery*. 2002;18(4):PII 10.1053/jars.2002.30638.

25. Li G, Rudy TW, Allen C, Sakane M, Woo SLY. Effect of Combined Axial Compressive and Anterior Tibial Loads on In Situ Forces in the Anterior Cruciate

Ligament: A Porcine Study. *Journal of Orthopaedic Research.* 1998;16(1):122-127.

26. Torzilli PA, Deng XH, Warren RF. The Effect of Joint-Compressive Load and Quadriceps Muscle Force on Knee Motion in the Intact and Anterior Cruciate Ligament-Sectioned Knee. *American Journal of Sports Medicine*. 1994;22(1):105-112

27. Wojtys EM, Huston LJ, Schock HJ, Ashton-Miller JA. Gender Differences in Muscular Protection of the Knee in Torsion in Size-matched Athletes. *Journal of Bone and Joint Surgery-American Volume*. 2003;85A(5):7820789.

28. Dienst M, Burks RT, Greis PE. Anatomy and biomechanics of the anterior cruciate ligament. *Orthopedic Clinics of North America*. 2002;33(4):605-620.

29. Girgis FG, Marshall JL, Monajem A. Cruciate Ligaments of Knee-Joint - Anatomical, Functional and Experimental Analysis. *Clinical Orthopaedics and Related Research.* 1975(106):216-31.

30. Shaw JA, Murray DG. The longitudinal axia of the knee and the role of the cruciate ligaments in controlling transverse rotation. *Journal of Bone and Joint Surgery-American Volume*. 1974;56A:1603-1609.

31. Li G, Rudy TW, Sakane M, Kanamori A, Ma CB, Woo SLY. The importance of quadriceps and hamstring muscle loading on knee kinematics land in-situ forces in the ACL. *Journal of Biomechanics*. 1999;32(4):395-400.

32. Gadikota HR, Wu JL, Seon JK, et al. Single-Tunnel Double-Bundle Anterior Cruciate Ligament Reconstruction With Anatomical Placement of Hamstring Tendon Graft. Can It Restore Normal Knee Joint Kinematics? *American Journal of Sports Medicine.* 2010;38(4):713-720.

33. Urabe Y, Kobayashi R, Sumida S, Tanaka K, Yoshida N, Nishiwaki GA, et al. Electromyographic analysis of the knee during jump landing in male and female athletes. *Knee*. 2005;12(2):129-34.

34. Russell KA, Palmieri RM, Zinder SM, Ingersoll CD. Sex differences in valgus knee angle during a single-leg drop jump. *Journal of Athletic Training.* 2006;41(2):166-171.

35. Dikeman JS. Experimental simulation of mechanism of injury for non-contact, isolated anterior cruciate ligament ruptures. *Master's Thesis, North Carolina State University*, 1998.

36. DeMorat G, Weinhold P, Blackburn T, Chudik S, Garrett W. Aggressive quadriceps loading can induce noncontact anterior cruciate ligament injury. *American Journal of Sports Medicine*. 2004;32(2):477-83.

37. Yamamoto Y, Hsu WH, Fisk JA, et al. Effect of the Iliotibial Band on Knee Biomechanics during a Simulated Pivot Shift Test. *Journal of Orthopaedic Research*. 2006;24(5):967-973.

CHAPTER 6

EFFECT OF TIBIAL ROTATION IN THE ACL–INTACT AND ACL–DEFICIENT KNEE UNDER SIMULSTED MUSCLE LOADS

6.1 Abstract

Few studies have evaluated rotational stability of the knee in anterior cruciate ligament (ACL) intact and deficient states under a joint compressive load. We tested the hypothesis that peak tibiofemoral axial rotation will not differ between the ACL-intact and -deficient knee when preloaded by simulated tibiofemoral muscle forces.

Eight cadaveric knees were tested with the ACL intact and transected. With the knee at 30^{o} of flexion, 10 Nm of internal or external torque was applied to produce rotation of the tibia relative to the femur. Three muscle loading conditions were tested in randomized order: (1) 'all muscles' pre-tensioned (quadriceps: 180 N, biceps femoris, medial hamstrings, medial and lateral heads of the gastrocnemius: 70 N each), (2) 'no muscles' pre-tensioned, and (3) all muscles pre-tensioned, except for semitendinosus and gracilis (termed 'hamstring harvest'). Tibiofemoral kinematics were captured using an optoelectronic motion tracking system.

There was no statistically significant difference in internal or external rotation of the tibia relative to the femur in the ACL-intact and -deficient states under each of the

muscle loading conditions tested. We found a significant difference between the loaded muscle conditions ('all muscles' and 'hamstring harvest') versus 'no muscles' in both ACL states.

There is no statistically significant difference in tibiofemoral rotation in the ACL-intact and -deficient states. Application of muscle preloads significantly affects rotation when compared with no muscle load, but there is still no difference between the two ACL states. Therefore, the presence or absence of the ACL does not significantly affect knee resistance to axial rotation.

6.2 Introduction

A number of studies have documented a high rate of radiographic knee osteoarthritis following anterior cruciate ligament (ACL) injury.[6,14,19] The cause of these degenerative changes is not understood, but they may be partly due to altered kinematics in the knee. For example, an ACL rupture removes the primary restraint to anterior translation of the tibia relative to the femur.[3] In addition, the ACL has been shown to augment resistance of the knee to axial rotation in the presence of tibiofemoral compression.[7,17]

Changes in the anterior-posterior translation and internal-external rotation of the knee after ACL rupture may accelerate the development of degenerative changes. Current ACL reconstruction techniques reduce anterior tibial translation, but have not been proven to decrease the rate of radiographic osteoarthritis. Rotational instability in the ACL-deficient knee that is not restored by ACL reconstruction may be responsible for the degenerative changes seen after ACL injury. *In vivo* studies of ACL-deficient knees

demonstrate increased internal tibial rotation relative to the femur.[1,9,16] Computer modeling suggests that this increase in internal tibial rotation alters tibiofemoral articular cartilage contact and accelerates thinning of the articular cartilage.[2,12]

Some authors have hypothesized that tibiofemoral muscle forces can help compensate for abnormal kinematics in the ACL deficient knee and thereby provide dynamic stability.[1,4] However, the contribution of these muscle forces to resisting axial rotation of the knee are difficult to quantify *in vivo*. Therefore, the purpose of this study was to test the hypothesis, *in vitro*, that three different combinations of knee preloading by simulated tibiofemoral muscle forces would not affect the peak tibiofemoral axial rotation in either the ACL-intact or -deficient knee placed under standardized internal and external torque loads.

6.3 Methods

Specimen Procurement and Preparation

Eight fresh-frozen human cadaveric knee specimens (mean age: 67.8 ± 17.4; range: 31-84 years) from individual male donors were obtained from the University of Michigan Anatomical Donations Program. There were four right and four left knees. The knees were physically and radiographically screened to be free of osseous and soft tissue abnormalities. The femur and tibia were cut approximately 25 cm from the joint line. The proximal fibula was rigidly fixed to the tibia in an anatomic position using a screw. The femur and tibia were mounted in pots using intramedullary screws and polymethylmethacrylate cement.

Soft tissues greater than 20 cm from the joint line were stripped to allow the specimen to be secured to the testing apparatus. The integrity of the soft tissue envelope within 20 cm of the joint line was maintained as much as possible. Through limited incisions, the tendon insertions of the quadriceps, medial hamstring (semimembranosus, semitendinosus, gracilis, and sartorius), biceps femoris, medial and lateral heads of the grastrocnemius muscles were isolated and sutured to tensioning devices acting along their anatomic lines of action. A medial parapatellar arthrotomy was performed for visual inspection of the articular surfaces as well as for transection of the ACL in later testing. The capsule was subsequently sutured closed prior to testing. The specimens were stored at -20^{o}C and thawed overnight at room temperature before testing. All testing was performed at room temperature and completed within 24 hours of thawing. Saline (0.9% sodium chloride) solution was used to keep the specimens moist throughout testing.

Knee Testing Apparatus

The specimens were mounted on a custom apparatus designed to allow application of rotational force on the tibia and joint compressive loads through knee flexors and extensors without constraining tibial motion (Figure 6.1).

The femoral component of the fixture consisted of a disc on which three tensioning devices were positioned in line with the anatomic pull of the quadriceps, biceps femoris, and medial hamstring muscles (Figure 6.2). A load cell [Transducer Techniques, Inc., Temecula, CA] connected to each muscle tensioning device provided force data for the individual muscles. A rod at the proximal end of the femoral

component allowed the apparatus to be mounted on a standard arthroscopic specimen stand with the knee positioned at $30^{o} \pm 3^{o}$ of flexion.

The tibial component of the apparatus consisted of a disc on which two tensioning devices and their respective load cells were positioned in line with the anatomic pull of the medial and lateral heads of the gastrocnemius muscle (Figure 6.3). At the distal end of the tibial component, two arms extended medially and laterally to allow application of a rotational load to the tibia without constraining tibial motion. A torque load cell [Eaton Corporation, Troy, MI] provided data on the external torque throughout each trial. Tibiofemoral kinematics was captured using the Optotrak Certus® Motion Capture System [Northern Digital Inc., Waterloo, Ontario] and analyzed with MotionMonitor™ software [Innovative Sports Training Inc., Chicago, IL]. Two sensor arrays containing three optoelectronic markers each were rigidly fixed to the femur and tibia using threaded Steinman pins (Figures 6.2 and 6.3, *). Osseous landmarks on the femur, tibia, and knee joint were then digitized with a stylus in order to create an anatomically-derived coordinate system to describe tibiofemoral motion.

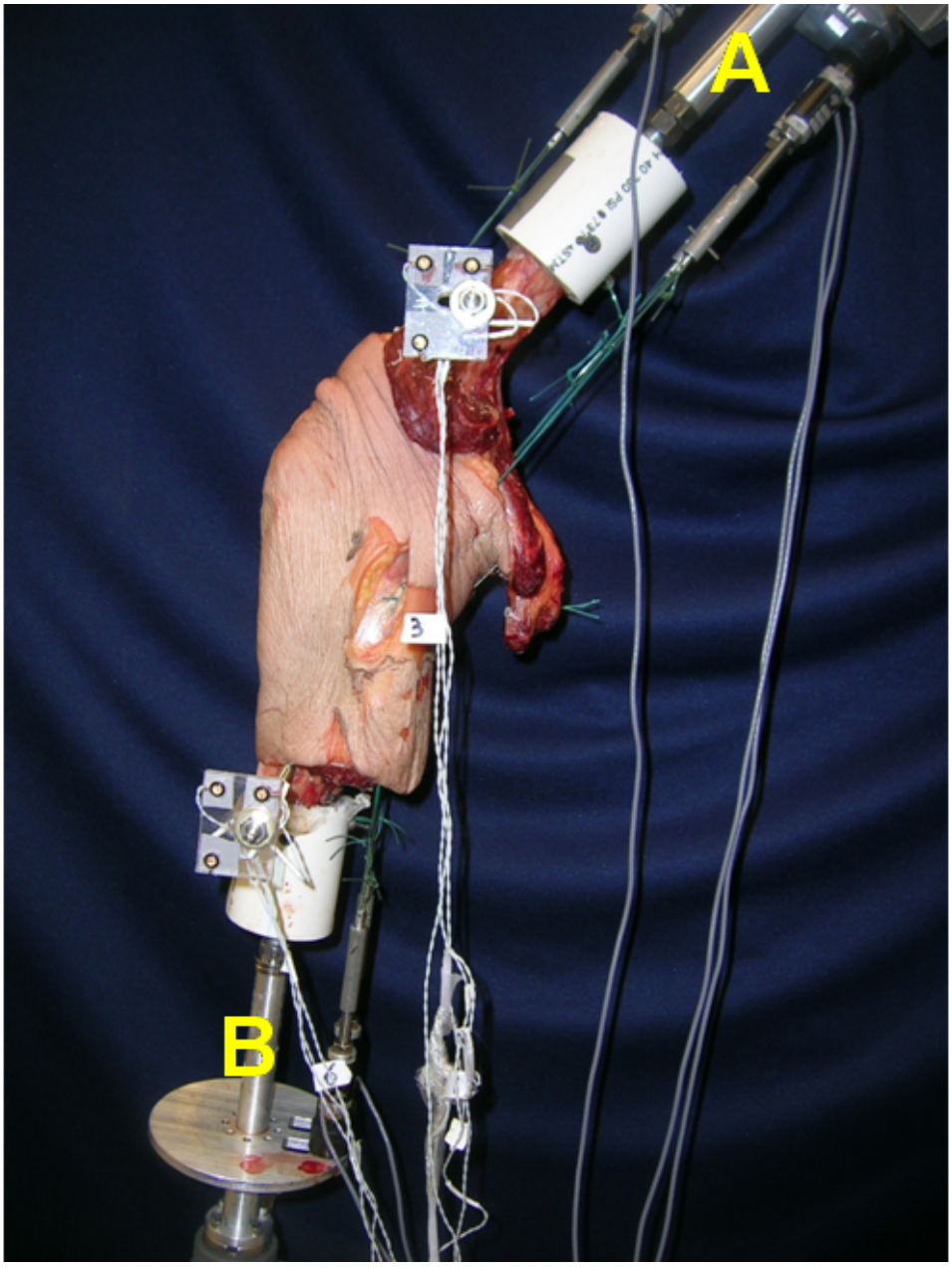

Figure 6.1 Knee specimen mounted in the testing apparatus. The femoral component (A) and tibial component (B) are threaded onto rods cemented within the intramedullary canals of the specimen. The entire apparatus is then mounted onto an arthroscopic specimen stand.

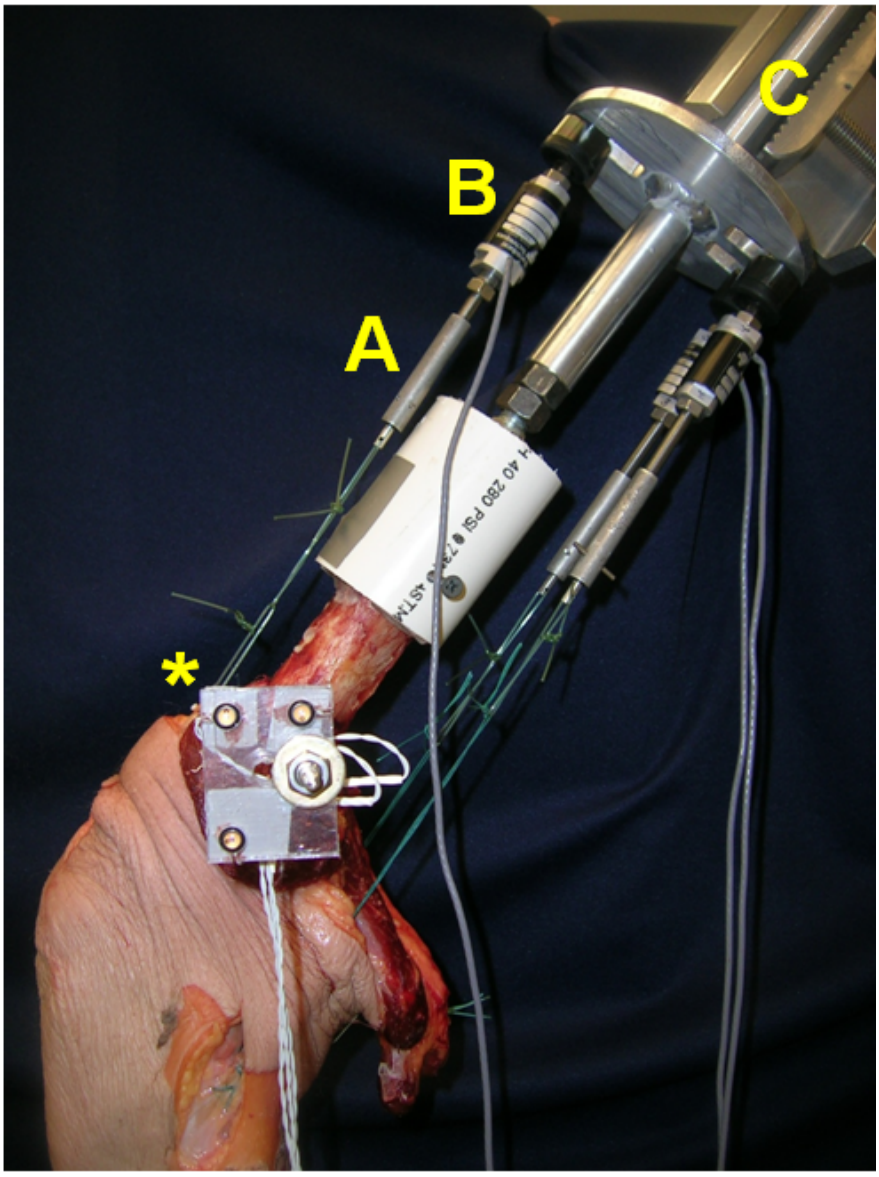

Figure 6.2 Femoral component. Three muscle tensioning devices (A) allow application of force in line with the anatomic pull of the quadriceps, biceps femoris, and medial hamstrings. Load cells (B) on each muscle tensioning device measure force data on the individual muscles. An arm at the proximal end (C) allows mounting on an arthroscopic specimen stand. A sensor array (*) containing three optoelectronic sensors for the motion tracking system is rigidly fixed to the femur.

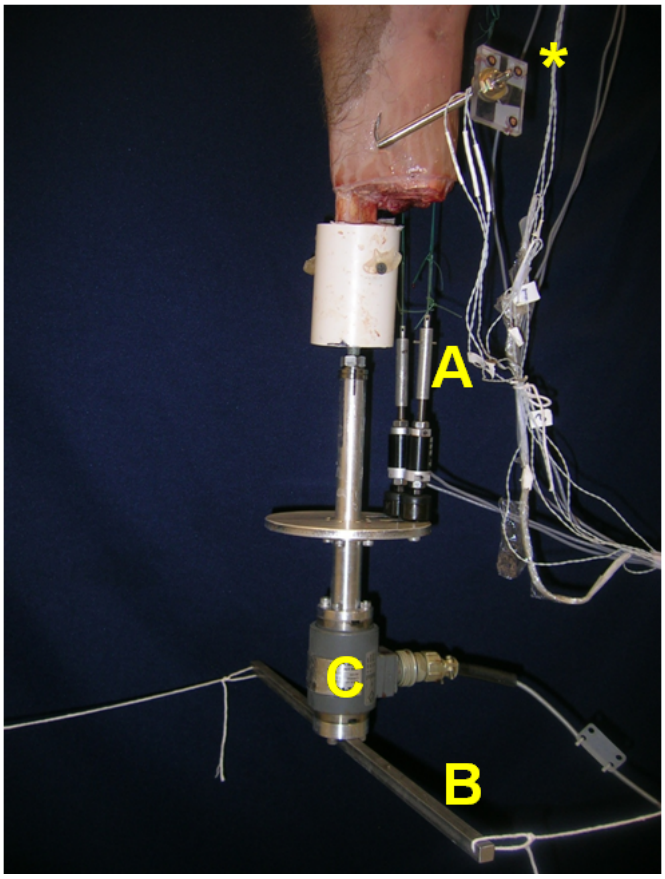

Figure 6.3 Tibial component. Two muscle tensioning devices (A) allow application of force along the anatomic line-of-action of the medial and lateral heads of the gastrocnemius. Arms extending medially and laterally at the distal end (B) allows application of a rotational load on the tibia. A torque load cell (C) measures rotational load. A sensor array (*) for the motion tracking system is rigidly fixed to the tibia.

Testing Protocol

Prior to testing, the knee was preconditioned with ten cycles each of: (1) passive movement through the full flexion-extension arc; (2) 10 Nm of internal followed by external torque was then applied to the tibia. Muscle preconditioning consisted of applying the testing preloads for each of the muscle groups and maintaining these loads

for 10 to 15 minutes prior to the start of testing. The preloads used were 180 ± 18 N for the quadriceps and 70 ± 7 N each for the medial hamstrings, lateral hamstrings, and medial and lateral heads of the gastrocnemius.[20] Loads on the five muscle groups, degrees of tibiofemoral rotation, knee flexion angle, and torque applied were recorded at 100 Hz.

We tested three muscle loading conditions: (1) 'all muscles' pre-tensioned, (2) 'no muscles' pre-tensioned, and (3) all muscles pre-tensioned except the semitendinosus and gracilis (termed 'hamstring harvest'). The third muscle group was designed to simulate conditions following hamstring autograft harvest. The order of testing for direction of rotation and loading conditions was randomized using a computer random sequence generator [www.random.org/sequences]. When the direction of rotation changed from one trial to the next, a preconditioning trial was performed. This preconditioning trial consisted of applying 10 ± 1 Nm of torque five times in the new direction of rotation. For each trial, 10 ± 1 Nm of static torque was applied for three seconds in a pure couple to the tibia using a system of weights and pulleys. Three trials were performed for each loading condition and the data averaged for statistical analysis. After each trial, muscle preloads were restored to initial values. The ACL was then transected through the medial parapatellar arthrotomy performed earlier. The capsule was again sutured closed. All specimens had positive Lachman's tests after transection of the ACL. Tests were then repeated with the three muscle conditions in random order.

Statistical Analysis

Within-subject differences were evaluated with a two-way repeated measures analysis of variance (ANOVA) with Bonferroni adjustment for multiple comparisons. Interactions between ACL state and muscle condition were evaluated using a level of significance of $p \leq 0.05$. Power was examined via a *post-hoc* power analysis. In external rotation, Cohen's D statistic ranged from 1.15 to 1.61 with a corresponding power of 0.57 to 0.85. In internal rotation, Cohen's D ranged from 2.17 to 3.17 with a corresponding power of 0.98 to >0.99.

6.4 Results

Peak tibiofemoral internal rotation with the ACL-intact under the 'all muscles', 'hamstring harvest', and 'no muscles' conditions was 9.3 ± 1.6^{o}, 9.1 ± 1.3^{o}, and 15.5 ± 2.4^{o} respectively. After transection of the ACL, peak tibiofemoral internal rotation under the same muscle conditions was 9.9 ± 2.0^{o}, 9.7 ± 2.0^{o}, and 15.4 ± 3.0^{o}. When comparing the ACL-intact and ACL-deficient states, there was no statistically significant difference ($p=1.00$) in peak tibiofemoral internal rotation under any of the muscle conditions tested (Figure 6.4).

Peak tibiofemoral external rotation with the ACL-intact under the 'all muscles', 'hamstring harvest', and 'no muscles' conditions was 13.9 ± 4.3^{o}, 13.8 ± 4.8^{o}, and 18.9 ± 4.2^{o} respectively. After transection of the ACL, peak tibiofemoral external rotation under the same muscle conditions was 13.6 ± 3.8^{o}, 13.5 ± 3.9^{o}, and 19.5 ± 3.5^{o} respectively. When comparing the ACL-intact and ACL-deficient states, there was no statistically

significant difference (p=1.00) in peak tibiofemoral external rotation under any of the muscle conditions tested (Figure 6.4).

There was a significant muscle effect on internal and external tibial rotation when comparing 'all muscles' versus 'no muscles' ($p<0.0001$) and 'hamstring harvest' versus 'no muscles' ($p<0.0001$). However, there was no significant difference between 'all muscles' and 'hamstring harvest' (p=1.00) in either the ACL-intact or -deficient states. There was no interaction effect between the ACL state and muscle loading condition.

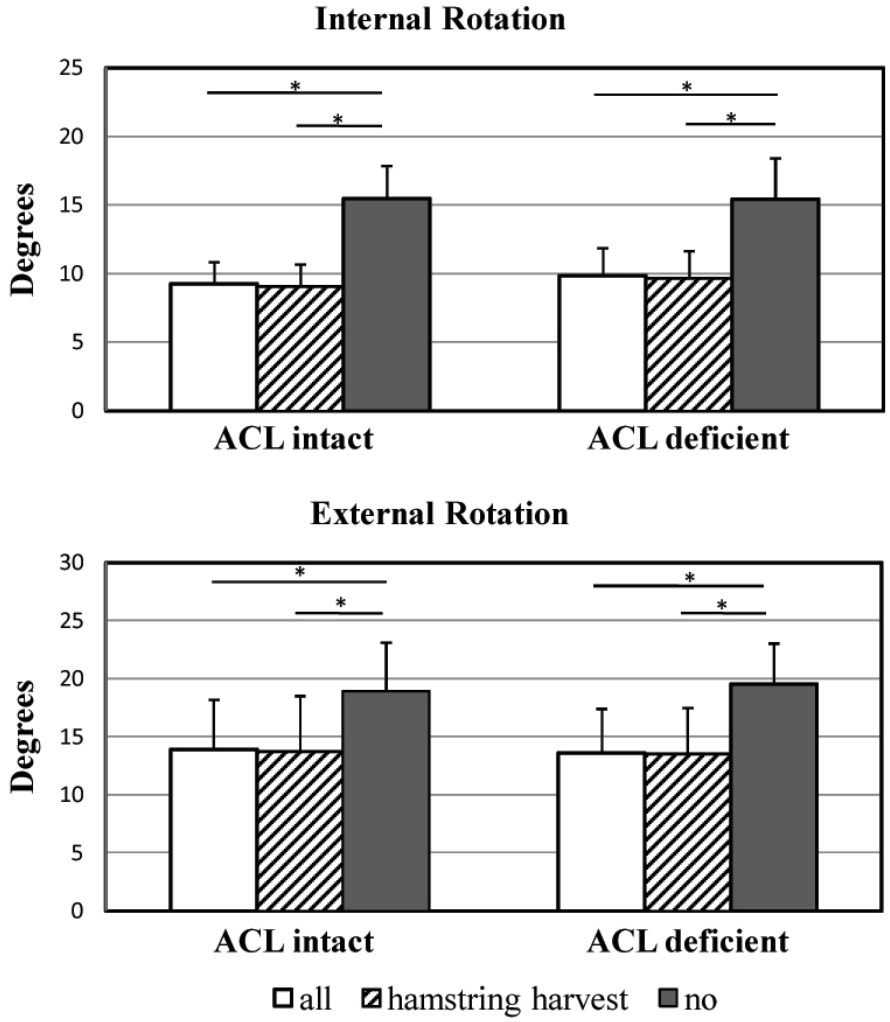

Figure 6.4 Tibial rotation in the ACL-intact and ACL-deficient states under simulated muscle loading conditions. Significant differences ($p\leq0.05$) indicated by asterisks. Error bars represent + 1 standard deviation.

6.5 Discussion

We investigated tibial rotation relative to the femur in the ACL-intact and -deficient knee under simulated muscle loads. No statistically significant differences were found between the ACL-intact and -deficient states. The application of a joint compressive force with 'all muscles' or 'hamstring harvest' conditions resulted in a significant difference in comparison to 'no muscles' in both ACL states. There was no difference when comparing 'all muscles' and 'hamstring harvest'.

Previous studies examining tibiofemoral rotation in the ACL-deficient knee have reported varying results. *In vivo* studies have demonstrated significantly increased internal tibial rotation during the swing phase of gait.[8,9,16] Georgoulis *et al.*[9] hypothesized that this is due to inactivity of the hamstring muscles and increased activity of the quadriceps and gastrocnemius muscles. However, these *in vivo* studies could not control for muscle forces acting across the knee joint.

Czerniecki *et al.*[5] investigated tibiofemoral rotation in subjects with unilateral ACL-deficiency during walking and running. They found increased tibiofemoral rotation with higher ambulation speed, but no difference when comparing the injured knee to the contralateral knee. Lane *et al.*[11] reported no difference between internal or external rotation in cadaveric specimens before and after ACL transection. In their study, the presence of a compressive load applied through the femur resulted in a significant change in external rotation, but not internal rotation. Previous authors hypothesize that rotational stability is influenced by several factors: (1) soft tissue structures, such as the ACL and menisci, (2) muscle forces and external loads, and (3) geometric factors, such as the contact of the femoral condyles against the tibial eminences.[15,18]

An *in vitro* study by Haimes et al. examining the motion limits of the knee with sequential sectioning of the ACL and the medial collateral ligament (MCL) found no significant change in external or internal rotation limits after sectioning of the ACL alone.[10] More recent work by Lo *et al.* investigated the effects of anterior tibial force and internal tibial torque on *in situ* ACL force during simulated weight-bearing knee flexion.[13] Their study demonstrated a significant increase in *in situ* ACL force with application of anterior tibial force, but not with internal tibial torque. The authors hypothesized that ACL force did not change because the application of muscles loads may have changed the knee flexion path or balanced the applied internal rotation torque.

The lack of significant change in rotation of the tibia relative to the femur after transection of the ACL in our study suggests that ACL condition alone does not determine rotational stability. By testing under simulated muscle loading conditions, this study provides new insight on the contribution of muscles to tibiofemoral rotation. Although no significant difference was found between the ACL-intact and -deficient states even under the various muscle loading conditions, there was a significant difference between the loaded muscle conditions, all muscles and hamstring harvest, and the no muscles condition. We believe this difference represents the interaction of muscle forces and geometric factors on tibiofemoral rotation.

Changes in muscle activity observed *in vivo* support this hypothesis. EMG examination of fully rehabilitated ACL-deficient subjects demonstrated increased vastus lateralis and biceps femoris activity during several functional activities.[4] The authors hypothesized this represents a “protective mechanism” to lessen the pivot shift

phenomenon. The presence or absence of this adaptation in muscle function may account for the variability in outcome after ACL injury.

Our findings also suggest that harvest of the semitendinosus and gracilis tendons does not significantly alter the dynamic stabilization provided by muscles crossing the knee joint. We hypothesize that with full rehabilitation of the medial hamstrings following hamstring autograft harvest there is no detrimental effect on tibiofemoral rotation in comparison to the intact knee.

The testing apparatus used in the current study has several modifications in comparison to previous rigs. Joint-compressive load was applied more naturally through simulated knee flexor and extensor muscles to better simulate *in vivo* loading conditions. By applying load through the knee flexor muscles, as opposed to the quadriceps alone, we minimized any abnormal shifts in neutral position seen in prior studies.[18] Our tibial component had minimal constraint on the tibia while still allowing us to apply a rotational torque.

There are limitations to the current study. The simulated muscle forces were selected based on previous studies performed in our laboratory.[20] These loads represent only a portion of body weight because of limitations in our testing apparatus. It is possible that larger differences in tibiofemoral rotation may be detected under greater loads. However, the differences observed between the conditions with muscle forces applied compared to no muscle forces would likely increase with more physiologic loads. Another limitation is the condition and age of the cadaveric specimens. Given the likely role of geometric factors on tibiofemoral rotation, the specimens tested in this experiment

may not best represent the population sustaining ACL injuries. We visually and radiographically examined each specimen to exclude specimens with degenerative changes or deformity that would markedly affect geometry of the tibiofemoral articulation. With application of the 180 N quadriceps force, we observed anterior translation of the tibia although we did not specifically record this with the motion tracking software. The amount of anterior translation also differed between the ACL-intact and -deficient states. However, our results support the findings of Haimes *et al*.[10], in which transection of the ACL alone resulted in increased anterior translation but no significant difference in internal or external rotation limits. Finally, our study needs to be replicated with a larger number of specimens. Although power was adequate to demonstrate differences in internal rotation, it was marginal for demonstrating differences in external rotation.

6.6 Conclusions

The lack of significant changes in tibiofemoral axial rotation following transection of the ACL in any of the three muscle loading conditions suggests that the condition of the ACL alone does not significantly affect knee resistance to axial rotation. Future studies measuring rotational stability might utilize larger (i.e. >460 N) and more dynamic compressive knee loading (e.g. Withrow *et al.*[20]) for a better representation of *in vivo* loading.

6.7 References

1. Andriacchi TP, Dyrby CO. Interactions between kinematics and loading during walking for the normal and ACL deficient knee. J Biomech. 2005; 38: 293-298.

2. Andriacchi TP, Briant PL, Bevill SL, Koo S. Rotational changes at the knee after ACL injury cause cartilage thinning. Clin Orthop. 2006; 442: 39-44.

3. Butler DL, Noyes FR, Grood ES. Ligamentous restraints to anterior-posterior drawer in the human knee. J Bone Joint Surg Am. 1980; 62-A: 259-270.

4. Ciccotti MG, Kerlan RK, Perry J, Pink M. An electromyographic analysis of the knee during functional activities II. The anterior cruciate ligament-deficient and -reconstructed profiles. Am J Sports Med. 1994; 22: 651-658.

5. Czerniecki JM, Lippert F, Olerud JE. A biomechanical evaluation of tibiofemoral rotation in anterior cruciate-deficient knees during walking and running. Am J Sports Med. 1988; 16: 327-331.

6. Daniel DM, Stone ML, Dobson BE, Fithian DC, Rossman DJ, Kaufman KR. Fate of the ACL-injured patient: A prospective outcome study. Am J Sports Med. 1994; 22: 632-644.

7. Delee JC, Drez D, Miller MD, eds. Delee & Drez's Orthopaedic Sports Medicine: Principles and Practice. 2nd ed. Philadelphia, PA: Saunders; 2002.

8. Dennis DA, Mahfouz MR, Komistek RD, Hoff W. In vivo determination of normal and anterior cruciate ligament-deficient knee kinematics. J Biomech. 2005; 38: 241-253.

9. Georgoulis AD, Papadonikolakis A, Papgeorgiou CD, Misou A, Stergiou N. Three-dimensional tibiofemoral kinematics of the anterior cruciate ligament deficient and reconstructed knee during walking. Am J Sports Med. 2003; 31: 75-79.

10. Haimes LJ, Wroble RR, Grood ES, Noyes FR. Role of the medial structures in the intact and anterior cruciate ligament-deficient knee: Limits of motion in the human knee. Am J Sports Med. 1994; 22: 402-409.

11. Lane JG, Irby SE, Kaufman K, Rangger C, Daniel DM. The anterior cruciate ligament in controlling axial rotation: an evaluation of its effect. Am J Sports Med. 1994; 22: 289-293.

12. Li G, Moses JM, DeFrate LE, Papannagari R, Pathare NP, Gill TJ. ACL injury alters tibiofemoral cartilage contact. Paper No: 0073; 53rd Annual Meeting of the Orthopaedic Research Society.

13. Lo J, Muller O, Wunschel M, Bauer S, Wulker N. Forces in anterior cruciate ligament during simulated weight-bearing flexion with anterior and internal rotational tibial load. J Biomech. 2008; 41: 1855-1861.

14. Lohmander LS, Ostenberg A, Englund M, Roos H. High prevalence of knee osteoarthritis, pain, and functional limitations in female soccer players twelve years after anterior cruciate ligament injury. Arthritis Rheum. 2004; 50: 3145-3152.

15. Reuben JD, Rovick JS, Schrager RJ, Walker PS, Boland AL. Three-dimensional dynamic motion analysis of the anterior cruciate ligament deficient knee joint. Am J Sports Med. 1989; 17: 463-471.

16. Ristanis S, Stergiou N, Patras K, Vasiliadis HS, Giakas G, Georgoulis AD. Excessive tibial rotation during high-demand activities not restored by anterior cruciate ligament reconstruction. Arthroscopy. 2005; 21: 1323-1329.

17. Shoemaker SC, Markolf KL. In vivo rotatory knee stability: ligamentous and muscular contributions. J Bone Joint Surg Am. 1982; 64-A: 208-216.

18. Torzilli PA, Deng X, Warren RF. The effect of joint-compressive load and quadriceps muscle force on knee motion in the intact and anterior cruciate ligament-sectioned knee. Am J Sports Med. 1994; 22: 105-112.

19. von Porat A, Roos EM, Roos H. High prevalence of osteoarthritis 14 years after an anterior cruciate ligament tear in male soccer players: a study of radiographic and patient relevant outcomes. Ann Rheum Dis. 2004; 63: 269-273.

20. Withrow TJ, Huston LJ, Wojtys EM, Ashton-Miller JA. The relationship between quadriceps muscle force, knee flexion, and anterior cruciate ligament strain in an in vitro simulated jump landing. Am J Sports Med. 2006; 34: 269-274.

CHAPTER 7

GENERAL DISCUSSION

7.1 Innovation

The goal of this dissertation was to provide fresh insights into the mechanism of non-contact ACL injuries. The current dogma is that valgus loading is thought to be the primary ACL injury mechanism (see Introduction)[1-4]. This is probably because an apparent knee valgus posture has been observed in actual ACL injury videotapes.[5-7] But in those same videotapes it is not possible to accurately estimate the magnitude of axial tibial rotation relative to the femur both because of skin motion and because of the relatively modest magnitude of the rotation.[8-9] As a result the role of axial tibial rotation in ACL injury causation has largely been ignored. This dissertation challenges current dogma by identifying the worst-case 3D compound impulsive loading direction that induces the most ACL strain, and it is not an abduction (or valgus) moment during the simulated landing. These results were supplemented by the results from the 3D computer model which, after being validated against experimental data, was used to explore 'what-if' scenarios. That knee model was purposely simplified to include the essence of knee mechanical behavior under 3-D loading, with a focus on exploring the role of frontal plane alignment, and sagittal plane tibial slope and concavity. The model permitted the

sensitivity of ACL strain to variations in morphological and biomechanical factors to be explored quickly and easily, at little expense, and at no danger to a subject.

A novel contribution in this dissertation is the design, construction and implementation of a novel torsional transformer device for applying axial moments to the tibia in internal or external rotation in the *in vitro* testing apparatus developed by Withrow et al.[10-11] In this way, a torsional loading capability was added to the existing capability of simulating realistic landing scenarios in the presence of simulated muscle forces. Withrow et al. used an impulsive compression force to mimic the ground reaction force that occurs during a jump landing, thereby applying a compressive force to the knee joint and simultaneously an impulsive flexion moment that suddenly increases the knee flexion angle. This increase in the knee flexion angle, in turn, induces a sudden stretch in the simulated quadriceps muscle thereby increasing its tension. The increase in quadriceps tension induces anterior tibial translation, and thereby an increase in ACL relative strain, via the patellofemoral mechanism. In addition, by applying the impulsive compressive force to knee specimens that were oriented in ab- or adduction relative to the compression force, it was possible for Withrow et al. to simultaneously apply a knee abduction or adduction moment in addition to the sagittal-plane loading conditions stated above.[10-11] In the present work, the torsional device can be set to apply an internal torque, an external torque, or even no tibial torque, to the knee in addition to other loading conditions stated above. Thus, the testing apparatus in this study provide a unique opportunity to explore the ACL strain behavior under impulsive 3-D compound loading conditions while the sagittal, frontal, and transverse plane tibiofemoral kinematics were measured simultaneously. It provides, for the first time, an apparatus and method that are

suited for providing new insights into ACL injury mechanisms involving significant internal tibial moments.

Chapter 2 demonstrated that AM-ACL relative strain were significantly greater under internal tibial torque than the external tibial torque in the presence of the realistic impulsive compressive force, flexion moment and muscle forces. This result corroborates the cited *in vitro* studies performed in a quasi-static manner.[12-14] More importantly, this finding helps to reduce the discrepancy between previous *in vitro* quasi-static studies[12-14] and the *post-hoc* injury video analyses[5-6]. For example, Meyer et al. showed that the external tibial rotation that occurred after the ACL failure was caused by an internal tibial torque, thereby suggesting that the observed external tibial rotation in *post hoc* injury video analyses might occur after the ACL was torn.[15] This chapter also reports the AM-ACL strain rate during dynamic loading trials. Little is known about the range of strain rate during a pivot landing. Thus, the chapter also provides strain rate data that should be useful for researchers wanting to know what sort of strain rates occur in pivot landings so they can properly evaluate the viscoelastic characteristics of tissue engineered bone-ligament-bone ACL constructs for human knee reconstructions.

Chapter 3 extends the Chapter 2 findings by showing that, contrary to current dogma, the *in vitro* experiment described in this chapter conclusively demonstrates that it is an internal tibial torque, rather than an abduction moment, that causes the most ACL relative strain. Then, the 3-D knee model simulation extends these findings by demonstrating that a knee abduction moment essentially increases ACL strain by *augmenting internal tibial rotation* due to the difference in slope between medial and lateral tibial plateaus. Another valuable insight from the model simulation is that quite a

large knee abduction moment is required in order to cause medial knee joint opening. Thus, in the model simulation, approximately 100 N-m of knee abduction moment was needed to cause the medial knee joint opening under an impulsive compressive force and the resultant quadriceps muscle force of 1~2 bodyweights and 1,000 N, respectively. This is a conservative result since these loading conditions are relatively modest compared to those acting during an actual injurious loading condition. Hence, the model simulation results imply that the knee abduction moment required to cause the medial knee joint opening would be even greater than 100 N-m during actual injurious loading conditions where the ground reaction force and the resultant quadriceps force would exceed the corresponding values used in this study. These findings help us to understand why concomitant MCL injuries are observed infrequently.[16] The quadriceps muscle contraction causes the tibia to translate anteriorly while the coupled internal tibial rotation would cause the medial tibia to translate posteriorly. Due to these opposing effects, the MCL is less likely to reach its ultimate tensile stress or strain and be injured.

In Chapter 4, a sensitivity analysis was performed for the effect of three selected morphological factors: lateral tibial slope, frontal plane limb alignment, and medial tibial concavity. In Chapter 3 the worst-case loading condition, as far as ACL strain is concerned, was found to be a given internal tibial torque combined with a knee abduction moment. The aim in Chapter 4 was to rank these morphological factors in terms of their contribution to increased ACL strain under the worst-case loading condition. Based on the MRI scans, the distal femur, proximal tibia, and patella were reconstructed. The 3D knee model based on the base geometries was first validated with the experimental data obtained from the Chapter 3. Then, the isolated effect of each morphological factor on the

ACL strain was extrapolated by changing the corresponding geometry, leaving any other conditions unchanged (i.e., geometry, locations of the origin and insertion for each ligamentous structure, and input loading conditions). Since there are large interindividual anatomical variations in the knee joint, these can make a comparison of the relative contributions of the morphological factors to ACL strain problematic. Hence, this modeling approach provided valuable insights into the risk factors for ACL injuries.

Finally, the goal in Chapter 5 was to investigate the role of the ACL in limiting axial tibial rotation by comparing ACL-Intact and ACL-Deficient states while simulating a realistic pivot landing scenario. It is a strength of this *in vitro* study that two different ACL states were compared on the same knee with little change to the testing set up under highly controlled conditions; such a well-controlled comparison would difficult or impossible to achieve *in vivo* given trial-to-trial variability.

The appendices provide the results of a published analysis of the relationship between tibiofemoral accelerations as well as the role of knee and hip flexion on hamstring muscle length.

7.2 Limitations of the Approach

In addition to the limitations discussed in each chapter, there are several other limitations to the present body of work. A first limitation is that the loading condition applied in this study is relatively modest compared to the corresponding loading condition in actual injury events. The relatively modest loading was chosen to prevent the ACL from accumulating damage throughout the *in vitro* dynamic loading trials. Under

the present modest jump landing scenario, the study found that internal tibial rotation plays a primary role in increasing the ACL strain. One can then ask the question: how much additional internal rotation would be required to cause an ACL rupture? In reality, isolated ACL injuries can occur without drastic axial tibial rotation. The results in this study demonstrated that the AM-ACL strain was increased because 1) the increased quadriceps muscle force directly contributed to the increase in the anterior tibial translation (i.e., baseline loading condition), and 2) the applied internal tibial torque augmented the coupled anterior tibial translation. If the ground reaction force and the resultant quadriceps muscle force were greater than the corresponding values in this study, a greater ACL strain would have been resulted. Besides, we would have needed a greater internal tibial torque in order to cause the same magnitude of an internal tibial rotation, because the knee joint becomes stiffer as the muscle contraction increases.[17] Thus, the results in this study imply that the ACL strain could reach an ACL injury threshold even without applying an unrealistically large internal tibial moment.

A second limitation is that it is possible that the AM-ACL strain values may have been overestimated by our test set-up. This is because each end of the knee specimen was connected to ground (i.e., the testing frame) via two universal joints. *In vivo*, a pivot landing involves the distal tibia being connected to the ground via the foot, but there is the possibility of attenuation of the impulsive reaction force at the hip joint via the tensile compliance of the hip muscles. That limitation can be explored using the model by comparing the effect of providing a rotational inertia, to represent the pelvis and torso, rather than the ground connection to the test frame. However, it is unlikely that the

qualitative results obtained would change had that rotational inertia been present; the magnitude of the effects might just be less.

A third limitation is that the menisci were not represented in the knee model simulations. This was deliberate choice because we wanted to examine the effect of tibial slope. We expect that the addition of the poroelastic menisci would decrease the relative motion between the femur and tibia, and thereby perhaps reduce the magnitude of the change in AM-ACL strain. But we do not believe that this limitation would alter the qualitative results found in this dissertation.

In summary, despite the known limitations of the *in vitro* experiments and the limitations of the knee model simulations, the main findings of this dissertation should remain valid. The dissertation clearly demonstrates for the first time that the worst-case dynamic knee loading as far as ACL strain is concerned is an internal tibial torque combined with a knee abduction moment. More importantly, it is an internal tibial torque that primarily causes large ACL strains during a jump landing and a knee abduction moment increases ACL strain by augmenting a coupled internal tibial rotation even without medial knee joint opening. These insights provide a better framework for understanding non-contact ACL injury mechanisms. The published tibiofemoral acceleration paper in the Appendix offers a framework for using miniature inertial measurement devices worn *in vivo* on the skin to screen for undue tibiofemoral accelerations.

7.3 Recommendations for Future Research

There remain many unresolved questions regarding non-contact ACL injury mechanisms and ACL reconstruction methods. In the following paragraphs, we outline possible directions for future research:

1) Although we showed that the test setup can cause ACL injuries in some specimens, it remains unknown how large an internal tibial torque is typically required to cause an ACL rupture under a 2*BW jump landing scenario. It is also unknown how the threshold for the allowable internal tibial torque varies with the impulsive compressive force and the resultant quadriceps muscle force.

2) In the present testing apparatus, the effects of muscles and ligamentous structures for the hip and ankle joints were not considered. It is known that the reduced strength in the hip abductor muscles can result in the increased knee valgus loading. The present study demonstrated that a knee abduction moment could increase the ACL strain by inducing an internal tibial rotation. Thus, a future study might investigate those effects on the ACL strain by adding torsional springs and a rotational inertia at the hip joint.

3) The behavior of the posterolateral (PL) bundle ACL under an internal or external tibial torque remains controversial. In the present study, it was difficult to get an unobstructed view in order to place a DVRT on the PL bundle from the anterior aspect. It also might be possible to measure ACL strain using radio-opaque beads combined with biplanar cineradiography rather than using a DVRT. A future study might explore the behavior of PL bundle under axial tibial torque by using a 3D knee model simulation.

4) It would be worth comparing the effect of several different ACL reconstruction methods on the tibiofemoral kinematics (i.e., a single-bundle reconstruction with more oblique graft vs. an anatomic double-bundle reconstruction) under the worst-case loading scenario found in the present study. A future study might also investigate the effect of the initial tension, orientation, and stiffness of the ACL graft on the tibiofemoral kinematics under the same loading conditions in order to better restore knee joint kinematics.

5) It might be worthwhile investigating the difference on ACL strain of landing on the forefoot versus the rear foot. In the case of the rearfoot, the ground reaction impulse is transmitted directly from the talocalcaneal joint up the tibia with little of any shock absorption. In the case of the forefoot, the calf and foot muscles can do negative work, thereby dissipating the impulsive load.

7.4 References

1. Hewett TE, Lindenfeld TN, Riccobene JV, Noyes FR. The effect of neuromuscular training on the incidence of knee injury in female athletes - A prospective study. Am J Sports Med. 1999;27:699-706.

2. Hewett TE, Myer GD, Ford KR, et al. Biomechanical measures of neuromuscular control and valgus loading of the knee predict ACL injury risk in female athletes: A prospective study. Am J Sports Med. 2005;33:492-501.

3. Lloyd DG. Rationale for training programs to reduce anterior cruciate ligament injuries in Australian football. J Orthop Sports Phys Ther. 2001;31:645-654.

4. Myer GD, Ford KR, Hewett TE. Rationale and clinical techniques for anterior cruciate ligament injury prevention among female athletes. J Athl Training. 2004;39:352-364.

5. Olsen OE, Myklebust G, Engebretsen L, Bahr R. Injury mechanisms for anterior cruciate ligament injuries in team handball a systematic video analysis. Am J Sports Med 2004;32(4):1002-1012.

6. Teitz CC. Video analysis of ACL injuries. In: Griffin LY, ed. Prevention of noncontact ACL injuries. Rosemont, IL: American Association of Orthopaedic Surgeons, 2001: 87–92.

7. Boden BP, Torg JS, Knowles SB, Hewett TE. Video analysis of anterior cruciate ligament injury: abnormalities in hip and ankle kinematics. Am J Sports Med 2009;37:252-259.

8. Krosshaug T, Nakamae A, Boden B, Engebretsen L, et al. Estimating 3D joint kinematics from video sequences of running and cutting maneuvers--assessing the accuracy of simple visual inspection. Gait Posture. 2007;26(3):378-85.

9. Krosshaug T, Slauterbeck JR, Engebretsen L, Bahr R. Biomechanical analysis of anterior cruciate ligament injury mechanisms: three-dimensional motion reconstruction from video sequences. Scand J Med Sci Sports. 2007;17(5):508-19.

10. Withrow TJ, Huston LJ, Wojtys EM, Ashton-Miller JA. The relationship between quadriceps muscle force, knee flexion, and anterior cruciate ligament strain in an in vitro simulated jump landing. *Am J Sports Med.* 2006;34(2):269-74.

11. Withrow TJ, Huston LJ, Wojtys EM, Ashton-Miller JA. The effect of an impulsive knee valgus moment on in vitro relative ACL strain during a simulated jump landing. *Clin Biomech.* 2006;21(9):977-83.

12. Arms SW, Pope MH, Johnson RJ, Fischer RA, Arvidsson I, Eriksson E. The biomechanics of anterior cruciate ligament rehabilitation and reconstruction. Am J Sports Med. 1984;12(1):8-18.

13. Fleming BC, Renstrom PA, Beynnon BD, et al. The effect of weightbearing and external loading on anterior cruciate ligament strain. J Biomech. 2001;34(2):163-170.

14. Markolf KL, O'Neill G, Jackson SR, McAllister DR. Effects of applied quadriceps and hamstrings muscle loads on forces in the anterior and posterior cruciate ligaments. Am J Sports Med. 2004;32(5):1144-1149.

15. Meyer EG, Haut RC. Anterior cruciate ligament injury induced by internal tibial torsion or tibiofemoral compression. J Biomech. 2008;41(16):3377-83.

16. Quatman CE, Quatman-Yates CC, Hewett TE. A 'plane' explanation of anterior cruciate ligament injury mechanisms - A systematic review. Sports Medicine. 2010:40(9);729-746.

17. Wojtys EM, Huston LJ, Schock HJ, Ashton-Miller JA. Gender Differences in Muscular Protection of the Knee in Torsion in Size-matched Athletes. Journal of Bone and Joint Surgery-American Volume. 2003;85A(5):7820789.

CHAPTER 8

CONCLUSIONS

The results from Chapter 2 through 6 and the Appendices enable the following conclusions to be drawn:

1) Internal tibial torque is a potent stressor of the ACL because it induces a 70% larger peak strain and strain rate in the anteromedial bundle of the ACL than does a corresponding external tibial torque (Chapter 2).

2) The worst-case dynamic knee loading as far as ACL strain is concerned is an internal tibial torque combined with a knee abduction moment. However, it is the internal tibial torque, rather than a knee abduction moment, that primarily causes large ACL strains during a jump landing (Chapter 3).

3) When the lateral tibial slope exceeds that of the medial tibial plateau, then a knee abduction moment causes coupled internal tibial rotation, and vice versa. Due to this coupling phenomenon, a knee abduction moment can increase ACL strain, even without medial knee joint opening (Chapter 3).

4) Under a large impulsive compressive force, an increased difference in the medial and lateral tibial slopes accentuates the coupled motion between internal tibial rotation and knee abduction angle, thereby increasing ACL strain. Thus, a steeper lateral tibial slope or a greater difference in medial and lateral tibial slope can be used as a predictor for ACL injury risk (Chapter 4).

5) A static frontal plane limb alignment was correlated with dynamic ACL strain. As static valgus limb alignment increased, the peak ACL strain increased, and vice versa. However, the overall effect of the static frontal plane limb alignment was minor compared to the effect of the lateral tibial slope (Chapter 4).

6) A medial tibial depth of concavity was negatively correlated with the peak AM-ACL strain. As the medial tibial concavity depth was decreased from the nominal depth, so as to make the medial tibial plateau shallower, the peak AM-ACL strain slightly increased. However, an increase in the medial tibial depth from the nominal depth resulted in a more pronounced decrease in peak AM-ACL strain. Thus, a shallow medial tibial concavity is a risk factor for ACL injury (Chapter 4).

7) ACL transection leads to a small increase in the internal tibial rotation, equivalent to a 13 % decrease in the dynamic rotational resistance, under the large impulsive forces associated with a simulated jump landing, but a significant increase in the anterior tibial translation. Hence, an ACL reconstruction that restores both ligament orientation and stiffness will provide major resistance to anterior tibial translation, but provide minor resistance to axial tibial rotation (Chapter 5).

8) The ACL alone does not significantly affect knee resistance to axial rotation, given the lack of significant changes in tibiofemoral axial rotation between the ACL-intact and ACL-deficient states. Muscle preloads significantly affect axial tibial rotation compared to the no-muscle load condition, regardless of whether the ACL is transected (Chapter 6).

9) It is unknown whether subjects can voluntarily set up a lengthening (eccentric) contraction of the hamstrings during a jump landing in order to reduce ACL strain. But if the hip commonly flexes twice as much as the knee during the first phase of the landing, then the hamstrings essentially contract isometrically, with no change in length (Appendix A).

10) A secondary analysis of the data in Chapter 2 shows that the increase in AM-ACL relative strain during a simulated jump landing is proportional to the peak posterior tibial acceleration (relative to the femur) in the sagittal plane (Appendix B).

APPENDIX A

HAMSTRING MUSCLE-TENDON UNIT FUNCTION DURING DROP AND HOP LANDINGS: IMPLICATIONS FOR ACL STRAIN

A.1 Abstract

Non-contact anterior cruciate ligament (ACL) ruptures frequently occur when landing from a jump. The maximum strain in the anterior cruciate ligament can be reduced by the hamstring tension, depending upon the angle of knee flexion at ground contact, and the ratio of the tensions in the quadriceps and hamstrings muscles. The tension in the hamstrings will depend on the level of preactivation, but also on whether the hamstrings shorten (tension will decrease), remain isometric (tension will remain constant) or lengthen (tension will increase) during the first 200 ms or so of the landing. We have previously shown that increases in hamstring tension can reduce maximum ACL strain by as much as 70% during a simulated jump landing. It is presently not known how and whether the lengths of the hamstrings change during the first 200 ms of a jump landing.

We hypothesized that certain combinations of hip and knee flexion can cause a lengthening of the hamstring muscle-tendon unit (MTU) during a jump landing. Methods: We dissected three cadavers to measure the change in hamstring length with

differing degrees of knee and hip flexion. We then performed a secondary analysis of the post-impact hip and knee angle changes measured in 48 young adults performing 317 drop and jump landings onto one leg. We then selected a representative cadaver, and mathematically predicted the changes in its hamstring MTU lengths based upon the premise that the cadaver could employ the same changes in hip and knee angles as those measured in the 317 jump landings.

The hamstring MTUs were found to undergo a quasi-isometric state in the first 100 ms of the landing phase in these natural landing trials. In the biceps femoris MTU, for example, a slight shortening was the most common response; but slight lengthening (<2%) occurred in 36% of the hop landings and 48% of the drop landings.

The hamstring MTUs function essentially quasi-isometrically during the first 100 ms of natural hop and drop landings. There is evidence for a lengthening state in some trials. It should be possible to enhance this effect by teaching an individual to increase hip flexion during the landing phase.

A.2 Introduction

Nearly 100,000 anterior cruciate ligament (ACL) injuries occur annually in the United States, 70% of which are defined as "non-contact" (Griffin, 2000). Non-contact ACL injuries, which involve foot-ground reaction and segmental gravitoinertial forces but no other external contact forces, commonly occur during unipedal jump landings (for example, Kirkendall, 2000). In a maximum height jump landing maximum ACL strain occurs at about 40 ms, with peak muscle forces of about 4,500 N, ~1,000 and ~500 N in the vasti, hamstring and gastrocnemius muscles (Pflum et al. 2004). If the landing phase

is defined as lasting from ground contact to peak knee flexion, then the landing phase of a jump lasts approximately 200 ms (*op cit*). During this phase the preactivated quadriceps muscles are stretched as they resist knee flexion to prevent the leg(s) from buckling, dissipate kinetic energy, and help to attenuate the downward momentum of the body. When an active muscle is stretched it undergoes a lengthening contraction (this terminology is preferred over "eccentric contraction" for reasons given by Faulkner 2003), and the tension in the muscle can nearly double (Brooks & Faulkner 1992). Hence, there is a significant stretch-related increase in quadriceps tension during the landing phase of any jump landing.

It has been demonstrated that an increase in quadriceps tension can significantly increase ACL strain, and even to rupture (Dikeman 1998, DeMorat et al. 2004, Withrow et al. 2006), by drawing the tibial plateau anteriorly relative to the femoral condyles via the patellofemoral mechanism. *In vivo* and computer modeling work by a number of investigators has shown that ACL strain is significantly affected by the relative quadriceps and hamstring muscle force balance (Bach, 1998; Berns, 1992; Beynnon, 1998; Draganich, 1990; Dürselen, 1995; Kain, 1988; Pandy, 1997; Renström, 1986; Shultz, 1999; Torzilli, 1994) in that the hamstrings can increasingly exert a posterior draw force on the proximal tibia as the knee flexes. But the magnitude of the hamstrings' tension will depend on their pre-existing tension at the moment of ground contact, and the state of muscle-tendon unit (MTU) over the next 200 ms. Tension in an actively contacting striated muscle will, if it suddenly is shortened, experience a decrease in contractile force. If the muscle contracts isometrically, it will remain isotonic. If on the other hand the active muscle is lengthened, it will undergo an abrupt increase in tension

that can nearly double its tension (for example, Brooks and Faulkner, 1992), all in the absence of any reflex modulation. In a cadaver model of a jump landing, we recently showed that an increase in hamstring tension during the landing phase can reduce ACL relative strain by an average of 70% (Withrow et al. 2006). Therefore, for a prophylactic reduction in ACL strain during the landing phase, the lengthening state is most preferable state. The isometric state is the next-most preferable state, and the shortening contraction state is the least preferable state. It is not known, however, whether the hamstring MTUs lengthen, act isometrically, or shorten during a drop or hop landing.

While ultrasonic measurements of muscle fascicle length can be made *in vivo* (Fukunaga et al. 1997) and have been made in the calf muscles during jump landings (Kurokawa et al. 2001), we are not aware of any such measurements having been made in the hamstring muscles. When the length of the muscle fascicle exceeds the width of the standard ultrasound probes, as it would in the hamstring muscles, it can be difficult to track each end of the muscle fascicle accurately during the landing phase. This is especially true given the possibility of probe motion artifact during such dynamic maneuvers.

We therefore used an alternative method to estimate hamstring MTU length. We hypothesized that lengthening contractions of the hamstring MTU do occur during natural hop and drop jump landings onto one leg. A goal of this study was to determine the frequency with which they occur. We first dissected three cadavers to measure the changes in hamstring MTU with knee flexion alone, hip flexion alone, and combined hip and knee flexion. Next, we performed a secondary analysis of two kinematic data sets: one set relating to measures of hip and knee flexion angles in 30 healthy young adults

performing 60 cm drop landings onto one leg (Russell et al. 2006) and the other set pertaining to knee and hip flexion angles in 21 healthy young adults landing on one leg following a 1-m forward hop (Palmieri-Smith et al., unpublished). We then predicted hamstring MTU length changes in each of the 102 trials of hop landings and 215 trials of drop landings. For each trial, the hamstring MTU length vs time relationship was categorized into one of six possible characteristic hamstring MTU length-time histories. We then calculated the frequency of each of the six types of hamstring length vs. time relationships in the hop and drop landing trials.

A.3 Methods

Cadaver Experiments

To test the first hypothesis we performed clear dissections of the lower extremities of three cadavers: a 92 yr-old female, a 74 year-old female, and a 77 year-old male without overt musculoskeletal abnormalities in the hips or knees. Heights and weights are given in the legend to Figure A.3. The origins and insertions of the biceps femoris (BF), semimembranosus (SM) and semitendinosus (ST) muscles were exposed and their 3-D locations hand digitized using an Opotrak Certus system (Northern Digital, Inc. Waterloo, Ont, Canada) to the nearest mm relative to bony prominence landmarks. Active marker triads were then attached to the posterior aspect of the pelvis, the mid-femur and proximal tibia using K-wires. A total of 35 trials were then conducted with each cadaver: five each while the knee was slowly flexed through 90° in the parasagittal plane with the hip fixed in up to five equal incremental angles between 0° and 75° in the parasagittal plane. A final five trials were conducted with the hip and knee being flexed

simultaneously by moving the ankle joint directly toward the hip joint in the frontal and parasagittal planes. Kinematic data from the active markers were obtained at 100 Hz using the Certus system. These data were filtered using a 4th order Butterworth low-pass filter. The lengths of each of the three hamstring MTUs were then calculated as the straight line distance between origin and insertion (Figure A.1) at each time interval using standard kinematic transformations and custom MATLAB^{R} routines.

We then mathematically modeled the relationship between MTU length and hip and knee angles in Cadaver #2. This cadaver was selected because the data were more internally consistent than from the other two cadavers (Figures A.3, A.4, A.5). This mathematical modeling was performed for each hamstring muscle by fitting a second order polynomial through the measured MTU length vs knee angle data for each hip angle (Figure A.2).

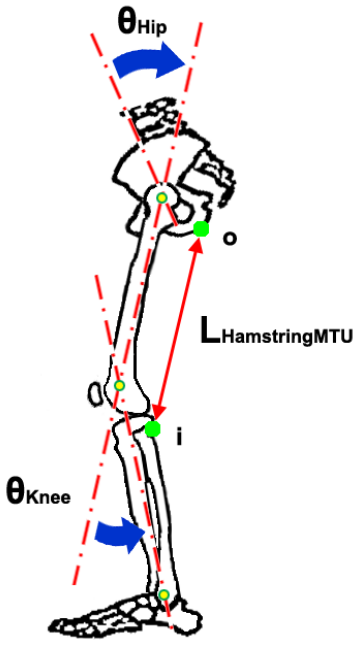

Figure A.1: Lateral view showing the definition of the hip (θ_h) and knee (θ_k) flexion angles along with the origin (o), insertion (i) and length ($L_{HamstringMTU}$) of a hamstring muscle-tendon unit.

Secondary Analysis of In Vivo Single Leg 1-m Forward Hop Landings:

Eleven young adult females (mean ± SD age: 24.0 ± 5.2 years, height: 162.8 ± 6.6 cm, mass: 55.9 ± 7.3 kg) and 10 males (age: 23.6 ± 3.8 years, height: 174.1 ± 7.0 cm, mass: 67.9 ± 7.3 kg) were asked to perform five trials of a 1 m-long forward hop on one leg. Hip and knee joint kinematics were recorded at 120 Hz using standard motion analysis techniques and a Vicon system as described in Russell et al. (2006), while force plate data of the landing were recorded at 1,200 Hz. Descriptive statistics were calculated for the mean (± SD) change in hip and knee angles from ground impact to 200 ms. We then predicted all three hamstring MTU lengths assuming that Cadaver #2 employed the same knee and hip angle trajectories as in the 102 hop landing trials, using the above *in vitro*-based model from Cadaver #2.

Secondary Analysis of In Vivo 60 cm Single Leg Drop Landings:

Thirty young adults (15 males (age = 24±5 years, height = 182.3±6.1 cm, mass = 84.6±9.8 kg) and 15 females (age = 21±6 years, height = 163.3±6.4 cm, mass = 62.1±9.1 kg) were asked to perform 8 trials of a 60 cm drop landing onto one leg (Russell et al. 2006). Data from three subjects were excluded because of technical problems. Using similar methods as for the above hop landing study, in each trial we first calculated the temporal change in hip and knee flexion angles from the raw data. We then used the above *in vitro* model to estimate the change in the three hamstring MTU lengths from ground contact to 200 ms in each trial. Descriptive statistics were again calculated for the change in hip and knee angles.

Analysis of Hamstring MTU Length and Velocity vs Time Relationships During the First 100 ms of the Landing Phase (100 ms post-ground contact)

For every knee angle data point in the first 100 ms (post-ground contact) of the data from the *in vivo* drop landings and hop landings (see above), a second order polynomial was used to find MTU length by interpolating between the five hamstring length vs hip angle polynomial curves that had been fit through the cadaver data shown in Figure A.4. The interval of 100 ms was chosen because the main impact loading on the knee occurs during this time (i.e., Withrow et al. 2006) and a longer interval would have required many more curve types to categorize all the different responses. Six possible hamstring MTU length vs time relationships (designated Curve Types 1-6) were defined and considered during this part of the landing phase (see Figures A.3, A.4, and A.5). For Curve Types 1-5, the increase in length (designated ΔL) of hamstring MTU was calculated in any region of the curve between the times of ground contact and 100 ms that was found to show lengthening mathematically. For Curve Type 4, two regions of MTU lengthening could occur (whose magnitudes was designated $\Delta L1$ and $\Delta L2$), and the maximum of $\Delta L1$ and $\Delta L2$ was then found and reported. For Curve Type 6, in which a monotonic decrease in MTU length could occur, the decrease in MTU length was calculated. The frequency of each of the six types of hamstring MTU length change vs. time relationships was found for the 102 hop landing and 215 drop landing trials. For each curve type, the mean (SD) change in length was also found, along with the minimum and maximum values. Changes in length of the hamstring MTU in Cadaver #2 may be compared with its length in the neutral posture (i.e., zero hip and knee angles) which was measured at 396 mm.

Peak muscle shortening or lengthening velocities were found after differentiating the MTU length – time relationships using a four-point scheme and filtering with a 4th order Butterworth low-pass filter.

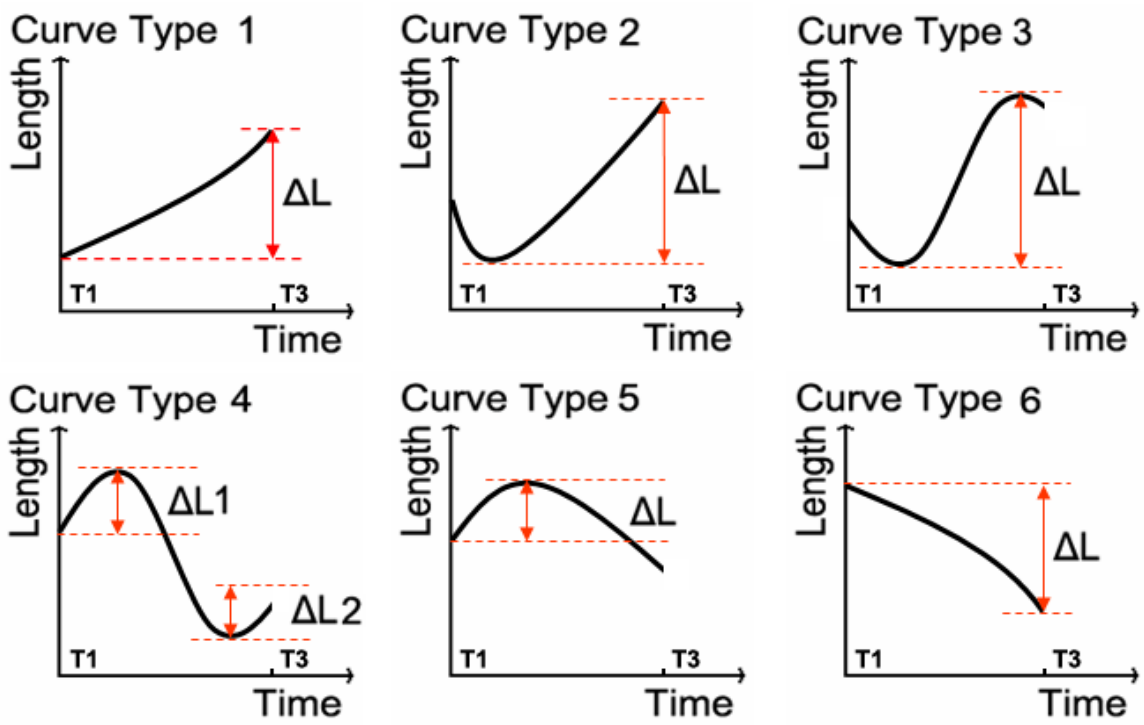

Figure A.2: Schematic drawing illustrating the six possible MTU length vs time relationships within 100 ms of ground contact. An increase in MTU length is designated by ΔL (or ΔL1 and ΔL2 when appropriate). T1 and T3 denote the instant of first ground contact, and 100 ms post-ground contact, respectively.

A.4 Results

Some of the *in vivo* trials contained data that could not be analyzed due to technical problems that included obscured markers. This left a total of 102 hop landing in 21 adults and 215 drop landing trials in 27 adults that could be analyzed successfully. In what follows, we report results from biceps femoris MTU for the sake of brevity, although the other muscles show substantially similar results.

Results from the In Vitro Study

Figure A.2 shows that for all three cadavers and all three hamstring MTUs the MTU length vs. knee angle relationship was characterized by curves with a generally negative slope. The positive offset of those curves was found to increase with increasing hip flexion angle. In the hamstring MTU vs. knee angle plotting space (Figure A.3), a lengthening of that muscle would be demonstrated by a positive slope, whereby the positive effect of hip flexion on hamstring MTU length exceeds the negative effect of knee flexion. So, for any given knee angle, each plot can be inspected to find out how much hip flexion is required to lengthen a hamstring MTU. For example, in Figure A.5, for lengthening of the biceps femoris MTU to occur when knee flexion increases from 0° to 30° during a landing, hip flexion would have increase by more than 25° (the difference between 30° and 55°).

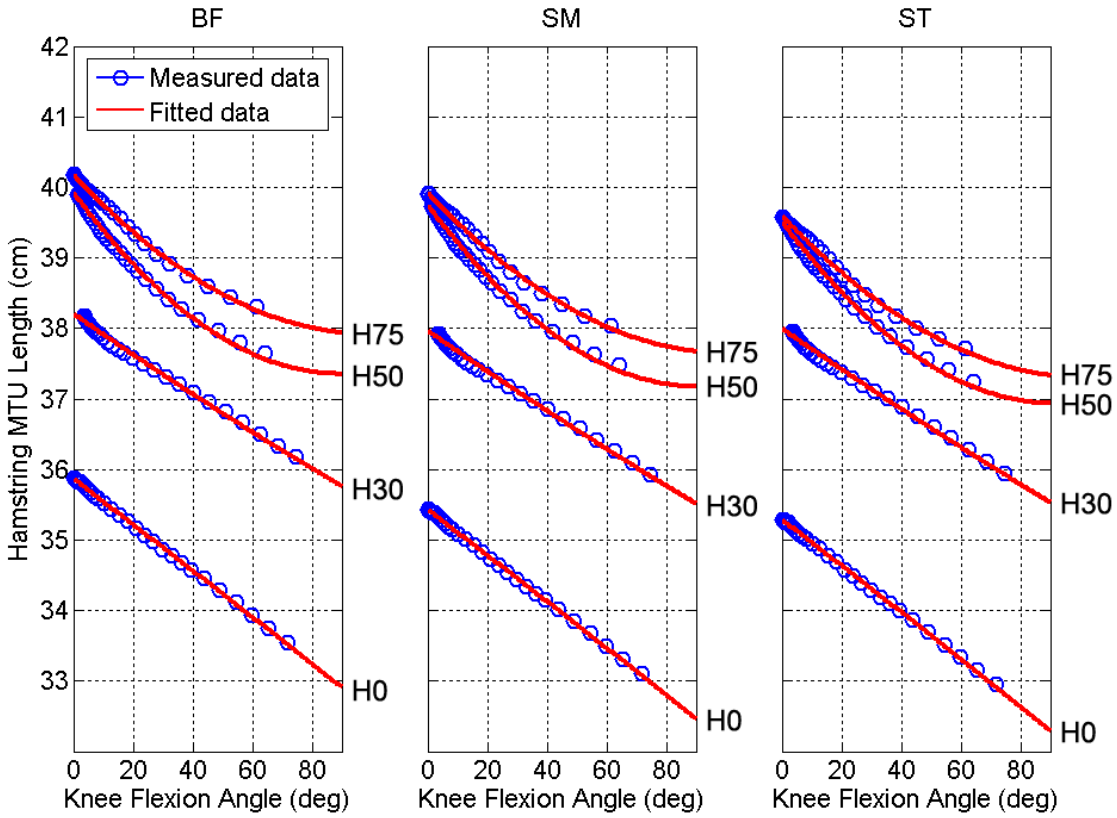

Figure A.3 Effect of increasing knee and hip flexion angles on the three hamstring muscle-tendon lengths from a 92 year-old female cadaver (cadaver #1**;** height: 1.75 m, weight: 70.3 kg) The points on each curve are the data points, while the continuous line through those data is a best-fit second order polynomial. H0, H15, H30, H45, H60 and H75 denote fixed hip angles of 0°, 15°, 30°, 45°, 60°, 75°, respectively.

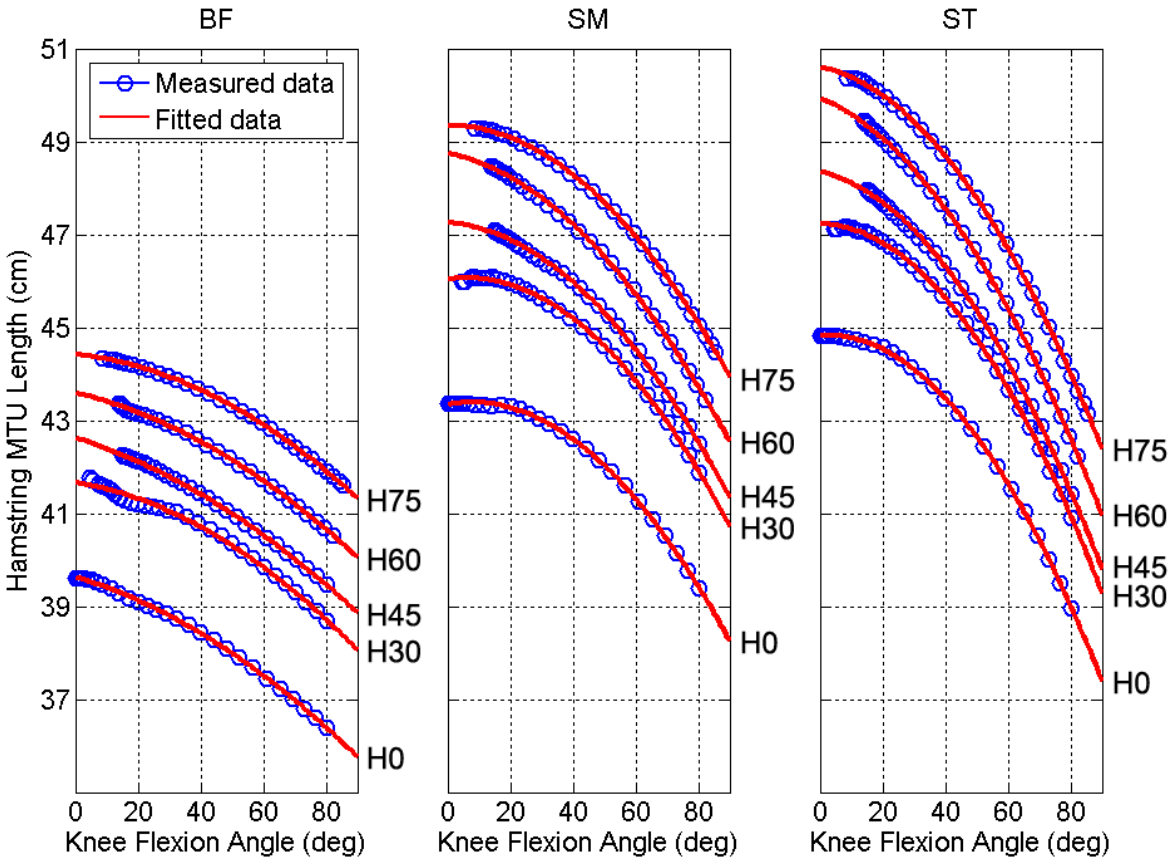

Figure A.4 Effect of increasing knee and hip flexion angles on the three hamstring muscle-tendon lengths from a 74 year-old female cadaver (cadaver #2**:** height: 1.42 m, weight: 59.0 kg).

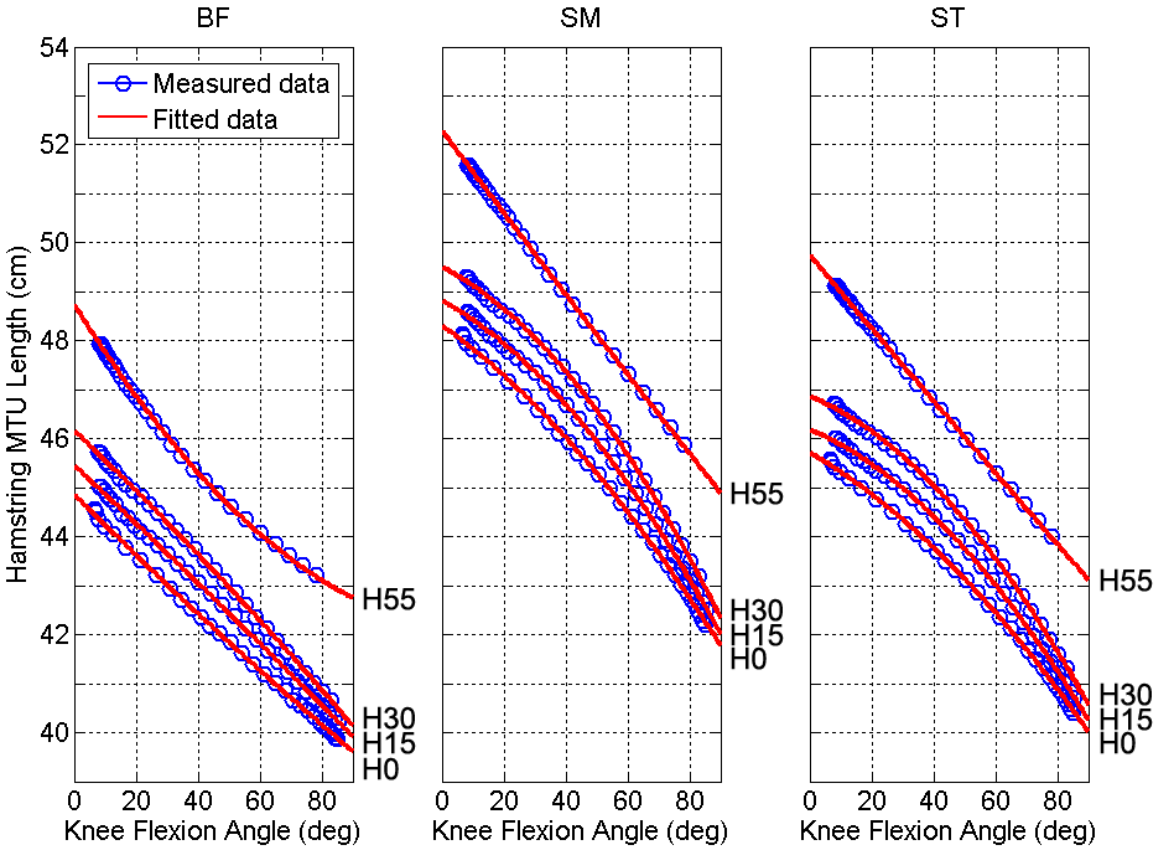

Figure A.5 Effect of increasing knee and hip flexion angles on the three hamstring muscle-tendon lengths from a 77 year-old male cadaver (cadaver #3**:** height: 1.85 m, weight: 90.7 kg).

1-m Forward Hop Landing Results

The most common curve type was Curve Type 6 (64% of the 102 trials) in which a monotonic shortening of the biceps femoris MTU occurred. The next most common curve type was Type 5 (30% of trials), which showed a rapid, but small, increase in MTU length followed by a decrease. The remaining curve types were rare.

The mean (SD) temporal changes in hip and knee angles are shown in Figure A.6, along with the trial closest to the mean response (in the thicker line type). The mean (SD) initial knee and hip angles at ground contact were 17.6° (8.1°) and 29.1° (9.6°), respectively. The mean (SD) increases in those angles were 39.3° (7.7°) and 5.5° (6.3°), respectively.

Figure A.7 shows the biceps femoris MTU length vs knee angle, as well as biceps femoris MTU length and velocity relationships vs time for the landing trial closest to the mean for Curve Type 6. These trials show quasi- isometric behavior for the biceps femoris MTU. The mean (SD) MTU shortening velocity within 200 ms of ground contact in the Type 6 curves was 10.1 (3.8) cm/s with maximum and minimum values of 24.4 and 3.6 cm/sec, respectively.

Table A.1 Frequency (%) of Curve Type for the 102 Hop Landing trials. The change in length (ΔL) of the Biceps Femoris MTU is also given in terms of the mean (μ) and standard deviation (σ).

Curve Type		1	2	3	4	5	6
Frequency (%)		0	1	4	1	30	64
ΔL	μ ± σ	-	0.3	0.5 ± 0.4	0.3	0.5 ± 0.9	-6.7 ± 2.8
(mm)	[min, max]	-		[0.1, 1.1]		[0.0, 4.8]	[-2.6, -20.3]

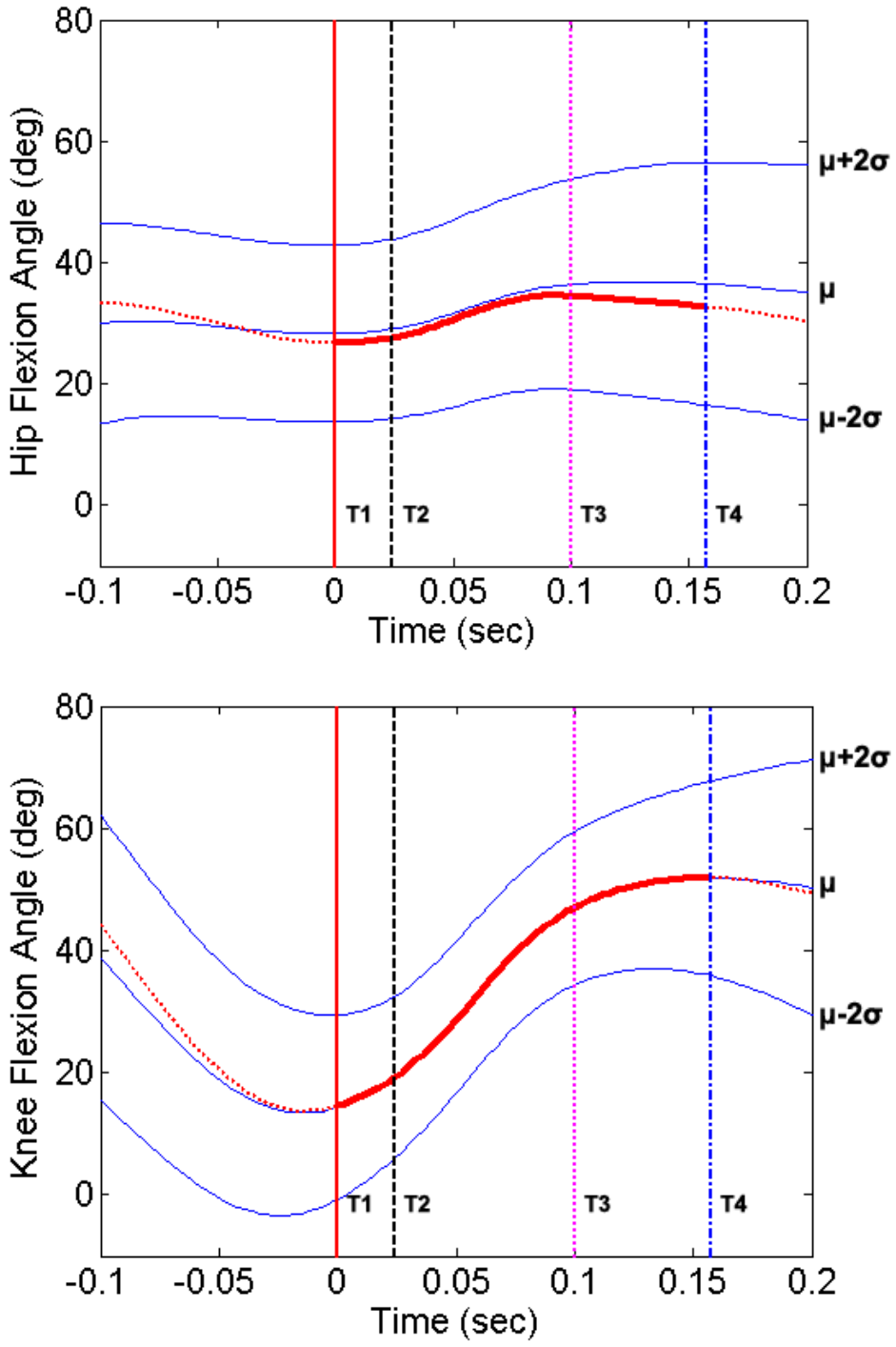

Figure A.6 Mean (+/-2SD) hip (top) and knee (bottom) angle vs. time data for 102 1-m forward hop landing trials from a total of 21 young adults are shown by the three thin-line curves in each figure. The thick line represents the single trial data that are closest to the mean. In all two figures T1, T2, T3 and T4 denote the instant of first ground contact, peak maximum ground reaction force, 100 ms post-ground contact, and the instant of maximum knee angle within 200 ms of ground contact, respectively.

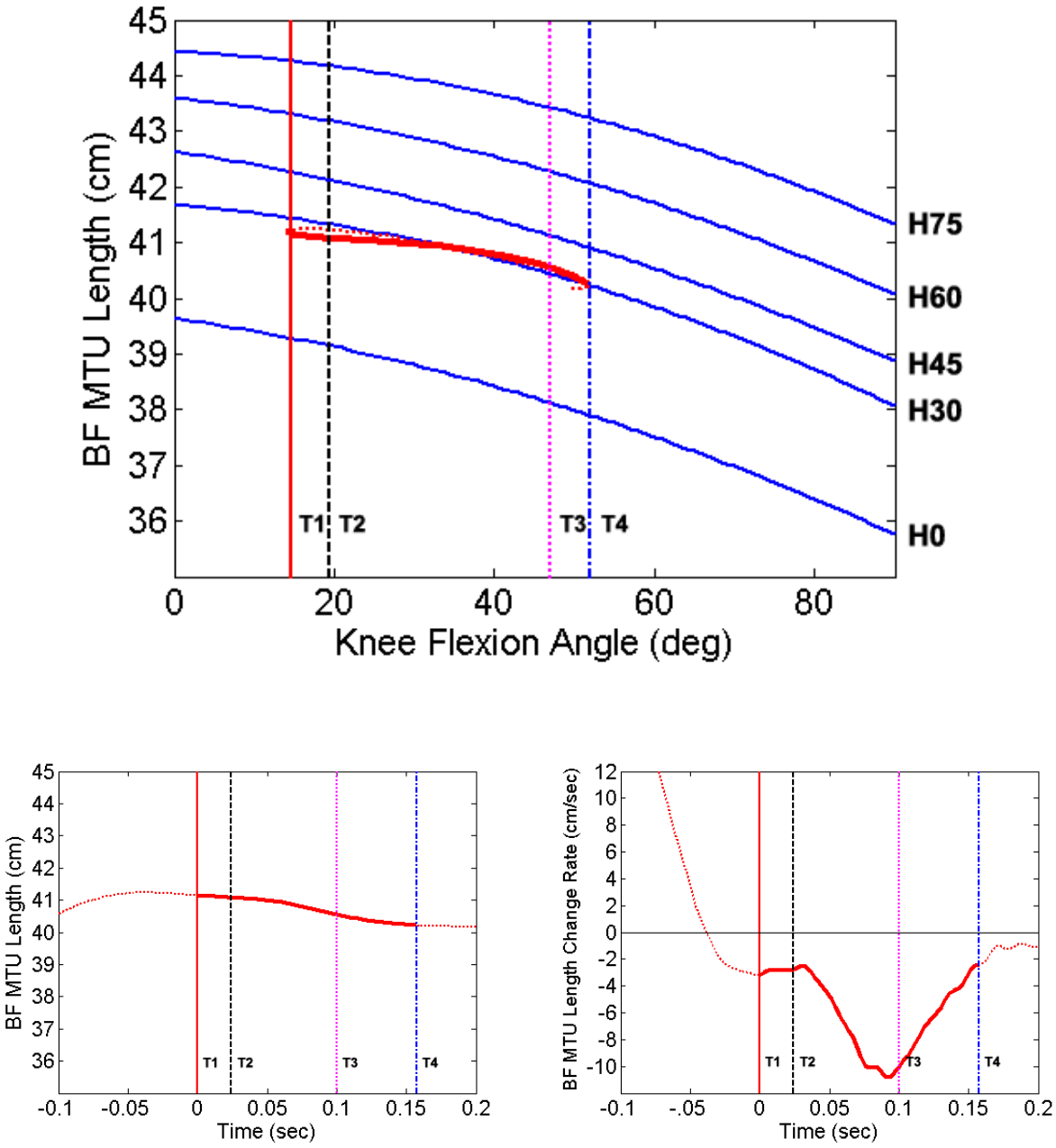

Figure A.7 1-m Forward Hop landing trial results. (Top figure) The five thin curves are replotted from Figure 2B and show the measured relationship between biceps femoris MTU length and knee flexion for different angles of hip flexion in cadaver #2. The thicker horizontal curve shows the predicted biceps femoris length during the single trial closest to the mean for the 102 hop landing trials. (Bottom left) Biceps femoris MTU length vs time data (Bottom left) and velocity vs time (Bottom right) for the single trial closest to the mean. In all three figures T1, T2, T3 and T4 denote the same quantities as in the preceding figure. A positive velocity denotes lengthening of the MTU.

60-cm Single Leg Drop Landing Results

Table A.2 shows that the most common curve type was Curve Type 6 (52% of 215 trials). The next most common curve type was Type 3 (26% of trials) in which a shortening phase was followed by a lengthening phase, while the third most common type was Type 5 (16% of trials) which had an initial lengthening phase. The other curve types were rare.

The mean (SD) initial knee and hip angles were 5.6° (4.2°) and 20.1° (5.9°), respectively. The mean (SD) increases in those angles were 49.2° (7.8°) and 15.1° (12.0°), respectively. The mean (SD) changes in hip and knee angles are shown in Figure A.8.

Figure A.9 shows the biceps femoris MTU length vs. knee angle, as well as biceps femoris MTU length and velocity relationships vs. time for the trial closest to the mean for Curve Type 6. These trials again show quasi-isometric behavior for the biceps femoris MTU. The mean (SD) shortening MTU velocity within 200 ms of ground contact in the Type 6 curves was 6.1 (2.0) cm/s with maximum and minimum values of 11.1 and 1.8 cm/sec, respectively.

Table A.2 Frequency (%) of each Curve Type among the 215 60-cm Drop Landing trials. The change in length (ΔL) of the Biceps Femoris MTU is given in terms of the mean (μ) and standard deviation (σ).

Curve Type		1	2	3	4	5	6
Frequency (%)		0.5	5	26	0.5	16	52
ΔL	μ ± σ	3.8	1.0 ± 1.3	1.2 ± 1.0	0.0	1.4 ± 1.2	-3.7 ± 1.4
(mm)	[min, max]		[0.0, 3.2]	[0.0, 3.4]		[0.2, 4.9]	[-1.1, -7.3]

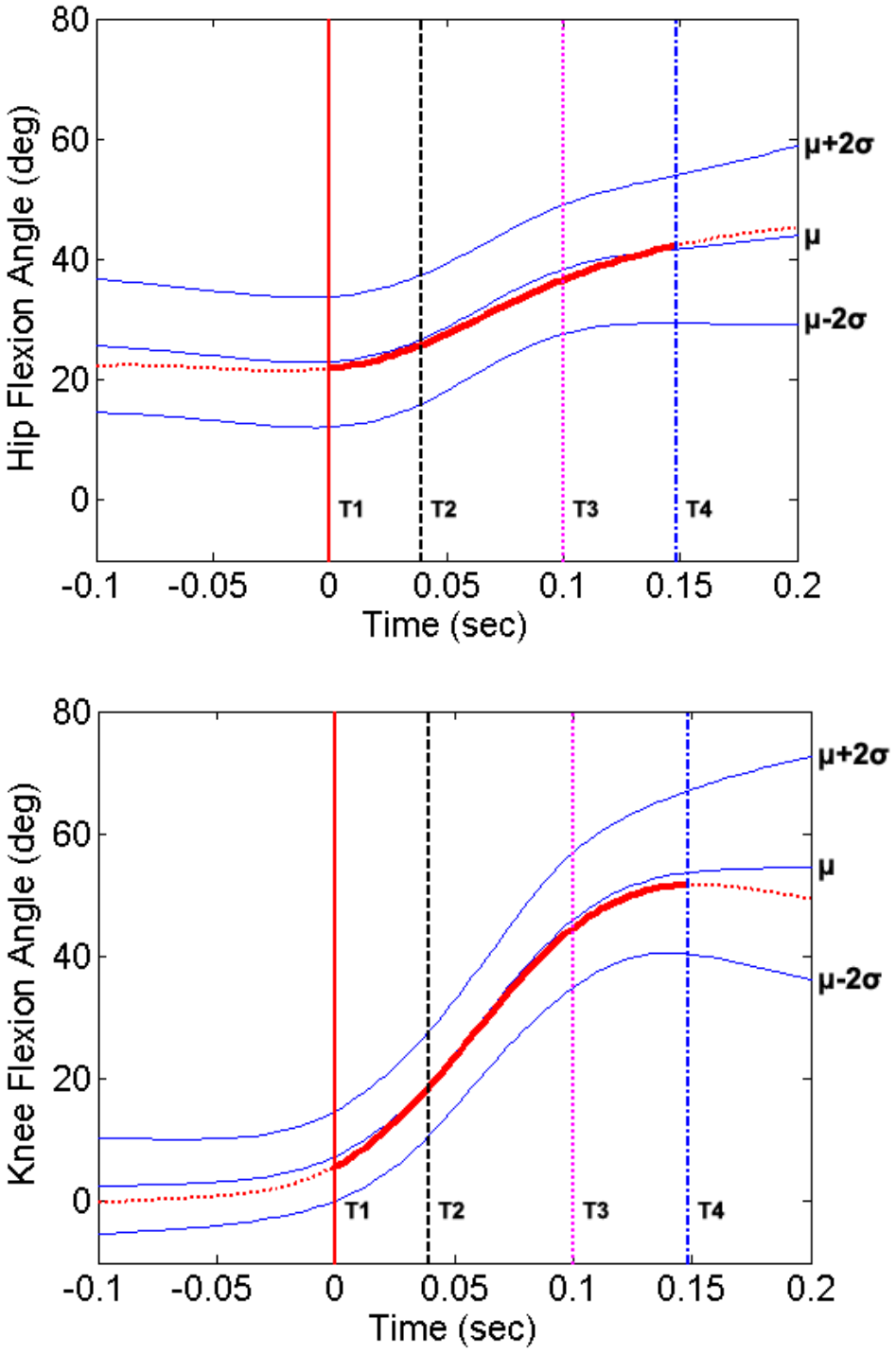

Figure A.8 Mean (+/-2SD) hip (top) and knee (bottom) angle vs. time data for 215 drop landing trials from a total of 27 young adults are shown by the three thin-line curves in each figure. The thick line represents the single trial data that are closest to the mean. T1-4 denotes the same time points as in Figure A.6.

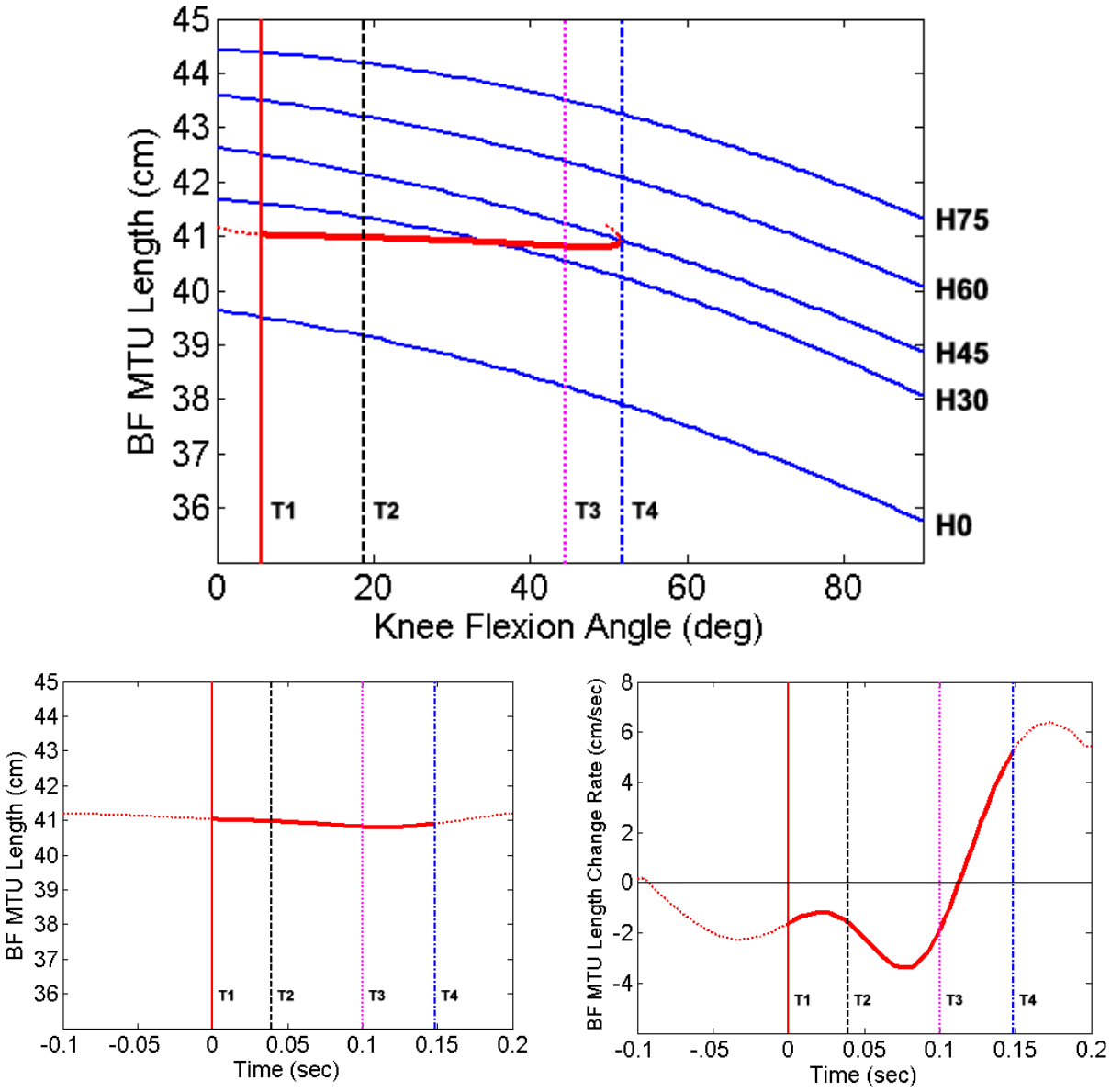

Figure A.9 Drop landing trial results. (Top figure) The five thin curves are replotted from Figure 2B and show the measured relationship between biceps femoris MTU length and knee flexion for different angles of hip flexion in cadaver #2. The thicker horizontal curve shows the predicted biceps femoris length during the single trial closest to the mean for the 215 drop landing trials. (Bottom left) Biceps femoris MTU length vs time data (Bottom left) and velocity vs time (Bottom right) for the single trial closest to the mean. In all three figures T1, T2, T3 and T4 denote the instant of first ground contact, peak maximum ground reaction force, 100 ms post-ground contact, and the instant of maximum knee angle within 200 ms of ground contact, respectively. A positive velocity denotes lengthening of the MTU.

A.5 Discussion

The significance of this paper is that it is the first time that the effect of hip motion on the state of the hamstring muscles has been examined during hop and drop landings onto one leg. The state of these muscles is important during such landings because they span the knee joint and have been shown to significantly limit ACL strain under some circumstances (see Introduction). The main result is that the hamstring MTUs appear to act quasi-isometrically during drop and hop landings onto one leg. This may help protect the ACL from excessive strain by restricting anterior tibial translation.

The results show that if an individual with given anthropometry (i.e., Cadaver #2) lands with the same hip and knee angle trajectories as these 27 adults landing on one leg from a 60 cm drop, or these 21 adults landing from a 1-m forward hop, then the biceps femoris MTU lengthened in 36 % of the hop landing trials (Curve Types 1-5) and 48% of the drop landing trials. The lengthening effect was subtle, ranging from 0 to 1.3% (Tables A.1 and A.2), and would likely be insufficient to set up a lengthening contraction of the actual hamstring muscle fibers because stretch of the MTU can instead occur in the tendon of the muscle, leaving the fibers themselves to act isometrically. Exactly this behavior has been observed ultrasonically in the calf muscle during jump landings (Kurokawa et al. 2001). We therefore conclude that in the present study, the biceps femoris was found to act quasi-isometrically during these jump landings. That is not say that different behavior may not be found when other types of jump landings are examined, or when out of sagittal plane hip motions (for example, internal or external rotation, with or without ab- or adduction) are included. These studies remain to be performed.

This quasi-isometric result is reasonable since the risk of muscle stretch injury is negligible during shortening or isometric contractions. Striated muscle can only be injured during lengthening contractions. The risk of muscle injury during a lengthening contraction is known to being proportional to the negative work done (the product of muscle tension times the amount of muscle stretch) during the lengthening contraction (Brooks et al. 1995). The good news is that training the muscle with lengthening contractions can significantly reduce its risk of injury over time (Brooks et al. 2001). This can be taken advantage of by purposely lengthening the hamstrings MTU during jump landings in order to limit maximum ACL strain.

An isometric hamstring state is not necessarily unhelpful in terms of the hamstrings' ability to counteract the action of the quadriceps muscle in straining the ACL during the landing phase, for it would ensure a constant hamstring tension throughout the first critical 100 ms of the landing phase. This would still be preferable to a sharp reduction in hamstring tension during this phase due to a marked shortening contraction. However, a lengthening contraction would be more preferable than an isometric contraction in terms of limiting ACL strain (see Introduction).

The curves in Figure A.3-5, A.6 and A.8 show that, had the subjects been instructed to volitionally land with greater increase in hip flexion during the early landing phase, then the effect on hamstring lengthening would have been greater. Conversely, landing with a smaller increase in hip flexion would increase biceps femoris MTU shortening.

One might have used a computer modeling program such as SIMM™ or ANYBODY™ instead of the cadaver to simulate these landings. While they are convenient in the way that they contain reasonable representations of muscle origin and insertions, bony geometry, as well as muscle wrapping in some cases, they do not necessarily reflect the correct rolling and sliding knee joint kinematics. Since the ACL strain is relatively sensitive to knee joint rolling and sliding kinematics during knee flexion, we felt it would be more accurate to use a real cadaver than these computer models to estimate the effect of hip and knee flexion on hamstring MTU state. Armed with the information in this paper, it would now be possible to run these computer models and compare their predictions of hamstring MTU length states with those in this paper.

The more extended a limb is at ground strike the higher is the impact force (Nigg 1985, Nisell et al. 1986). The range of initial knee and hip angles at ground contact in the present study are consistent with published results of 25°-32° for 25 and 50 cm drop landings (Fagenbaum et al. 2003; Pflum et al. 2004) and 20°-28° in Stop-Jumps (Yu, 2004). More recently in maximum height jump landings, mean (± SD) initial knee flexion angles of 11° (±3°) at toe contact, and 28° (±7°) at heel contact have been measured (Urabe et al. 2005). These results can be compared with data from Olsen et al. (2004), who used injury videotapes to estimate the knee flexion angle at the time of ACL injury as averaging 16°. So, the range of initial knee and hip angles studied in this paper, and the post-contact intervals during which changes in those angles occur, are pertinent to the mechanisms of ACL injury.

The idea of studying the variation in jump landing kinematics in the 48 adults was to be able to quantify the variance in natural jump landing styles. Since jump landing

styles can be modified by instruction, it is important to first understand the normal range of behavior. Since hip and knee angles are non-dimensional, the variation in landing styles means that this variation can be applied to a single cadaver in order to study how that variation would affect hamstring MTU length changes. It would have been beneficial to run the calculations in a larger number of cadavers, but that was simply not practical. Individual differences in muscle lever arms between cadavers would tend to bias the results toward more or less hamstring lengthening, but probably would not affect the overall qualitative results or the variation due to intrasubject and intratrial variations in hip and knee angles.

We chose one-legged jump landings to analyze in this study because this is a common scenario for ACL injury. The axial loading on the single extremity is considerably higher than in a bipedal landing as the limb attenuates the downward momentum of the superincumbent body mass.

Slight variations in the character of the family of curves in Figure A.3, A.4, and A.5 exist, especially in Cadavers 1 and 3. These variations may reflect slight differences in the orientation of the foot in the frontal plane as it was manually moved to flex the knee and/or hip joints.

The six Curve Types shown in Figure A.2 arise because of variations in the relative hip and knee angular velocities throughout the time interval considered, 100 ms. The fact that only two or three Curve Types predominated lends credence to systematic behaviors being identified.

Limitations include the limited number of cadavers studied, and the fact that the effect of muscle wrapping was not studied. This latter effect can be expected to increase the calculated muscle length change at greater angles of hip flexion, but not knee flexion. Hence, the present estimates of the lengthening effects on hamstring MTU are probably conservative. It was also a limitation that we did not examine gender effects in this study, but it would be worthwhile doing this in the future given the known gender difference in ACL injury rates. Finally, we only used one cadaver to run the MTU predictions. This being a female it might have been better to only apply data from the female subjects. It was also a limitation that we applied data from live healthy young adults to an older expired individual. Nonetheless, these limitations should not affect the overall qualitative results that were obtained.

The results show that the hamstring MTU function is essentially quasi-isometric during the first 100 ms of natural hop and drop landings. Due to the trial-to-trial and subject-to-subject kinematic variations in hip and knee angles there was evidence for a lengthening hamstring MTU state in some trials. It should be possible to enhance this effect by teaching an individual to preprogram increased hip flexion during the early landing phase. Conversely, a reduction in hamstring pretension prior to landing, or a lack of hip flexion during the early landing phase, such as can occur during an out-of-control landing involving a backward fall, would increase hamstring MTU shortening and thereby directly reduce its tension and the prophylactic effect it usually has in limiting peak ACL strain during the impact loading associated with the landing (Withrow 2008).

Lastly, our results may partially explain the decrease in ACL injury rates reported after training with the Cincinnati Sportsmetrics (Hewett et al. 1999) or the PEP ACL

injury prevention programs (Mandelbaum et al. 2005). Both of these programs focus on functional hip and knee positioning during jump landing and pivoting maneuvers and they emphasize hip flexion. An increase in preprogrammed hip flexion, developed by the 6 or 8 week training intervention, could result in a consistent isometric or even lengthening hamstring muscle contraction during jump landings. This could be a fruitful area for further sports medicine research.

A.6 Conclusions

The hamstring MTUs function essentially quasi-isometrically during the first 100 ms of natural hop and drop landings. There is evidence for a lengthening state in some trials. It should be possible to enhance this effect by teaching an individual to increase hip flexion during the landing phase.

A.7 References

1. Bach JM, Hull ML. Strain inhomogeneity in the anterior cruciate ligament under application of external and muscular loads. *J Biomech Eng* 1998;120:497-503.

2. Berns GS, Hull ML, Patterson HA. Strain in the anteromedial bundle of the anterior cruciate ligament under combination loading. *J Orthop Res* 1992;10:167-176.

3. Brooks SV. Faulkner JA. Isometric, shortening, and lengthening contractions of muscle fiber segments from adult and old mice. *Am J Physiol* 1992;267(2 Pt 1):C507-13.

4. Brooks SV, Opiteck JA and Faulkner JA. Injury to muscle fibres after single stretches of passive and maximally stimulated muscles in mice. *J Physiol (Lond)* 1995;488(Pt 2): 459-469.

5. Brooks SV, Zerba E, Faulkner JA. Conditioning of skeletal muscles in adult and old mice for protection from contraction-induced injury. *J Gerontol A Biol Sci Med Sci.* 2001;56(4):B163-71.

6. DeMorat G, Weinhold P, Blackburn T, Chudik S, Garrett W. Aggressive quadriceps loading can induce non-contact anterior cruciate ligament injury. *Am J of Sports Med* 2004;32, 477-483.

7. Dikeman JS. Experimental simulation of mechanism of injury for non-contact, isolated anterior cruciate ligament ruptures. *Master's Thesis, North Carolina State University,* 1998.

8. Draganich LF, Vahey JW. An in vitro study of anterior cruciate ligament strain induced by quadriceps and hamstring forces. *J Orthop Res* 1990;8: 57-63.

9. Dürselen L, Claes L, Kiefer H. The influence of muscle forces and external loads on cruciate ligament strain. *Am J Sports Med* 1995;23:129-136.

10. Fagenbaum R, Darling WG. Jump landing strategies in male and female college athletes and the implications of such strategies for anterior cruciate ligament injury. *Am J Sports Med* 2003;31:233-240.

11. Faulkner JA. Terminology for contractions of muscles during shortening, while isometric, and during lengthening. *J App Physiol* 2003;95:455-459.

12. Fukunaga T, Ichinose Y, Ito M, Kawakami Y, Fukashiro S. Determination of fascicle length and pennation in a contracting human muscle in vivo. *J. Appl. Physiol.* 1997;82(1): 354–358.

13. Kurokawa S, Fukunaga T, Fukashiro S. Behavior of fascicles and tendinous structures of human gastrocnemius during vertical jumping. *J Appl Physiol* 2001;90: 1349-1358.

14. Griffin LY, Agel J, Albohm MJ, et al: Non-contact anterior cruciate ligament injuries: risk factors and prevention strategies. *J Am Acad Orthop Surg* 2000;8: 141-150.

15. Hewett TE, Lindenfeld TN, Riccobene JV, Noyes FR. The effect of neuromuscular training on the incidence of knee injury in female athletes. *Am J Sports Med* 1999;27:699-706.

16. Kain CC, McCarthy JA, Arms S, Pope MH. An in-vitro analysis of the effect of transcutaneous electrical stimulation of the quadriceps and hamstrings on anterior cruciate ligament deformation. *Am J Sports Med* 1988;16:147-152.

17. Kirkendall DT, Garrett WE: The anterior cruciate enigma. Injury mechanisms and prevention. *Clin Orthop Rel Res* 2000;372: 64-8.

18. Mandelbaum BR, Silvers JH, Eatanabe DE, et al. Effectiveness of a neuromuscular and proprioceptive training program in preventing anterior cruciate ligament injuries in female athletes: 2-year follow up. *Am J Sports Med* 2005;33:1003-1010.

19. Nigg BM. Biomechanics, load analysis and sports injuries in the lower extremities. *Sports Med* 1985;2:367-379.

20. Nisell R, Nemeth G, Ohlsen H. Joint forces in extension of the knee. *Acta Orthop Scand* 1986;57:41-46.

21. Olsen OE, Myklebust G, Engebretsen L, Bahr R. Injury Mechanisms for Anterior Cruciate Ligament Injuries in Team Handball. *Am J Sports Med* 2004;32:1002-1012.

22. Palmieri-Smith RM (Unpublished data).

23. Pandy MG, Shelburne KB. Dependence of cruciate-loading on muscle forces and external load. *J Biomech* 1997;30:1015-1024.

24. Pflum MA, Shelburne KB, Torry MR, Decker MJ, Pandy MG. Model prediction of anterior cruciate ligament force during drop landings. *Med Sci Sports Exerc* 2004;36:1949-1958.

25. Renström P, Arms SW, Stanwyck TS, Johnson RJ, Pope MH. Strain within the anterior cruciate ligament during hamstring and quadriceps activity. *Am J Sports Med* 1986;14:83-87.

26. Russell KA, Palmieri RM, Zinder SM, Ingersoll CD. Sex differences in valgus knee angle during a single-leg drop jump. *J Athl Train* 2006;41:166-71.

27. Shultz SJ, Perrin DH. The role of dynamic hamstring activation in preventing knee ligament injury. *Athletic Therapy Today* 1999;4:49-53.

28. Torzilli PA, Deng X, Warren RF. The effect of joint-compression load and quadriceps muscle force on knee motion in the intact and anterior cruciate ligament-sectioned knee. *Am J Sports Med* 1994;22:105-112.

29. Urabe Y, Kobayashi R, Sumida S, Tanaka K, Yoshida N, Nishiwaki GA, Tsutsumi E, Ochi N. Electromyographic analysis of the knee during jump landing in male and female athletes. *The Knee* 2005;12:129-134.

30. Withrow TJ, Huston LJ, Wojtys EM, Ashton-Miller JA. The relationship between quadriceps muscle force, knee flexion and ACL strain in and in vitro simulated jump landing. *Am J Sports Med* 2006;34:269-274.

31. Withrow TJ, Huston LJ, Wojtys EM, Ashton-Miller JA. The effect of varying hamstring tension on ACL strain during the knee flexion caused by axial impact loading of the lower extremity in vitro. J Bone Jt Surg 2008;90(4):815-23

32. Yu B, McClure SAB, Onate JA, Guskiewicz KM, Kirkendall DT, Garrett WE. Age and gender effects on lower extremity kinematics of youth soccer players in a stop-jump task. *Am J Sports Med* 2004;33:1356-1364.

APPENDIX B

THE RELATIONSHIP BETWEEN ANTERIOR TIBIAL ACCELERATION, TIBIAL SLOPE AND ACL STRAIN DURING A SIMULATED JUMP LANDING TASK

B.1 Abstract

Knee joint morphology contributions to ACL loading are rarely considered within the injury prevention model. This may be problematic since the knee mechanical response may be influenced by these underlying morphological factors. The goal of this study, therefore, was to explore the relationship between posterior tibial slope, recently postulated to influence knee and ACL loading, impact-induced anterior tibial acceleration and resultant ACL strain during a simulated single leg landing.

Eleven female lower limb cadaveric specimens (65±10.5 years) were mounted in a testing apparatus to simulate single-limb landings in the presence of pre-impact knee muscle forces. After preconditioning, specimens underwent 5 impact (1297.9 ± 210.6 N) trials, while synchronous 3-D joint kinetics, kinematics and relative anteromedial bundle (AMB) strain data were recorded. Mean peak tibial acceleration and AMB strain were quantified over 200 ms post-impact. These, along with radiologically-defined posterior

tibial slope measures, were submitted to individual and step-wise linear regression analyses.

Mean (± SD) peak AMB strain (3.35 ± 1.71 %) was significantly correlated ($r = 0.79$; $p = 0.004$; $\beta = 0.791$) with anterior tibial acceleration (7.87 ± 2.77 $m.s^{-2}$), with the times to respective peaks (66 ± 7 ms; 66 ± 4 ms) also significantly correlated ($r = 0.82$; $p = 0.001$; $\beta = 0.818$). Posterior tibial slope (7.8 ± 2.1º) was significantly correlated with both peak anterior tibial acceleration ($r = 0.79$; $p = 0.004$; $\beta = 0.786$) and peak AMB strain ($r = 0.76$; $p=0.007$; $\beta = 0.759$).

Impact-induced ACL strain is directly proportional to anterior tibial acceleration, with this relation being moderately dependent on the posterior slope of the tibial plateau. Anterior tibial acceleration is associated with AMB strain during simulated landings. The magnitude of the impact-induced accelerations governing the strain response is additionally correlated with the posterior slope of the tibial plateau. Further exploration of the effect of other knee morphological variables on ACL strain during simulated high-risk landings appears warranted.

B.2 Introduction

When landing from a jump, the ground reaction force induces transient segmental accelerations that are transmitted from the foot to the head[7-8] . These accelerations are attenuated by the resistance of bone as well as passive and active soft tissues to deformation[8-9]. When accelerations induced in a restraining structure cause deformations (strains) that approach its failure tolerance, the potential for injury increases[10-11]. Inadequate shock attenuation is commonly implicated in overuse injuries during

repetitive high impact running or jumping tasks, where fatigued muscles provide inadequate damping[12]. Impact-induced tibio-femoral accelerations during a landing may similarly cause ACL strains approaching those sufficient to cause rupture. Specifically, in instances when an ineffective overarching neuromuscular strategy prevails, it is feasible that impact-induced sagittal plane anterior tibial accelerations could be large enough to compromise the passive ligamentous restraint mechanism.

A number of knee morphologic variables have been identified as risk factors for ACL injury, with many also demonstrating sex-dependence. A small femoral notch, higher than-normal BMI and increased joint and ACL laxity, for example, prospectively predicted ACL injury risk in US military cadets[13]. Variations in lower limb alignment, such as increased anterior pelvic tilt[14], femoral anteversion[14-15] and genu recurvatum[14,16] are also proposed to impact ACL loading and resultant risk. Because morphologic contributions to injury risk are largely unmodifiable, they have not been considered within the injury prevention model. Worth noting, however, is that the underlying knee morphology directly influences joint mechanics[17] and hence the potential for injurious load states. Therefore, elucidating the interaction between key knee morphologies and joint and ligament loading during high risk landings seems particularly worthwhile. The posterior tibial plateau slope has been identified as a risk factor for ACL injury[18-20]. Individuals previously suffering an ACL injury[21], particularly females[22], possessed larger posterior tibial slopes compared to matched controls. Speculation exists regarding how posterior tibial slope may implicate within the ACL injury mechanism[18,20,23]. Recently, for example, execution of a "provocative" (decreased ankle plantar flexion and increased knee extension and hip flexion) compared to safe lower limb landing was suggested to

orient the tibial slope more vertically at impact, resulting in greater anterior tibial thrust[23]. It seems reasonable from a biomechanical perspective that during such movements an increased posterior tibial slope may increase ACL strain by directly increasing the impact-induced anterior tibial accelerations with respect to the femur.

The goal of this study was to test the primary hypothesis that during a simulated dynamic single-limb landing, peak relative AMB strain is directly associated with both posterior tibial slope and peak anterior tibial acceleration. We also tested a secondary hypothesis that the timing of the peak acceleration and strain magnitudes are highly correlated. Because these postulates were tested under simulated "safe" landing scenarios, one cannot extrapolate outcomes to ACL injury scenarios. This study remains important, however, as it represents an initial examination of the interaction between morphological factors and the dynamics of the knee and the ACL response to controlled impulsive loading.

B.3 Methods

Hypotheses were tested in an *in vitro* repeated measures laboratory experiment. A prehoc power analysis employing regression coefficients obtained from Withrow et al24 showed that a minimum of 10 same-sex specimens were required to achieve statistical power of 0.90 with a nominal alpha of 0.05. Data were therefore collected on unembalmed female lower limb cadaveric specimens (mean age = 65±10.5 years). All specimens were procured from the University of Michigan Anatomical Donations Department and fresh frozen at -20º C until 12 hours prior to testing[24]. Limbs were visually checked and those presenting with scars, indications of surgery, deformities prior

to procurement, radiographic abnormalities or osteophytes, cartilage erosion, exposed bone and/or any ACL tears were discarded. Specimens were then dissected, leaving the joint capsule, ligaments and other passive joint tissues intact. Muscle tissue from the quadriceps, medial and lateral hamstrings and medial and lateral gastrocnemius tendons was also removed. Following dissection, specimens were cut transtibially and transfemorally, approximately 24 cm from the joint line and potted within two 7.6 cm diameter polymethylmethacrylate cylinder blocks of height 5.1 cm.

Once potted, each knee specimen was mounted in the Withrow et al.[24] apparatus to simulate, in the presence of muscle forces, the 3-D impulsive loads associated with a jump landing[24,72] (Figure B.1). A double loop of nylon cord (~2 mm diameter, tensile stiffness of ~2 kN/cm) simulated the *in vivo* tensile stiffness of the quadriceps muscle tendon unit under sudden stretch.[24-25] This cord was attached to the quadriceps tendon via a cryoclamp and run along the quadriceps muscle line-of-action to the potted fixture end.[25-26] Constant force springs simulated medial and lateral hamstrings and gastrocnemius muscle-tendon units. Pre-impact quadriceps tension was set to 180 N, with the tension in each hamstring and gastrocnemius muscle being set to 70 N, similar to those calculated[27] previously for landing maneuvers. Specimens were mounted with an initial knee flexion angle of 15º so as to be consistent with typical single leg landings *in vivo*[28] .

Each specimen underwent approximately ten consecutive simulated impact trials. The first five trials preconditioned the specimen[25] , with data from the next five successful trials used in statistical analyses. To successfully simulate the impulsive knee

loads, a weight of approximately 178 N was released vertically in line with the tibial end of the specimen from a height between 7 cm and 9 cm. This release height was adjusted over the preconditioning trials to simulate a 2 x body weight (BW) impact for each specimen.

The weight struck the end of an impact 1 rod in series with the distal tibia with an impulsive compressive force averaging approximately 1,200 N that peaked at approximately 50 ms.[25] This value is consistent with that estimated or quantified during *in vivo* landings.[27,29] In all trials, knee specimens were oriented with the base of the mounting pot placed directly below the impact rod and the line-of-action of the impulsive distal tibia force acting 4 cm posterior to the knee joint center. This resulted in an impulsive compression and flexion moment being exerted about the knee joint, generating femoral and tibial momenta and an increase in knee flexion angle[24-26]. The 3-D forces and moments applied to the knee joint by the distal tibia and proximal femur were recorded for 2 seconds post-impact via 6–axis load cells (AMTI, Watertown, Massachusetts).

A miniature (3-mm stroke) differential variable reluctance transducer (DVRT; MicroStrain, Inc., Burlington, VT) was inserted into the distal third of the ACL's anteromedial bundle (AMB)[25-26] to measure change in length relative to its initial length. This initial length value corresponded to the pre-impact DVRT length, as recorded with balanced pre-tensioned muscle and gravitational forces and the static knee flexion angle (15º).[25] Using this baseline measure, DVRT length changes were recorded for each trial over the same 2 second post-impact period via a 16-bit analog-to-digital converter and converted to relative AMB strain.

Specimen 3-D knee kinematics were recorded during each impact trial via three infrared emitting diodes (IREDS) rigidly attached to the tibial plateau and the femoral condyle. A Certus system (Northern Digital, Waterloo, Ontario, Canada) acquired the 3-D location of each IRED at 400 Hz for 2 seconds immediately post-impact with a resolution of 0.1 mm, from which 3-D tibiofemoral kinematics were quantified to the nearest degree and millimeter[25]. The knee was assigned 6 degrees of freedom corresponding to motion along or about three orthogonal axes[30] passing through a fixed joint center, the mid-point of the femoral condyles at the height of the most proximal point on intercondylar notch[24]. Kinematic data recorded during each impact trial were expressed relative to the specimen's pre-impact (neutral) posture.

Following testing, specimens were removed from the loading frame and had true lateral radiographs taken. Specifically, images were taken at a fixed distance of 2 meters, with the tibia aligned vertically and the primary ray focused at the height of the tibial surface, perpendicular to tibial long axis. From the resulting radiographic images, tibial slope measures were made in blinded fashion based on previous methods[18,31] . The anterior and posterior cortices of the tibial shaft were first determined at points approximately 4 cm apart on the distal radiograph (Figure B.2). The midpoints of the two lines connecting these points were then quantified and the sagittal plane longitudinal axis was constructed such that it passed through each midpoint.[18] The peak anterior and posterior points of the medial tibial plateau, as observed on the radiograph (Points A and B), were subsequently defined. The slope angle was calculated as the enclosed angle between the line passing through these two points and the line perpendicular to the sagittal plane longitudinal axis.[18]

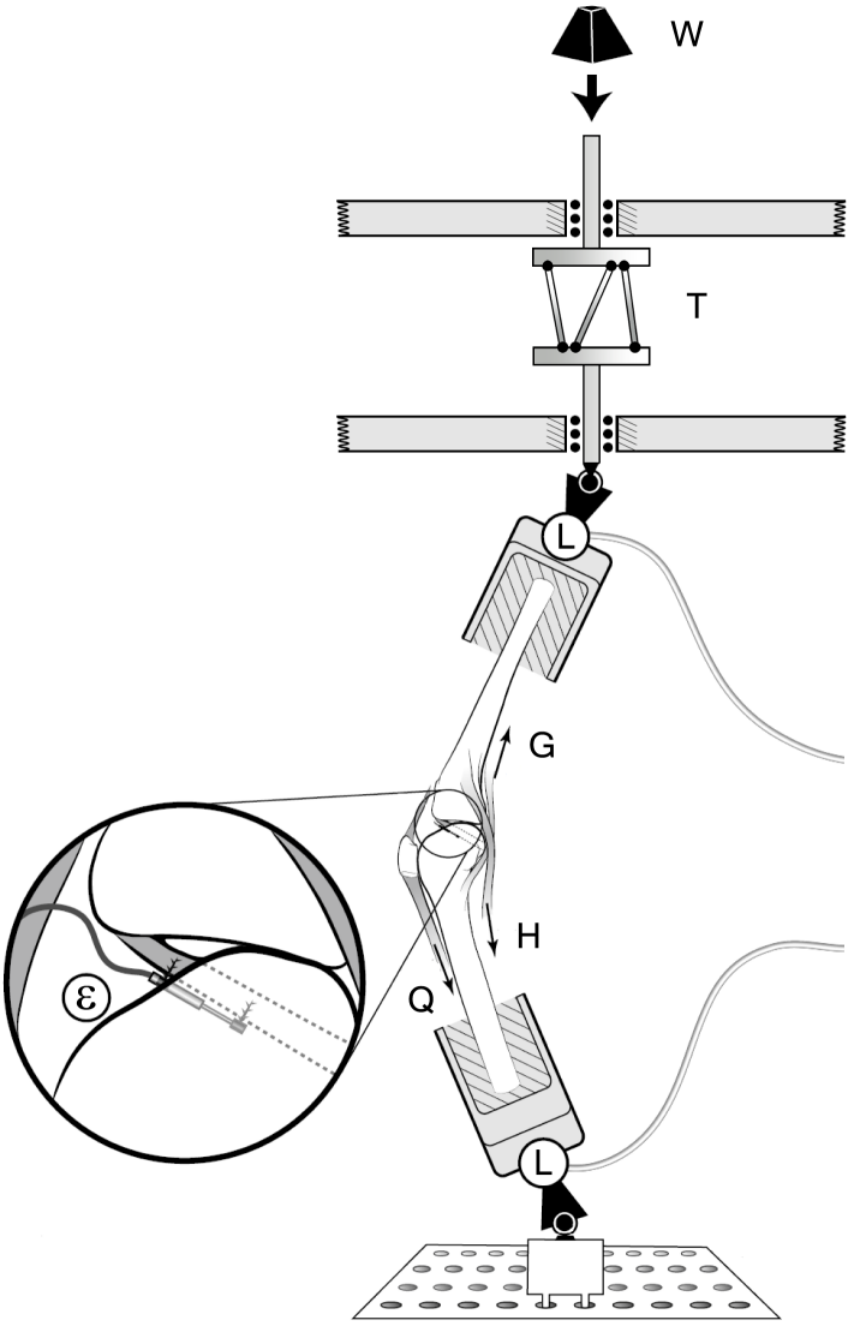

Figure B.1 Schematic of test setup, showing the knee mounted for testing as well as the applied impulsive loading (W) and three axis load cells (L). Lines of action of the quadriceps (Q), hamstring (H), gastrocnemius (G) muscle-tendon units are also visible. The inset drawing shows the differential variable reluctance transducer attached to the anteromedial region of the anterior cruciate ligament in order to measure the relative strain (b).

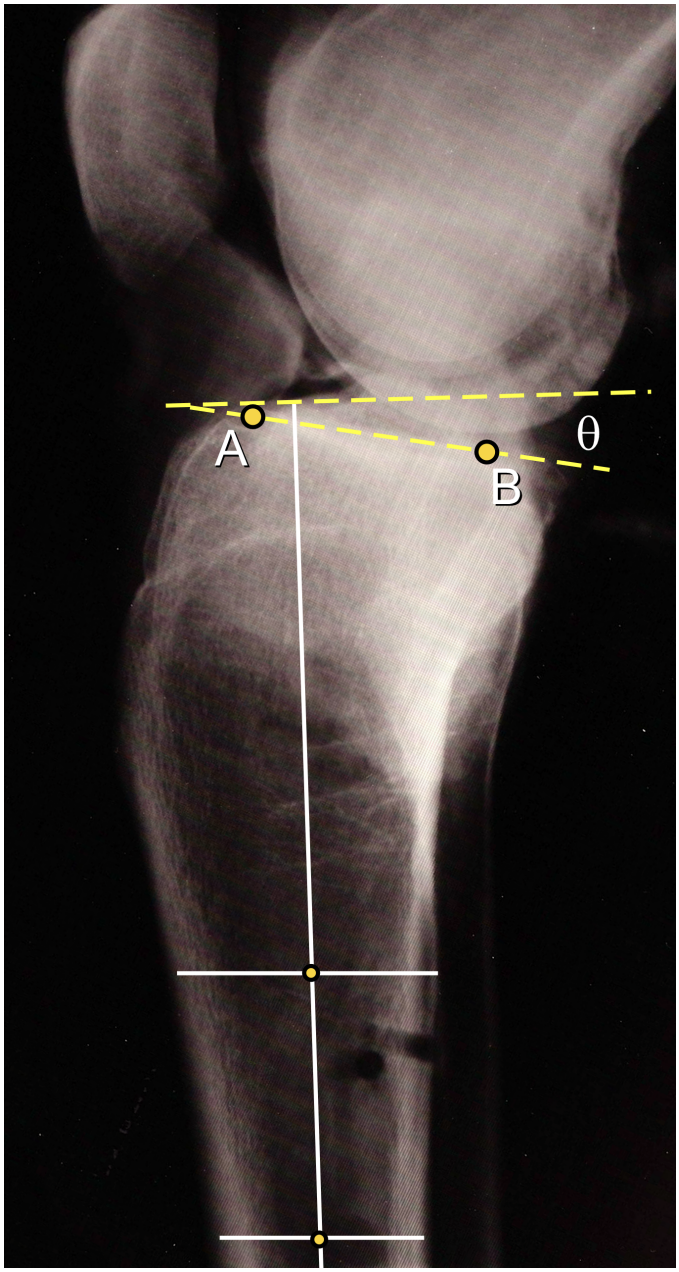

Figure B.2 Method used to calculate the posterior slope angle of the tibial plateau as defined within a standard lateral radiograph. A line passing through the midpoints of two lines connecting the anterior and posterior cortices of the tibial shaft, located approximately 4 cm apart defined the sagittal plane longitudinal axis of the tibia. The peak anterior (A) and posterior (B) points on the medial tibial plateau were then identified, with the slope angle defined as the enclosed angle between the line perpendicular to the longitudinal axis and the line joining points A and B.

Statistical Methods

The relative 3D translations and rotations between the femur and tibia were calculated over the duration of each trial.[20,32] Anterior tibial displacement data were then low-pass filtered with a cubic smoothing spline with a 50 Hz cut-off frequency[33] and double differentiated to provide accelerations. From these data, the peak anterior tibial acceleration over the first 200 ms post-impact was recorded. The peak relative AMB strain was similarly determined for each trial over this same time period. To assess tibial slope measurement reliability, three researchers initially quantified slope angles in each specimen on three consecutive days. Intra-class (within – 3,k; between – 3,1) correlation coefficients (ICC) were subsequently quantified within a 2-way mixed model. ICC values less than 0.4 were viewed as poor, from 0.4 to 0.74 were considered fair to good, and greater than 0.75 excellent[34] . ICC's calculated for intra- and inter-rater agreement in tibial slope measures were greater than 0.914, suggesting they could be submitted to statistical treatment with confidence. Posterior tibial slope values were thus averaged across the three measurements obtained for each specimen and submitted to the analyses.

To test the primary research hypothesis, individual regression analyses were first conducted to examine potential associations between both peak anterior tibial acceleration and posterior tibial slope and resultant peak AMB strain. Based on the outcomes of these preliminary analyses, a multiple linear step-wise regression model was adopted to examine the extent to which specimen-based peak AMB strain measures were predicted by posterior tibial slope, peak tibial acceleration and the interaction between these terms. Significance levels for inclusion and exclusion within this model were set at $p < 0.05$ and $p < 0.1$ respectively. To test our secondary hypothesis, the relative timings

of specimen based peak AMB strain and peak anterior tibial acceleration were also submitted to a simple linear regression model. Regression coefficients for all treatments were regarded as significant for $p < 0.05$. All analyses were performed using SPSS software version 17.0 (SPSS, Chicago, IL)

Source of Funding

This study was funded, in part, through the National Institutes of Health (AR054821-01). This funding was used to assist in specimen procurement, building the impact-loading device, purchasing equipment/materials used in the cadaveric testing and the funding of graduate students working on this project.

B.4 Results

Following testing, each joint was visually examined for damage. No gross morphologic changes were found in the ACL of any specimen, with each ligament remaining functionally intact. The mean (± SD) peak impact force applied to the distal tibia was 1,297.9 ± 210.6 N (range = 1,002.5 N – 1,783.1 N), occurring 50.6 ± 2.8 ms (range = 46 ms – 56 ms) following impact. Time series data depicting impact-induced anterior tibial acceleration and associated AMB strain measures over the first 200 ms of the impact phase are presented for a random sample (n=4) of specimens in Figure B.1. The duration of the anterior tibial acceleration pulse was 37.2 ± 6.0 msec. Definitive peaks were evident in both anterior tibial accelerations (8.31 ± 2.77 $m.s^{-2}$; range = 5.19 $m.s^{-2}$ – 14.45 $m.s^{-2}$) and AMB strain magnitudes (3.35 ± 1.71 %; range = 1.15 % - 6.67

%) for all specimens, occurring 66 ± 7 ms (range = 51 ms – 76 ms) and 66 ± 4 ms (range = 60 ms – 73 ms) post-impact, respectively (Figure B.3 and Table B.1). The posterior tibial slope across specimens was 7.8 ± 2.1º (range = 4.7º – 10.5º**).**

Table B.1 Mean specimen-based peak impact-induced anterior tibial acceleration magnitudes and associated peak relative AMB strain measures quantified during simulated (n = 5 trials) single leg landings. Posterior tibial slope angles for each specimen are also presented.

Specimen	Peak Anterior Tibial Acceleration ($m.s^{-2}$)	Peak Relative AMB Strain (%)	Posterior Tibial Slope Angle (deg)
1	6.73	1.15	4.9
2	14.45	5.01	10.5
3	5.79	1.36	6.3
4	8.42	2.48	6.1
5	6.41	3.42	6.7
6	10.32	4.32	9.2
7	6.93	3.76	8.0
8	8.40	3.93	10.2
9	6.01	3.50	4.7
10	5.19	1.27	6.5
11	12.72	6.67	10.0

In testing the primary hypothesis, peak AMB strain was significantly correlated (r = 0.79; p = 0.004) with peak anterior tibial acceleration (Figure B.4A), explaining 62% of the associated variance (b = 0.791). Specifically, for every $1 m.s^{-2}$ increase in peak anterior tibial acceleration, the AMB will experience a 0.4% greater peak relative strain. Peak impact-induced anterior tibial acceleration was also significantly correlated (r = 0.79; p = 0.004) with posterior tibial slope (Figure B.4B), which explained 61.8% of the variance (b = 0.786). Here, for every, the peak anterior tibial acceleration increased by $1.11 m.s^{-2}$.

In testing the secondary hypothesis the timing of the peak anterior tibial acceleration was significantly correlated ($r = 0.82$; $p = 0.001$) with the timing of peak AMB strain (Figure B.4D), explaining 67% of the variance ($b = 0.818$). Peak relative AMB strain was also significantly correlated ($r = 0.76$; $p = 0.007$) with posterior tibial slope (Figure B.4C), explaining 58% of the variance ($b = 0.759$). In this instance, for every 1º increase in posterior tibial slope, the AMB experienced 0.6% greater peak relative strain. Including both peak anterior tibial acceleration and posterior tibial slope within the full step-wise linear regression model did not significantly ($p = 0.304$) improve peak relative AMB strain predictions. Specifically, the posterior tibial slope term only explained an additional 4.9% of the variance observed in peak relative AMB strain beyond that explained by peak anterior tibial acceleration alone.

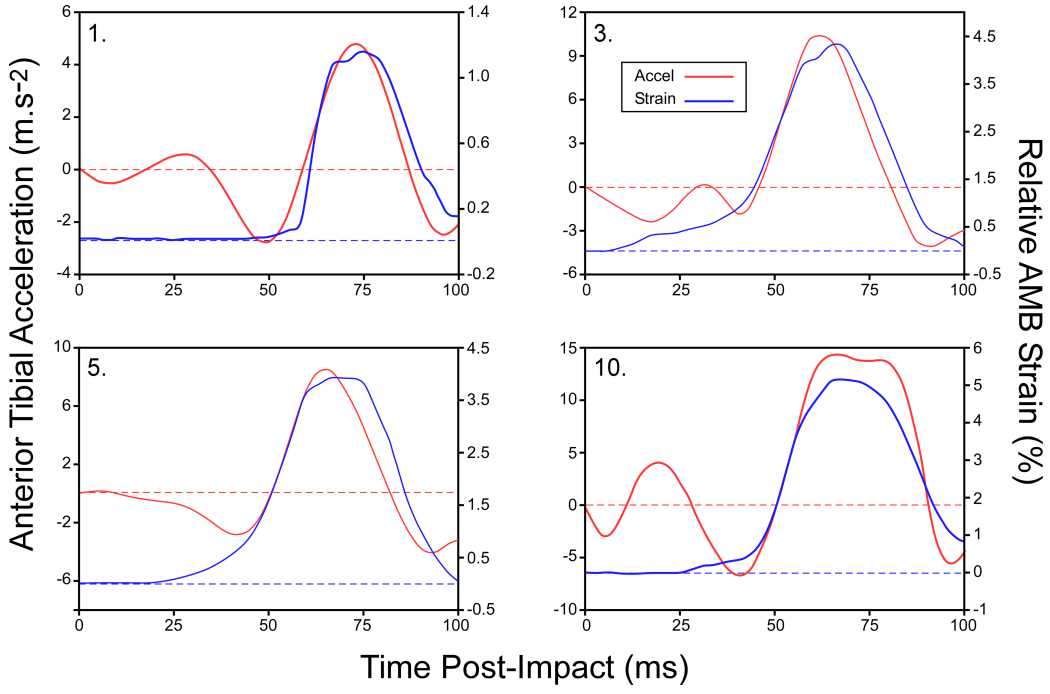

Figure B.3 Impact-induced anterior tibial acceleration and associated AMB strain measures over the first 200 ms of the impact phase for a random sample (n=4) of specimens.

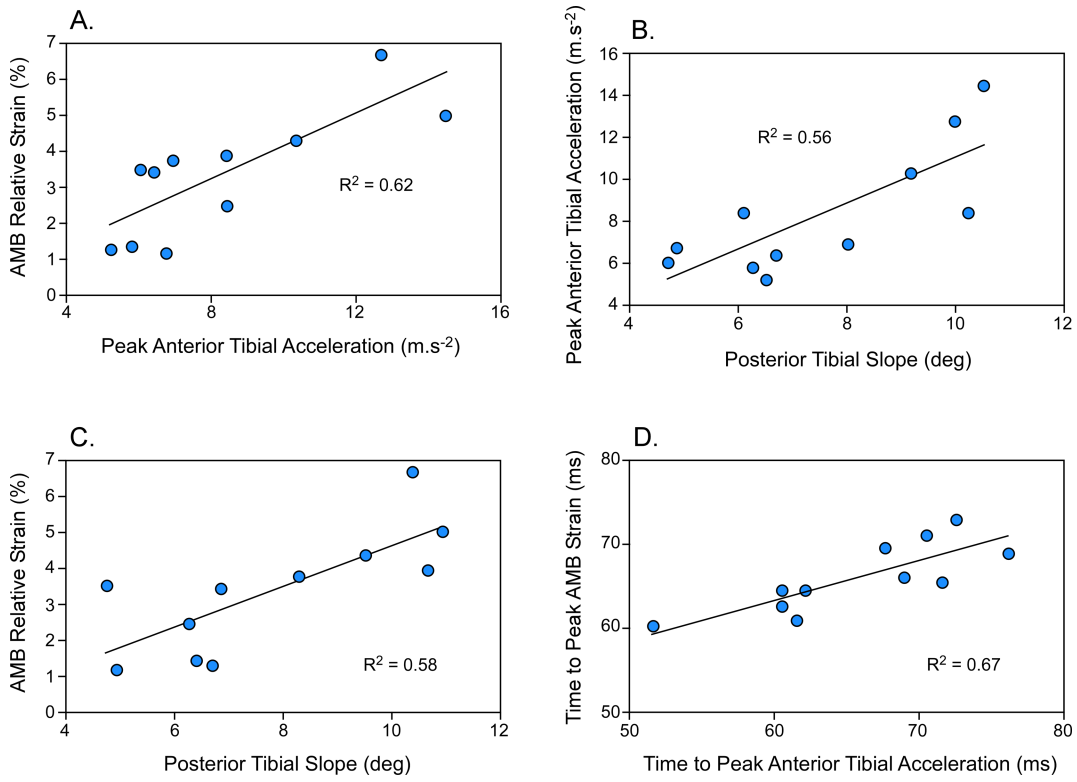

Figure B.4 Associations between mean subject-based peak impact induced anterior tibial acceleration and peak relative AMB strain (A), posterior tibial slope angle and impact induced anterior tibial acceleration (B), posterior tibial slope angle and peak relative AMB strain (C) and the respective timings of peak impact-induced anterior tibial acceleration and peak relative AMB strain (D).

B.5 Discussion

This is the first study to demonstrate significant associations between impact-induced anterior tibial acceleration, posterior tibial slope and AMB-ACL strain for dynamic high impact jump landings. Understanding relations between knee morphology and resultant mechanics during such tasks is ultimately critical to improved neuromuscular-based ACL injury prevention methods. We of course did not induce ACL

injury in any trial as this was not a goal of the study. It would thus be worthwhile for a future study to examine the relationships between peak anterior tibial acceleration, tibial slope and ACL rupture.

Regardless, current outcomes provide substantial insights into key morphological and mechanical interactions that directly impact ACL loading during high-risk landing maneuvers. A relatively large anterior tibial acceleration peak was evident in all specimens soon after impact, coinciding directly with peaks in the AMB strain response. Further, increases in the magnitude of the acceleration peak predicted similar increases in AMB strain. It is well documented that the ACL is the primary passive restraint to anterior tibial translations and loads[35-36]. Acceleration transients at the proximal tibia during abrupt deceleration tasks have similarly been shown to generate tibiofemoral shear forces that load the passive knee structures.[37-38] A feasible and somewhat intuitive explanation for our observed relation is obtained when one additionally considers Newton's second law of motion (F = ma). Specifically, greater anterior tibial acceleration will result in greater force being imparted on the ACL. This increased force will in turn increase the relative strain experienced within the ligament, as it attempts to restrain the accelerating tibia.

Using the same impact loading apparatus, Withrow 1 et al.[24] demonstrated that AMB strain also correlates well with the knee flexion moment, flexion angle and quadriceps force. This paper extends their initial finding by showing that these parameters may affect AMB strain via their contributions to the large transient tibial acceleration pulse, over 35 msec in duration and peaking at 65 msec post-landing impact, coinciding almost exactly with the instant of peak AMB strain.

The fact that our peak strain magnitudes were consistent with those measured during movements eliciting substantially smaller knee joint accelerations[39-40] may initially seem counterintuitive. Considering strain was measured "locally" in each instance, outcome comparisons may be compromised due to the sensitivity of the strain response to DVRT placement along the ligament tissue. The extent to which AMB strain behaviors vary along its length remains unknown and appears worthy of further exploration. It should be noted, however, that our peak strain measures were extremely consistent with those measured previously *in vivo* for similar high-impact landing scenarios[41]. We are thus confident that our observed strain outcomes and resultant anatomical – mechanical relations are viable. Regardless, the above inconsistencies strongly suggest that greater insights into how the complex interactions between knee joint and ACL geometric, structural, and mechanical factors dictate the ACL strain response under dynamic loading is warranted.

Impact-induced peak tibial acceleration magnitudes varied over a wide range across specimens. With both impact load and pre-impact muscle forces being constant, therefore, between-specimen variations in acceleration 1 and strain profiles must have been dictated by additional joint factors. Based on previously demonstrated links to ACL injury risk[21-22], we had initially posited posterior tibial slope to be one such factor. The posterior tibial slope has been suggested to induce potentially hazardous ACL loads during landing tasks via the promotion of a larger anterior tibial translation and/or thrust[23]. Explicit relationships between tibial slope, knee kinematics and ACL load, however, had only been quantified under clinically relevant joint loading conditions (eg., anterior drawer and Lachman test) [18,42-43]. Furthermore, the tibial translation and ACL

strain profile observed in these instances was not affected by slope under constrained anterior-posterior load applications. Our results suggest that at least for high-impact landings under the same external load constraints, tibial acceleration and resultant ACL strain are sensitive to the posterior tibial slope. A larger-than-normal slope orients the ACL more in an anterior-posterior direction[44] , and shifts the tibiofemoral contact point anteriorly[43] . This latter adjustment is posited to increase the anterior tibial shear load component of the tibial compressive force when transitioning from non-weight-bearing to weight-bearing[18,45,] causing greater ACL loads[46] . A similar chain of events may prevail during high-impact landing scenarios, where high-rate compressive joint loading transfers to an equally high anterior tibial shear load rate, culminating in a greater anterior tibial acceleration pulse and ACL strain. These relations may precipitate even greater tibial accelerations and ACL strains for an individual exhibiting the earlier discussed "provocative" landing postures, where the effect of tibial slope may be even greater [23] .

Others have also shown that at least for clinical load states, the posterior tibial slope transfers a component of axial compressive tibial loading into anterior tibial translation and hence ACL strain.[43] Further work is necessary to determine whether tibial slope contributions to high-impact 3-D knee joint loading similarly extrapolate to cause actual ACL injury.

We currently defined tibial slope as the angle of the medial tibial plateau, measured indirectly within a standard lateral radiograph[31,47] . These measures were also significantly correlated (R^2 = 0.97; p = 0.00001) with slope measures made directly on each specimen based on recently published methods[48] , suggesting they could be made with confidence. The fact that we were able to clearly establish relations between slope

and both acceleration and strain using this simple indirect radiographic technique thus advocates its' en-mass screening potential. Hashemi et al.[20] recently demonstrated, however, that links between posterior tibial slope and ACL injury may be more complex, with the medial tibial slope magnitude and its depth of concavity presenting with additional risk. Delineation of these different slopes, including cartilage contributions to slope variations[49-50] , is not possible on plane radiographs, so 3-D computed tomography or magnetic resonance imaging may be necessary[18,20,51] . Regardless, additional insights into ACL loading during landings seem likely by expanding current analyses to consider 3-D knee joint morphologic-mechanical interactions.

Compressive joint loads (~2 x BW) during the impact simulations were less than those of landings in which ACL injury is common[20,29,52-53] . As noted, however, associations between posterior tibial slope, tibial acceleration and ACL strain appear governed by standard mechanical principals. Hence, larger ACL strains in the presence of larger impact loads are likely. A larger impact load for a 1 knee with an increased posterior tibial slope will similarly induce a larger anterior shear component of the tibial compressive force, tibial acceleration and ACL strain. This relation between impact load, tibial acceleration and ACL strain profiles may also explain why a larger body mass index prospectively predicts ACL injury risk13 . We also examined relations between slope, kinematics and ACL strain within the sagittal plane only. While ACL injury has been suggested possible via a purely sagittal plane loading mechanism[29,54] , it is increasingly speculated that a more complex 3D scenario prevails[55] . Hence, the tibial slope acceleration mechanism could contribute to injury risk without being the only critical factor.

While not examining injury scenarios explicitly, our study supports the growing notion that the posterior tibial slope is an important risk factor for ACL injury [20,23,56] . In particular, a steeper slope increases the propensity for potentially traumatic impact induced anterior tibial accelerations and resultant ACL strains. While we did not simulate muscle activation strategies associated with an entire landing maneuver, risk does appear greater when an ineffective overarching neuromuscular strategy presents. In such instances, the rapidly moving tibia must be further restrained by the passive ACL, potentially inducing injury-causing load magnitudes. A simulation of actual injury scenarios within our cadaveric model would provide important additional insights here and we will do so in our ongoing efforts. Current outcomes may also provide immediate improvements to en-mass ACL injury risk assessment methods. In addition to possible radiologic assessments, for example, ongoing advances in body-worn sensor technologies[57-58] with integrated accelerometery may 1 ultimately afford improved risk screening based on safe, non-invasive segment acceleration measures. The success of targeted training interventions may similarly be evaluated by determining whether large impact-induced tibial accelerations can be consistently reduced for a variety of landing scenarios. In any case, quantifying impact-induced tibial accelerations during dynamic landings in which ACL injuries are common appears worthy of further exploration.

Our study had several limitations that should be considered alongside current outcomes. The plane film x-rays, for example, do not afford measurement of the tibial plateau depth of concavity, a known predictor of ACL injury[27] . Another potential limitation relates to the reliability of our tibial slope measure. Several such methods are proposed in the literature[20,59] and it is unclear whether the associations between slope,

acceleration and strain would exist if other methods were used. With slope definitions appearing reasonably correlated, however [59-60] , similar outcomes seem likely. The high reliability we observed for these measures also adds strength to their efficacy. While slope measures were reliable, however, study outcomes may still have been compromised if these and AMB strain measures were inaccurate. This seems particularly true considering the relatively small between-specimen variations in each of these parameters. We measured both slope and strain data using well established techniques. There is little data currently available, however, reporting their true accuracies, suggesting current outcomes should be viewed in light of this potential shortcoming. Regardless, considering the strengths of association observed between slope, tibial acceleration and AMB strain measures, we still feel current outcomes make an important contribution to our understanding of knee morphologic-mechanical interactions.

A limitation common in this type of testing was that we were unable to quantify the true AMB resting length with the specimen positioned within the loading frame[61-62]. We defined length changes in terms of relative AMB strain, using the length of the DVRT for the static muscle pre-load state as the reference value[24] . Additionally, only local ACL AMB strain was recorded; attaching even a miniature gage on the posteriolateral bundle of the ACL risks compromising the posterior joint capsule[63] or incurring measurement artifact[24] . However, the strain behavior of the ACL-AMB does provide a reasonable representation of the entire ligament strain response[39,64] . The recent work of Mizuno et al. supports this contention with general agreement between local AMB strain and ACL *in situ* loads[19,65] observed under clinical load applications. A final limitation is the extent to which data obtained from aged cadaveric specimens can be used to infer ACL injury

causality in a young healthy population. Although advancing age is known to impact knee joint and ACL tissue properties[66] , however, we would still expect results in younger specimens to exhibit similar qualititative trends, but with different absolute values.

B.6 Conclusions

Impact-induced ACL strain is directly proportional to anterior tibial acceleration, with both of these factors also being dependent on the posterior slope of the tibial plateau.

B.7 References

1. Griffin LY, Albohm, MJ, Arendt, EA, Bahr, R, Beynnon, BD, et al. Understanding and preventing noncontact anterior cruciate ligament injuries: a review of the Hunt Valley II meeting, January 2005. Am J Sports Med. 2006;34:1512-32.

2. Renstrom P, Ljungqvist, A, Arendt, E, Beynnon, B, et al. Non-contact ACL injuries in female athletes: an International Olympic Committee current concepts statement. Br J Sports Med. 2008;42:394-412.

3. Hewett TE, Lindenfeld, TN, Riccobene, JV, Noyes, FR. The effect of neuromuscular training on the incidence of knee injury in female athletes. A prospective study. Am J Sports Med. 1999;27:699-706.

4. Myklebust G, Engebretsen, L, Braekken, IH, Skjolberg, A, Olsen, OE, Bahr, R. Prevention of anterior cruciate ligament injuries in female team handball players: a prospective intervention study over three seasons. Clin J Sport Med. 22 2003;13:71-8.

5. Agel J, Arendt, EA, Bershadsky, 1 B. Anterior cruciate ligament injury in national collegiate athletic association basketball and soccer: a 13-year review. Am J Sports Med. 2005;33:524-30.

6. Mihata LC, Beutler, AI, Boden, BP. Comparing the incidence of anterior cruciate ligament injury in collegiate lacrosse, soccer, and basketball players: implications

for anterior cruciate ligament mechanism and prevention. Am J Sports Med. 2006;34:899-904.

7. Derrick TR. The effects of knee contact angle on impact forces and accelerations. Med Sci Sports Exerc. 2004;36:832-7.

8. Lafortune MA, Lake, MJ, Hennig, EM. Differential shock transmission response of the human body to impact severity and lower limb posture. J Biomech. 1996;29:1531-7.

9. Coventry E, O'Connor, KM, Hart, BA, Earl, JE, Ebersole, KT. The effect of lower extremity fatigue on shock attenuation during single-leg landing. Clin Biomech (Bristol, Avon). 2006;21:1090-7.

10. Moran KA, Marshall, BM. Effect of fatigue on tibial impact accelerations and knee kinematics in drop jumps. Med Sci Sports Exerc. 2006;38:1836-42.

11. Voloshin AS, Mizrahi, J, Verbitsky, O, Isakov, E. Dynamic loading on the human musculoskeletal system -- effect of fatigue. Clin Biomech (Bristol, Avon). 1998;13:515-520.

12. Elvin NG, Elvin, AA, Arnoczky, SP. Correlation between ground reaction force and tibial acceleration in vertical jumping. J Appl Biomech. 2007;23:180-9.

13. Uhorchak JM, Scoville, CR 1 , Williams, GN, Arciero, RA, St Pierre, P, Taylor, DC. Risk factors associated with noncontact injury of the anterior cruciate ligament: a prospective four-year evaluation of 859 West Point cadets. Am J Sports Med. 2003;31:831-42.

14. Nguyen AD, Shultz, SJ. Sex differences in clinical measures of lower extremity alignment. J Orthop Sports Phys Ther. 2007;37:389-98.

15. Braten M, Terjesen, T, Rossvoll, I. Femoral anteversion in normal adults. Ultrasound measurements in 50 men and 50 women. Acta Orthop Scand. 1992;63:29-32.

16. Trimble MH, Bishop, MD, Buckley, BD, Fields, LC, Rozea, GD. The relationship between clinical measurements of lower extremity posture and tibial translation. Clin Biomech (Bristol, Avon). 2002;17:286-90.

17. Amiri S, Cooke, D, Kim, IY, Wyss, U. Mechanics of the passive knee joint. Part 2: interaction between the ligaments and the articular surfaces in guiding the joint motion. Proc Inst Mech Eng [H]. 2007;221:821-32.

18. Hashemi J, Chandrashekar, N, Gill, B, Beynnon, BD, Slauterbeck, JR, Schutt, RC, Jr., Mansouri, H, Dabezies, E. The geometry of the tibial plateau and its influence on the biomechanics of the tibiofemoral joint. J Bone Joint Surg Am. 2008;90:2724-34.

19. Mizuno K, Andrish, JT, van den Bogert, AJ, McLean, SG. Gender dimorphic ACL strain in response to combined dynamic 3D knee joint loading: implications for ACL injury risk. Knee. 2009;16:432-40.

20. Hashemi J, Chandrashekar, N 1 , Mansouri, H, Gill, B, Slauterbeck, JR, Schutt, RC, Jr., Dabezies, E, Beynnon, BD. Shallow medial tibial plateau and steep

medial and lateral tibial slopes: new risk factors for anterior cruciate ligament injuries. Am J Sports Med. 2010;38:54-62.

21. Brandon ML, Haynes, PT, Bonamo, JR, Flynn, MI, Barrett, GR, Sherman, MF. The association between posterior-inferior tibial slope and anterior cruciate ligament insufficiency. Arthroscopy. 2006;22:894-9.

22. Todd MS, Lalliss, S, Garcia, E, Deberardino, TM, Cameron, KL. The Relationship Between Posterior Tibial Slope and Anterior Cruciate Ligament Injuries. Am J Sports Med. 2010;38:63-67.

23. Boden BP, Breit, I, Sheehan, FT. Tibiofemoral alignment: contributing factors to noncontact anterior cruciate ligament injury. J Bone Joint Surg Am. 2009;91:2381-9.

24. Withrow TJ, Huston, LJ, Wojtys, EM, Ashton-Miller, JA. The relationship between quadriceps muscle force, knee flexion, and anterior cruciate ligament strain in an in vitro simulated jump landing. Am J Sports Med. 2006;34:269-74.

25. Withrow TJ, Huston, LJ, Wojtys, EM, Ashton-Miller, JA. Effect of varying hamstring tension on anterior cruciate ligament strain during in vitro impulsive knee flexion and compression loading. J Bone Joint Surg Am. 2008;90:815-23.

26. Withrow TJ, Huston, LJ, Wojtys, EM, Ashton-Miller, JA. The effect of an impulsive knee valgus moment on in vitro relative ACL strain during a simulated jump landing. Clin Biomech (Bristol, Avon). 2006;21:977-83.

27. Pflum MA, Shelburne, KB 1 , Torry, MR, Decker, MJ, Pandy, MG. Model prediction of anterior cruciate ligament force during drop-landings. Med Sci Sports Exerc. 2004;36:1949-58.

28. Kernozek TW, Torry, MR, Iwasaki, M. Gender differences in lower extremity landing mechanics caused by neuromuscular fatigue. Am J Sports Med. 2008;36:554-65.

29. Yu B, Lin, CF, Garrett, WE. Lower extremity biomechanics during the landing of a stop-jump task. Clin Biomech (Bristol, Avon). 2006;21:297-305.

30. Grood ES, Suntay, WJ. A joint coordinate system for the clinical description of three-dimensional motions: application to the knee. J Biomech Eng. 1983;105:136-44.

31. Genin P, Weill, G, Julliard, R. [The tibial slope. Proposal for a measurement method]. J Radiol. 1993;74:27-33.

32. DeGoede KM, Ashton-Miller, JA. Fall arrest strategy affects peak hand impact force in a forward fall. J Biomech. 2002;35:843-8.

33. Woltring HJ, Huiskes, R, de Lange, A, Veldpaus, FE. Finite centroid and helical axis estimation from noisy landmark measurements in the study of human joint kinematics. J Biomech. 1985;18:379-89.

34. Portney LG, Watkins, MP. Foundations of Clinical Research. Edited by Norwalk, C. T., Appleton and Lange, 2000.

35. Butler DL. Kappa Delta Award paper. Anterior cruciate ligament: its normal response and replacement. J Orthop Res. 1989;7:910-21.

36. Markolf KL, 1 Burchfield, DM, Shapiro, MM, Shepard, MF, Finerman, GA, Slauterbeck, JL. Combined knee loading states that generate high anterior cruciate ligament forces. J Orthop Res. 1995;13:930-5.

37. Bryant AL, Newton, RU, Steele, J. Successful feed-forward strategies following ACL injury and reconstruction. J Electromyogr Kinesiol. 2009;19:988-97.

38. Lafortune MA. Three-dimensional acceleration of the tibia during walking and running. J Biomech. 1991;24:877-86.

39. Beynnon BD, Fleming, BC. Anterior cruciate ligament strain in-vivo: a review of previous work. J Biomech. 1998;31:519-25.

40. Beynnon BD, Fleming, BC, Johnson, RJ, Nichols, CE, Renstrom, PA, Pope, MH. Anterior cruciate ligament strain behavior during rehabilitation exercises in vivo. Am J Sports Med. 1995;23:24-34.

41. Cerulli G, Benoit, DL, Lamontagne, M, Caraffa, A, Liti, A. In vivo anterior cruciate ligament strain behaviour during a rapid deceleration movement: case report. Knee Surg Sports Traumatol Arthrosc. 2003;11:307-11.

42. Fening SD, Kovacic, J, Kambic, H, McLean, S, Scott, J, Miniaci, A. The effects of modified posterior tibial slope on anterior cruciate ligament strain and knee kinematics: a human cadaveric study. J Knee Surg. 2008;21:205-11.

43. Giffin JR, Vogrin, TM, Zantop, T, Woo, SL, Harner, CD. Effects of increasing tibial slope on the biomechanics of the knee. Am J Sports Med. 2004;32:376-82.

44. Li G, Papannagari, R, DeFrate, LE, Yoo, JD, Park, SE, Gill, TJ. Comparison of the ACL and ACL graft forces before and after ACL reconstruction: an in-vitro robotic investigation. Acta Orthop. 2006;77:267-74.

45. Beynnon BD, Fleming, BC, 1 Labovitch, R, Parsons, B. Chronic anterior cruciate ligament deficiency is associated with increased anterior translation of the tibia during the transition from non-weightbearing to weightbearing. J Orthop Res. 2002;20:332-7.

46. Petersen W, Zantop, T. Anatomy of the anterior cruciate ligament with regard to its two bundles. Clin Orthop Relat Res. 2007;454:35-47.

47. Yoo JH, Chang, CB, Shin, KS, Seong, SC, Kim, TK. Anatomical references to assess the posterior tibial slope in total knee arthroplasty: a comparison of anatomical axes. J Arthroplasty. 2008;23:586-92.

48. de Boer JJ, Blankevoort, L, Kingma, I, Vorster, W. In vitro study of inter individual variation in posterior slope in the knee joint. Clin Biomech (Bristol, Avon). 2009;24:488-92.

49. Hudek R, Schmutz, S, Regenfelder, F, Fuchs, B, Koch, PP. Novel measurement technique of the tibial slope on conventional MRI. Clin Orthop Relat Res. 2009;467:2066-72.

50. Espregueira-Mendes JD, da Silva, MV. Anatomy of the proximal tibiofibular joint. Knee Surg Sports Traumatol Arthrosc. 2006;14:241-9.

51. Simon RA, Everhart, JS, Nagaraja, HN, Chaudhari, AM. A case-control study of anterior cruciate ligament volume, tibial plateau slopes and intercondylar notch dimensions in ACL-injured knees. J Biomech. 2010;43:1702-7.

52. McLean SG, Samorezov, JE. Fatigue-induced ACL injury risk stems from a degradation in central control. Med Sci Sports Exerc. 2009;41:1661-72.

53. Blackburn JT, Padua, DA 1 . Sagittal-plane trunk position, landing forces, and quadriceps electromyographic activity. J Athl Train. 2009;44:174-9.

54. DeMorat G, Weinhold, P, Blackburn, T, Chudik, S, Garrett, W. Aggressive Quadriceps Loading Can Induce Noncontact Anterior Cruciate Ligament Injury. Am J Sports Med. 2004;32:477-483.

55. McLean SG, Huang, X, Su, A, Van Den Bogert, AJ. Sagittal plane biomechanics cannot injure the ACL during sidestep cutting. Clin Biomech (Bristol, Avon). 2004;19:828-38.

56. McLean SG, Lucey, SM, Rohrer, S, Brandon, C. Knee joint anatomy predicts high-risk in vivo dynamic landing knee biomechanics. Clin Biomech (Bristol, Avon). 2010;25:781-8.

57. Bergmann JH, Mayagoitia, RE, Smith, I. A portable system for collecting anatomical joint angles during stair ascent: a comparison with an optical tracking device. Dyn Med. 2009;8:3.

58. Favre J, Aissaoui, R, Jolles, BM, de Guise, JA, Aminian, K. Functional calibration procedure for 3D knee joint angle description using inertial sensors. J Biomech. 2009;42:2330-5.

59. Han HS, Chang, CB, Seong, SC, Lee, S, Lee, MC. Evaluation of anatomic references for tibial sagittal alignment in total knee arthroplasty. Knee Surg Sports Traumatol Arthrosc. 2008;16:373-7.

60. Brazier J, Migaud, H, Gougeon, F, Cotten, A, Fontaine, C, Duquennoy, A. [Evaluation of methods for radiographic measurement of the tibial slope. A study of 83 healthy knees]. Rev Chir Orthop Reparatrice Appar Mot. 1996;82:195-200.

61. Fleming 1 BC, Beynnon, BD, Tohyama, H, Johnson, RJ, Nichols, CE, Renstrom, P, Pope, MH. Determination of a zero strain reference for the anteromedial band of the anterior cruciate ligament. J Orthop Res. 1994;12:789-95.

62. Hashemi J, Breighner, R, Jang, TH, Chandrashekar, N, Ekwaro-Osire, S, Slauterbeck, JR. Increasing pre-activation of the quadriceps muscle protects the anterior cruciate ligament during the landing phase of a jump: An in vitro simulation. Knee. 2010;17:235-241.

63. Bach JM, Hull, ML. Strain inhomogeneity in the anterior cruciate ligament under application of external and muscular loads. J Biomech Eng. 1998;120:497-503.

64. Butler DL, Kay, MD, Stouffer, DC. Comparison of material properties in fascicle bone units from human patellar tendon and knee ligaments. J Biomech. 1988;19:425-32.

65. Kanamori A, Woo, SL, Ma, CB, Zeminski, J, Rudy, TW, Li, G, Livesay, GA. The forces in the anterior cruciate ligament and knee kinematics during a simulated pivot shift test: A human cadaveric study using robotic technology. Arthroscopy. 2000;16:633-9.

66. Woo SL, Hollis, JM, Adams, DJ, Lyon, RM, Takai, S. Tensile properties of the human femur-anterior cruciate ligament-tibia complex. The effects of specimen age and orientation. Am J Sports Med. 1991;19:217-25.